

**Univerzita Karlova**

**2. lékařská fakulta**

Doktorský studijní program: Biochemie a patobiochemie



**Mgr. Matej Gazdarica**

**The role of SGIP1 protein in the control of cannabinoid receptor 1**

Úloha proteinu SGIP1 v řízení Kanabinoidního receptoru 1

Disertační práce

Školitel: MUDr. Jaroslav Blahoš, Ph.D

Praha, 2023

**Prohlášení:**

Prohlašuji, že jsem závěrečnou práci zpracoval samostatně a že jsem řádně uvedl a citoval všechny použité prameny a literaturu. Současně prohlašuji, že práce nebyla využita k získání jiného nebo stejného titulu

Souhlasím s trvalým uložením elektronické verze mé práce v databázi systému meziuniverzitního projektu Theses.cz za účelem soustavné kontroly podobnosti kvalifikačních prací.

V Praze, 16.10.2023

Mgr. Matej Gazdarica

.....

Podpis

## **Acknowledgments**

Firstly, I would like to thank doc. MUDr. Jaroslav Blahoš, Ph.D. for the opportunity to work on this fascinating project and be the part of his scientific team. I also want to thank Laurent Prézeau, Ph.D., and Jean Philippe Pin, Ph.D., for letting me conduct my research at the Laboratory of Neuroreceptors, dynamics and function at IGF at Montpellier as well as for their thoughtful approach and inspiring ideas. I owe a debt of gratitude to the whole Department of Molecular Pharmacology at the Institute of Molecular Genetics AS CR, v.i.i., namely to Irina Cheveleva, Judith Noda Mayor, Lucie Pejšková, Michaela Dvořáková and Oleh Durydivka for creating and an excellent working environment filled with inspiration and felicity. Many thanks also belong to my friends for bringing joy to my life. Furthermore, I would like to thank Jordi Haubrich, Joan Font Ingles, Cédric Soulié, and others who made my stay in Montpellier unforgettable. Last but not least, I would like to thank my mother, father, and sister, who supported me my whole life.

## Abstrakt

Dvě oblasti na C-konci kanabinoidního receptoru 1 (CB1R), <sup>425</sup>SMGDS<sup>429</sup> a <sup>460</sup>TMSVSTDTS<sup>468</sup>, obsahují shluky serinových a treoninových zbytků, které mohou být fosforylovány a společně hrají zásadní roli při desenzitizaci a internalizaci aktivovaného CB1R. Pomocí metod bioluminiscenčního rezonančního přenosu energie spolu s farmakologickými inhibitory jsme v této práci zkoumali úlohu fosforylace těchto serinových/treoninových klastrů při zprostředkování protein-proteinových interakcí CB1R s molekulami důležitými pro desenzitizaci a internalizaci tohoto receptoru. Ukázali jsme, že interakce CB1R s G proteinem spřaženou receptorovou kinázou 3 (GRK3) a  $\beta$ -arrestinem2 závisí na odlišných vzorcích fosforylace C-konce CB1R. Kromě toho musí být GRK3 pro interakci s CB1R v aktivní formě. Dále byl zkoumán vliv proteinu SGIP1 (Src homology 3-domain growth factor receptor-bound 2-like (endophilin) interacting protein 1) na dynamiku signalosomu CB1R a desenzitizaci CB1R. SGIP1 zásadně mění interakci CB1R s GRK3 a  $\beta$ -arrestinem2 a modifikuje vazbu GRK3 na  $\beta\gamma$  podjednotky G proteinů. V této práci charakterizujeme nově identifikované sestřihové varianty SGIP1 a ukazujeme, že změny způsobené alternativním sestřihováním v doménách SGIP1 nemají vliv na inhibiční účinek SGIP1 na internalizaci CB1R. Výsledky této studie podrobně popisují molekulární mechanismy zprostředkující signalizaci a desenzitizaci CB1R. Popis těchto jevů pomáhá pochopit kanabinoidní signalizaci a vývoj tolerance.

**Klíčová slova:**  $\beta$ -arrestin2, desenzitizace receptoru, fosforylace, G proteinem spřažená receptorová kináza 3, receptory spřažené s G proteinem, kanabinoidní receptor 1, SGIP1.

## Abstract

Two regions within the cannabinoid receptor 1 (CB1R) C-tail, <sup>425</sup>SMGDS<sup>429</sup> and <sup>460</sup>TMSVSTDTS<sup>468</sup>, contain clusters of serine and threonine residues that can be phosphorylated and collectively play an essential role in the desensitization and internalization of activated CB1R. First, I studied the role of phosphorylation of the aforementioned serine/threonine clusters in protein-protein interaction between CB1R and molecules relevant to the receptor desensitization and internalization using the Bioluminescence Resonance Energy Transfer method in tandem with pharmacological inhibitors. I show that CB1R interaction with G protein-coupled receptor kinases 3 (GRK3) and  $\beta$ -arrestin2 depends on distinct C-tail phosphorylation patterns. Furthermore, the activation of GRK3 is required for its interaction with CB1R. Second, I studied the impact of Src homology 3-domain growth factor receptor-bound 2-like endophilin interacting protein 1 (SGIP1) on the dynamics of CB1R signalosome and CB1R desensitization. SGIP1 altered CB1R interactions with GRK3,  $\beta$ -arrestin2 and GRK3-G $\beta\gamma$  coupling. Further, I characterize newly identified splice variants of SGIP1 and demonstrate that alternative splicing-based alterations in SGIP1 domains do not affect the inhibitory effect of SGIP1 on CB1R internalization. This study's outcomes describe the molecular mechanisms mediating CB1R signaling and desensitization. Such details help to understand cannabinoid signaling in the brain and drug tolerance development.

**Key words:**  $\beta$ -arrestin2, cannabinoid receptor 1, G protein-coupled receptors, G protein-coupled receptor kinase 3, phosphorylation, receptor desensitization, SGIP1

This work was carried out in the Laboratory of Molecular Pharmacology at the Institute of Molecular Genetics ASCR, with the support of grants GAČR GA16-24210S, GAČR GA21-02371S. The work was also supported by the IMG International Mobility 2 (CZ.02.2.69/0.0/0.0/16\_027/0008512, Ministry of Education, Youth and Sports).

Tato práce byla provedena v Laboratoři molekulární farmakologie Ústavu molekulární genetiky AV ČR s podporou grantů GAČR GA16-24210S, GAČR GA21-02371S a ÚMG Mezinárodní mobilitou 2 (CZ.02.2.69/0.0/0.0/16\_027/0008512, Ministerstvo školství, mládeže a tělovýchovy).

## List of abbreviations

- 2-AG – 2-arachidonoylglycerol
- AEA – Anandamide
- AP-2 – Adaptor protein complex 2
- APA – AP2 activator
- BRET – Bioluminescence resonance energy transfer
- cAMP – cyclic adenosine triphosphate
- CB1R – Cannabinoid receptor 1
- CB2R – Cannabinoid receptor 2
- CBD – Cannabidiol
- CCP – Clathrin-coated pits
- CME – Clathrin-mediated endocytosis
- CNS – Central neuros system
- CRIP1a – Cannabinoid receptor interacting protein 1a
- cGMP – Cyclic guanosine monophosphate
- DAMGO - (D-Ala<sup>2</sup>, N-MePhe<sup>4</sup>, Gly-ol)-enkephalin
- DDT – dithiothreitol
- DMSO – dimethyl sulfoxide
- eCBs – Endocannabinoids
- ECS – Endocannabinoid system
- EPS15 – EGFR pathway substrate 15
- ERK – Extracellular signal-regulated kinases
- FAAH – Fatty acid amide hydrolase
- FCHO – FCH domain only proteins
- F-BAR – FCHO1/2 N-terminus consists of the Fer-CIP4 homology-BAR
- GASP1 – G protein coupled receptor associate protein 1
- GDP – Guanosine diphosphate
- GIRK – G protein-coupled inwardly rectifying potassium channels
- GPCR – G protein-coupled receptor
- GRK – G protein-coupled receptor kinase
- GTP – Guanosine triphosphate
- hCB1R – Human cannabinoid receptor 1

HEK293 – Human embryonic kidney cells 293  
HTRF – Homogenous Time-Resolved FRET  
IP1 – Inositol monophosphate  
JNK – c-Jun N-terminal kinases  
mBRET – milliBRET  
mCB1R – Mouse cannabinoid receptor 1  
MAGL – Monoacylglyceride lipase  
MAPK – Mitogen-Activated Protein Kinases  
MP – Membrane phospholipid  
PFC – Prefrontal cortex  
PI3K – Phosphoinositol 3-kinase  
PKA – Protein kinase A  
PKB – Protein kinase B  
PKC – Protein kinase C  
PPAR – Peroxisome proliferator-activated receptor  
Proline rich domain – PRD  
rCB1R – Rat cannabinoid receptor 1  
Rluc – *Renilla luciferase*  
SGIP1 – SH3-containing GRB2-like protein 3-interacting protein 1  
Syp1 – Suppressor of yeast profilin deletion 1  
SH3 – Src homology 3  
Terbium cryptate – SNAP-Lumi4-Tb  
THC – (-)-trans- $\Delta^9$  –tetrahydrocannabinol  
TRPV1 – Transient receptor potential cation channel subfamily V member 1  
 $\mu$ HD –  $\mu$  homology domain  
YFP – Yellow fluorescent protein  
WT CB1R – wild type cannabinoid receptor 1  
WIN - WIN 55,212-2 mesylate

## Table of Contents

1. Introduction .....	12
1.1. Cellular signaling .....	12
1.2. G protein-coupled receptors .....	12
1.2.1 GPCR families .....	13
1.2.2. Activation of GPCR .....	14
1.2.3. GPCR ligands.....	14
1.2.4. GPCR signaling.....	15
1.2.5. Signaling via G proteins .....	15
1.2.6. Termination and regulation of GPCR signaling .....	17
1.2.7. GPCR desensitization.....	18
1.2.8. GPCR phosphorylation .....	19
1.2.9. G protein-coupled receptor kinases - GRKs .....	19
1.2.10. Arrestins .....	21
1.2.11. GPCR internalization .....	22
1.2.12. Clathrin-mediated endocytosis .....	23
1.3. Endocannabinoid system .....	25
1.3.1. Endocannabinoids .....	25
1.3.2. Phytocannabinoids and synthetic cannabinoids.....	26
1.3.3. Cannabinoid receptors.....	27
1.3.4. Cannabinoid receptor 1.....	28
1.3.5. Cannabinoid receptor 1 structure.....	30
1.3.6. Cannabinoid receptor 1 signaling.....	30
1.3.7. Cannabinoid receptor 1 biased signaling .....	31
1.3.8. Cannabinoid receptor 1 desensitization and internalization .....	32
1.3.9. Role of CB1R C-tail in the desensitization and internalization.....	33
1.4. Src homology 3-domain growth factor receptor-bound 2-like (endophilin) interacting protein 1 (SGIP1) .....	35
1.4.1. SGIP1 structure.....	36
1.4.2. SGIP1 and CB1R.....	37
1.4.3. SGIP1 splice variants .....	38
2. Aims and hypotheses .....	40
3. Material and methods.....	41
3.1. Chemicals, enzymes and kits    Producer .....	41
3.2. Antibodies    Producer .....	42
3.3. Expression vectors.....	42

3.4.	Laboratory devices Manufacturer .....	42
3.5.	Transformation of competent <i>E. coli</i> .....	44
3.6.	Bacterial glycerol stock.....	44
3.7.	Agarose gel electrophoresis .....	44
3.8.	DNA Mini Prep.....	45
3.9.	DNA Midi Prep.....	45
3.10.	DNA sequencing .....	45
3.11.	Cell culture and transient transfection .....	45
3.12.	Long-term storage and thawing of cell lines.....	46
3.13.	Bioluminescence resonance energy transfer assays.....	46
3.14.	Microscopy .....	48
3.15.	SDS page and Western blot.....	48
3.16.	Animals used .....	49
3.17.	Inositol monophosphate accumulation .....	49
3.18.	Internalization assay.....	49
3.19.	Statistical analysis.....	50
4.	Results .....	51
4.1.	Activation of GRK3 is necessary for its optimal association with G $\beta\gamma$ .....	51
4.2.	GRK3 has to be in active form to interact with CB1R.....	52
4.3.	GRK2/3 inhibitor cmpd101 impedes CB1R-driven recruitment of $\beta$ -arrestin2.....	53
4.4.	Mutagenesis and characterization of CB1R C-tail phosphorylation mutants .....	54
4.5.	G protein activation and signaling are not altered in CB1R phosphorylation mutants ...	57
4.6.	CB1R phosphorylation state partially affects the formation of GRK3-G $\beta\gamma$ complexes....	58
4.7.	SGIP1 augments and prolongs GRK3-G $\beta\gamma$ coupling .....	59
4.8.	The two CB1R C tail motifs control dynamics of the CB1R-GRK3 association .....	60
4.9.	SGIP1 enhances CB1R-GRK3 association.....	62
4.10.	CB1R C tail phosphorylation is crucial for $\beta$ -arrestin2 recruitment .....	62
4.11.	The presence of SGIP1 increases CB1R- $\beta$ -arrestin2 association in $\beta$ -arrestin2- interacting CB1R phosphorylation mutants.....	64
4.12.	Unique phosphorylation patterns mediate GRK3 and $\beta$ -arrestin2 interactions with CB1R	64
4.13.	Expression of new SGIP1 splice variants in HEK293 cells.....	66
4.14.	SGIP1 splice variants attenuate CB1R internalization.....	67
5.	Discussion.....	69
5.1.	Activation of GRK3 is crucial for CB1R desensitization .....	69
5.2.	Two regions of CB1R C-terminus play an essential role in mediating CB1R interactions with GRK3 and $\beta$ -arrestin2 .....	71

5.3.	SGIP1 enhances GRK3-G $\beta$ $\gamma$ , CB1R-GRK3, and CB1R- $\beta$ -arrestin2 interactions.....	76
5.4.	Characterization of novel SGIP1 splice variants.....	77
6.	Conclusions .....	79
7.	Summary .....	80
8.	Shrnutí.....	81
9.	List of references.....	82
10.	List of publications .....	95
11.	Appendices.....	96

# **1. Introduction**

## **1.1. Cellular signaling**

Cell signaling arose from the needs of a cell to perceive and correctly process information from the environment and to coordinate intrinsic cellular processes vital for its survival. Eventually, cellular signaling further evolved into a plethora of complex molecular mechanisms that mediate a wide range of cellular processes, including cell-cell communication or coordination of physiological processes to maintain delicate homeostasis in multicellular organisms. In general, cellular signaling consists of two components: a receptor and a ligand.

A receptor is a molecule that recognizes a specific type of a signaling agent - a ligand, and is able to transduce signals. Based on the cellular location, two categories of receptors can be distinguished: intracellular receptors and membrane receptors.

Intracellular receptors are a class of proteins found in the cytoplasm or nucleus of the cell. Upon binding a ligand, typically a hydrophobic molecule, intracellular receptor undergoes conformational changes that reveal a DNA-binding site. The ligand-receptor complex then translocates into the nucleus, binding directly to DNA and regulating gene expression.

While membrane receptors consist of several receptor families that transduce signals through a different mechanisms, they all share several key structural features: an extracellular ligand-binding domain, a hydrophobic transmembrane domain that anchors receptors in the plasma membrane, and a cytoplasmic domain. Upon binding of a ligand, the membrane receptor undergoes conformation changes in the extracellular domain that activate cytoplasmic domain-linked signal-transducing machinery. Membrane receptors are classified into three categories: ionotropic receptors, receptor kinases and G protein-coupled receptors.

## **1.2. G protein-coupled receptors**

G protein-coupled receptors (GPCRs), also called seven-transmembrane receptors, are the largest superfamily of transmembrane cell signaling proteins. Between 800 and 1000 genes encode the GPCR receptor superfamily, involved in signaling processes that modulate behavior and mood, blood pressure, cognition, immune system, smell, taste, and homeostasis

(Thomsen, Frazer, & Unett, 2005). Given their role in virtually all physiological processes, GPCRs represent attractive pharmacological targets. It is estimated that approximately 35% of approved drugs target GPCRs (Sriram & Insel, 2018).

While the members of this superfamily greatly vary in protein sequence, they all share certain structural and functional features (Josefsson, 1999). The general topology of GPCR consists of an N-terminal extracellular domain, seven transmembrane helices connected by loop regions, and an intracellular C-terminal domain (Palczewski et al., 2000). A prominent feature of GPCRs is the ability to couple and activate the heterotrimeric G proteins that facilitate signal propagation.

### **1.2.1 GPCR families**

After more than four decades of GPCR research, several classifications of GPCRs rose based on distinct criteria. In vertebrates, GPCRs are classified into five families based on structural and sequence comparison of domains and functional similarities: rhodopsin-like receptors (A), secretin-like receptors (B), metabotropic glutamate receptors (C), adhesion receptors (D), and frizzled/taste receptors (F) (Rosenbaum, Rasmussen, & Kobilka, 2009).

The family of rhodopsin-like receptors accounts for 85% of mammalian GPCRs and is responsible for physiological roles like the sense of smell and vision (Schiøth & Fredriksson, 2005). The family of secretin receptors is formed by receptors that are activated by large peptides such as secretin, glucagon, growth hormone-releasing hormone, or parathyroid hormone (Miller, Dong, & Harikumar, 2012). The family of metabotropic glutamate receptors executes various functions in the central and peripheral nervous system, including behavioral and mood modulation (Pin, Galvez, & Prezeau, 2003). The next group of GPCRs, the adhesion receptors family, is characterized by the presence of a large extracellular region linked to the N-terminus (Yona, Lin, Siu, Gordon, & Stacey, 2008). Many receptors of this family are orphan receptors without known signaling pathways (Gupte et al., 2012). The last GPCR family – frizzled/taste are receptors for Wnt proteins and play a vital role in the regulation of cell polarity, embryonic development, and regulation of proliferation (Huang & Klein, 2004).

### **1.2.2. Activation of GPCR**

The canonical pathway of GPCR activation involves ligand binding to the extracellular domain and subsequent rearrangement of transmembrane helices that induces conformation change of a receptor leading to activation of heterotrimeric G protein and cellular signaling. While this process was previously described by a two-state model, in which receptor changes conformation between inactive and active states, the discovery of allosteric modulators, biased agonists or heteromerization of GPCRs extended the complexity behind GPCR activation and signaling (Park, Lodowski, & Palczewski, 2008).

Furthermore, many GPCRs, for example dopamine receptor 1, spontaneously achieve active conformation (Tiberi & Caron, 1994). This type of receptor conformation is characterized by a basal constitutive ligand-independent signaling activity.

### **1.2.3. GPCR ligands**

GPCRs are activated by a broad spectrum of stimuli that range from chemical compounds like lipids or peptides to physical agents like photons. Ligands can be divided into several categories based on the receptor response type.

An agonist is a signaling agent that produces a response upon binding to a receptor. Agonists can be further divided, based on the efficacy to activate a receptor, into full agonists that induce maximal response and partial agonists that exert only partial receptor response. On the other hand, an antagonist is a ligand that, upon binding to the receptor, does not produce a response and thus does not possess efficacy. Instead, upon binding to a receptor, the antagonist blocks the receptor from being activated by an agonist. An inverse agonist is an agent that, upon binding to a receptor, evokes an opposite pharmacological response than an agonist. Unlike antagonists with affinity but no efficacy for receptors, inverse agonists suppress the basal activity of constitutively active receptors (Bond & Ijzerman, 2006).

The above categories are not absolute – a ligand can be an antagonist, inverse agonist, or even agonist for different receptors or have specific activity dependent on the ligand concentration. Moreover, ligands known as biased ligands selectively activate only specific receptor-associated signaling pathways, thus effectively modifying the signaling outcomes

of a stimulated receptor in a process called biased signaling (Seyedabadi, Ghahremani, & Albert, 2019).

Most ligands are orthosteric regulators, meaning they bind to the receptor's active (orthosteric) site. Allosteric modulators are compounds that furthermore modify receptor response upon ligand binding. These compounds bind to allosteric sites, stabilizing GPCR in unique conformations leading to the altered effect of orthostatic ligand binding. Allosteric modulators present an attractive therapeutic target due to the possibility of modulating the effect of pharmacological drugs (Lindsley et al., 2016).

#### **1.2.4. GPCR signaling**

Activated GPCRs transduce signals via several signaling pathways. Canonical signaling transduction via GPCRs is mediated through the G proteins signaling pathway. Activation of G proteins, in turn, recruits secondary messengers that further propagate and amplify the signaling. While G protein signaling is described as the classical GPCR signal transduction mechanism, GPCRs can also signal via G protein-independent pathways through molecules like  $\beta$ -arrestins or G protein-coupled receptor kinases (GKRs) (Gurevich, Tesmer, Mushegian, & Gurevich, 2012; Peterson & Luttrell, 2017).

#### **1.2.5. Signaling via G proteins**

G protein signaling is dependent on receptor-induced activation of heterotrimeric G proteins, composed of three subunits:  $G\alpha$ ,  $G\beta$ , and  $G\gamma$ . Based on sequence homology, four families of human  $G\alpha$  proteins have been classified:  $G\alpha_s$ ,  $G\alpha_{i/o}$ ,  $G\alpha_{q/11}$ , and  $G\alpha_{12/13}$  (Downes & Gautam, 1999).

Heterotrimeric G proteins are anchored in the cytoplasmatic membrane, where they are functionally coupled to GPCRs. During the receptor-unstimulated state, the  $G\alpha$  subunit is associated with a guanosine diphosphate molecule (GDP) that renders the heterotrimeric G protein complex inactive. The binding of a ligand to GPCR induces a conformation change of the receptor that catalyzes the exchange of GDP for guanosine triphosphate molecule (GTP) in the  $G\alpha$  subunit (Higashijima, Ferguson, Sternweis, Smigel, & Gilman, 1987). This exchange promotes a conformation change that induces dissociation of the  $G\alpha$  subunit from the  $G\beta\gamma$  complex, thus leading to their activation. Both subunits bind and modulate a

different set of downstream effectors, providing further signal amplification.  $G\alpha$  targets enzymes like adenylyl cyclases, phospholipase C or cyclic guanosine monophosphate (cGMP) phosphodiesterase while  $G\beta\gamma$  complex recruits G protein-coupled receptor kinases (GRKs) to the cellular membrane, modulates ion channels or mitogen-activated protein kinases (Daaka et al., 1997; Khan et al., 2013; Milligan & Kostenis, 2006).  $G\alpha$  subunits possess intrinsic GTPase activity, thus once GTP is hydrolyzed into GDP, the  $G\alpha$  becomes inactive, leading to reassociation with the  $G\beta\gamma$  complex (Fig. 1). Human genome encodes 18 different  $G\alpha$  subunits that can be grouped into four categories based on their sequence and function:  $G\alpha_s$ ,  $G\alpha_i$ ,  $G\alpha_q$ , and  $G\alpha_{12}$  (Table 1.)

Due to the fact that both receptors and G proteins can diffuse in the cytoplasmic membrane, a single GPCR can catalyze GDP/GTP exchange on multiple heterotrimer G proteins, thus substantially amplifying a signal (Ross, 2014). For instance, in a phototransducing cascade, a single photon exciting (activating) rhodopsin receptor can activate about 60 G proteins that further translate into hydrolysis of as many as 72 000 molecules of cGMP (Arshavsky & Burns, 2014). Due to this phenomenon of signal amplification, the activation of the receptors with a low surface expression can still have a profound outcome on the cell.

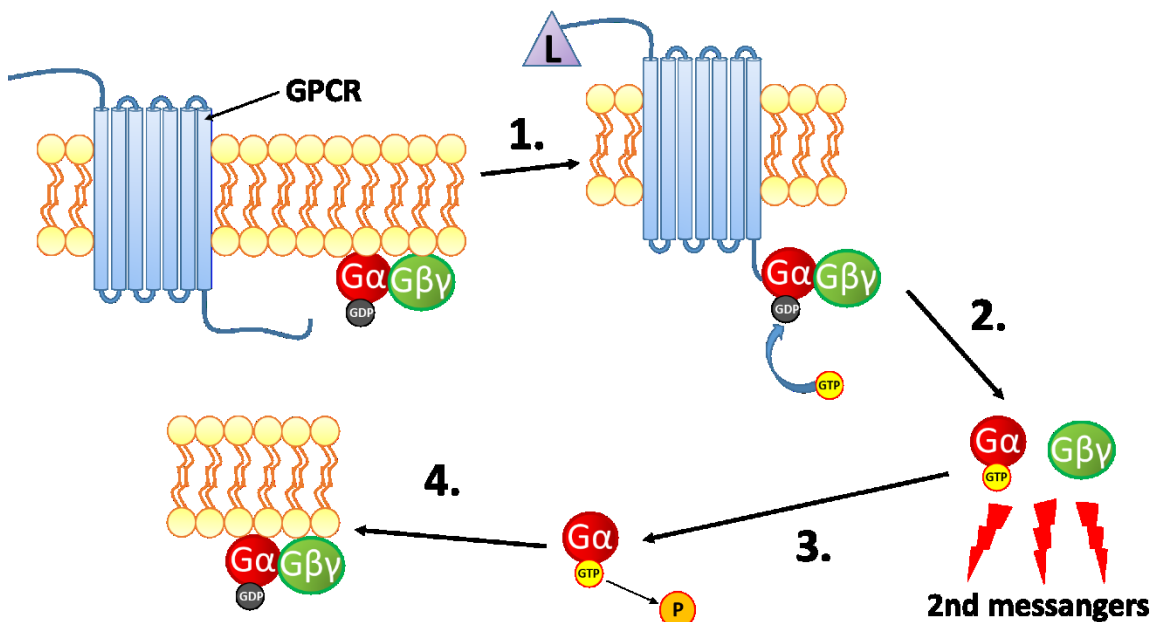


**Figure 1. The activation of G proteins by GPCRs.** Inactive GDP-bound heterotrimeric G proteins are anchored in the cytoplasmic membrane. 1) Activation of GPCR by ligand (L) induces a conformation change of GPCR that catalyzes the exchange of GDP for GTP in the  $G\alpha$  subunit. 2) Binding of GTP causes dissociation of  $G\alpha$  from  $G\beta\gamma$  leading to activation of these subunits and their subsequent interaction with secondary messengers, ultimately producing a signaling cascade. 3) The intrinsic GTPase activity of  $G\alpha$  (or the activity of

regulatory molecules of G proteins) catalyzes the hydrolysis of GTP to GDP by the release of monophosphate (P). 4) GDP-bound  $G\alpha$  reassociates with  $G\beta\gamma$  forming inactive G protein heterotrimers.

### 1.2.6. Termination and regulation of GPCR signaling

While signal transduction is an essential process for literally every cell, abnormal signaling or even overstimulation can be detrimental to the cell's fate, leading to cell death or, on the contrary, to uncontrolled cell growth and cancer. For instance, excessive levels of neurotransmitter glutamate can overstimulate glutamate receptors and cause neuronal damage in the process called glutamatergic excitotoxicity (Manev, Favaron, Guidotti, & Costa, 1989). The activated receptor and corresponding signaling have to be terminated in order to ensure dynamic reactivity to physical and chemical cues. Consequently, through the course of evolution, cells have developed numerous mechanisms that tightly control and regulate signaling. The signaling of GPCRs is mainly regulated via processes of desensitization and internalization, and downregulation.

**Table 1. List of human  $G\alpha$  subunits.** The human genome encodes four groups of  $G\alpha$  subunits that have distinct effects on cellular signaling (Syrovatkina, Alegre, Dey, & Huang, 2016).

Family of $G\alpha$	Members and expression	Signal transduction effect
<b><math>G\alpha_s</math></b>	$G\alpha_s$ – ubiquitously expressed $G\alpha_{olf}$ – olfactory neurons	Activation of adenylyl cyclase
<b><math>G\alpha_{i/o}</math></b>	$G\alpha_{i1}$ – widely distributed $G\alpha_{i2}$ – widely distributed $G\alpha_{i3}$ – ubiquitously expressed $G\alpha_{oA}$ – neurons $G\alpha_{oB}$ – neuroendocrine cells $G\alpha_{t1}$ – retinal rods, taste cells $G\alpha_{t2}$ – retinal cones $G\alpha_g$ – brush cells, taste cells $G\alpha_z$ – platelets, neurons	Inhibition of adenylyl cyclase Activation of phosphodiesterase Open $K^+$ channels Close $Ca^{2+}$ channels
<b><math>G\alpha_q</math></b>	$G\alpha_q$ – ubiquitously expressed $G\alpha_{11}$ – ubiquitously expressed $G\alpha_{14}$ – lungs, liver, kidneys $G\alpha_{15}$ – hematopoietic cells $G\alpha_{16}$ – hematopoietic cells	Inhibition of adenylyl cyclase
<b><math>G\alpha_{12}</math></b>	$G\alpha_{12}$ – ubiquitously expressed $G\alpha_{13}$ – ubiquitously expressed	Activation of the Rho family of GTPases

### 1.2.7. GPCR desensitization

GPCR desensitization is a process characterized by signal attenuation followed by a decrease in response to consecutive stimulation. The response of activated receptors can be decreased via homologous desensitization (mediated by GRKs) that occurs after prolonged agonist exposure. Alternatively, signal attenuation can be mediated via ligand-independent heterologous desensitization that is facilitated by second messenger-mediated protein kinase A (PKA) or protein kinase C (PKC) (Hausdorff, Caron, & Lefkowitz, 1990; Zhang & Kim, 2017).

In GPCRs, a highly conserved two-step mechanism accomplishes the cessation of G protein signaling. The first step involves phosphorylation of the cytoplasmic part of the activated receptor by GRKs or second messenger-activated protein kinases followed by  $\beta$ -arrestin recruitment, which uncouples G protein from GPCR, effectively leading to the diminution of second messenger generation (Lefkowitz, 1998). During the second step, the desensitized receptor is packed into an endosome that is either targeted for degradation in lysosomes or is recycled back to the cellular membrane as a receptor ready to be activated again (Lefkowitz, 1998; Pavlos & Friedman, 2017) (Fig. 2).

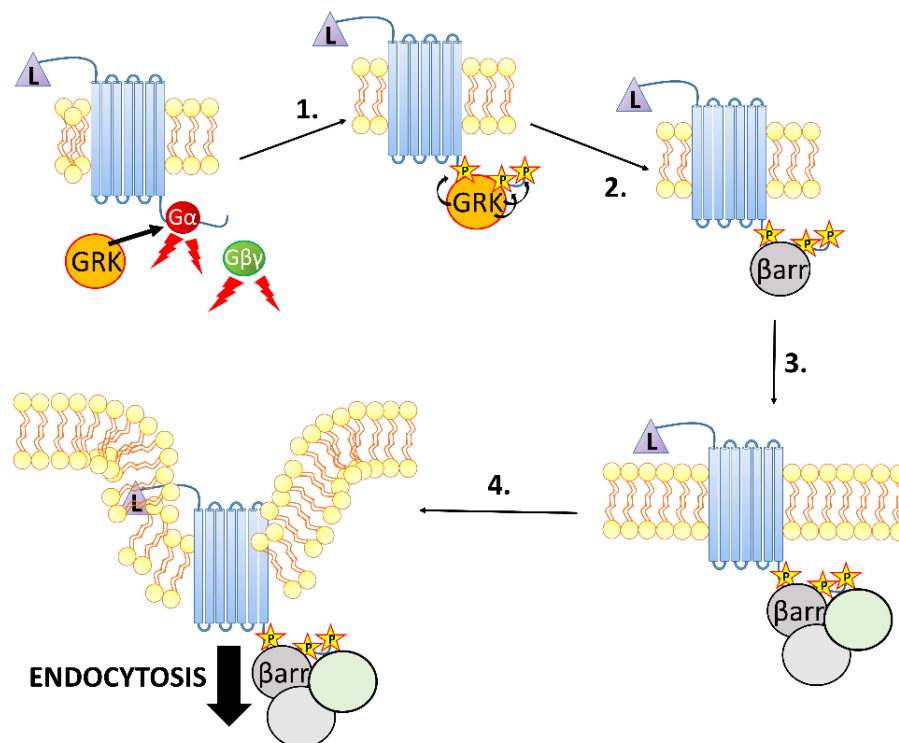


**Figure 2. Desensitization of activated GPCR.** Ligand-activated receptor and activated G proteins induce translocation of GRK to the proximity of the receptor. **1)** GRK is recruited to the cytoplasmic portion of the receptor (C-tail), which phosphorylates serine and threonine residues. **2)** Phosphorylation of C-tail serves as a recruitment signal for  $\beta$ -arrestin that

attenuates G protein signaling by binding to activated GPCR and uncoupling it from G protein. **3)** GPCR-bound  $\beta$ -arrestin serves as a molecular scaffold for the recruitment of regulatory proteins involved in endocytosis (shown as light grey and light green circles). **4)** Desensitized receptor is packed into endosome by endocytosis and targeted for degradation or recycling back to the plasma membrane.

### **1.2.8. GPCR phosphorylation**

Upon ligand binding and subsequent activation of GPCRs, these receptors are phosphorylated on their intracellular loops or C-tails. The multisite phosphorylation is mediated by two distinct groups of serine/threonine kinases: second messenger-dependent kinases (PKA and PKC) and second messenger-independent kinases – G protein-coupled kinases (GRKs) (Lefkowitz, 1998). Interestingly, the kinase activity itself does not decouple the active G proteins from GPCR. Instead, the phosphorylation of receptors triggers the recruitment of  $\beta$ -arrestins that sterically block the interaction of GPCR with their cognate G proteins (Gainetdinov, Premont, Bohn, Lefkowitz, & Caron, 2004).

The phosphorylation of the activated GPCR is not a single uniform action but rather a highly multifarious process where different kinases facilitate distinct phosphorylation patterns leading to various outcomes. This phenomenon, called the Barcode hypothesis, postulates that distinct ligands stabilize various receptor conformations that induce specific patterns of receptor phosphorylation and downstream signaling (Butcher et al., 2011; Nobles et al., 2011).

### **1.2.9. G protein-coupled receptor kinases - GRKs**

GRKs is a family of protein kinases responsible for the first step in GPCR signaling termination. GRKs recognize active GPCRs and mediate multisite phosphorylation of serine/threonine residues within the receptor's third intracellular loop and C-tail. While kinases of the GRK family share several features, including common structural architecture and the ability to phosphorylate GPCRs, they are enzymes with distinct substrates and regulatory characteristics. Based on sequence homology, GRKs can be further divided into three subfamilies: GRK1/7, GRK2/3, and GRK4 subfamily containing GRK4, GRK5, and GRK6.

The underlying structure of the GRK family is highly conserved and consists of a short N-terminal  $\alpha$ -helical domain, a regulator of G protein signaling homology domain (RH domain), a catalytic domain responsible for kinase activity, and a variable C-terminal domain unique for each subfamily of GRKs (Homan & Tesmer, 2014; Siderovski, Hessel, Chung, Mak, & Tyers, 1996) (Fig. 3). The C-terminal domain is responsible for cellular localization of GRKs as well as ligand-induced translocation to cytoplasmic membrane by interaction with lipids and membrane-bound proteins (Penela et al., 2006; Pitcher et al., 1992). GRKs exist in two distinct forms: open catalytically inactive conformation and closed catalytically active conformation. During the inactive state, GRKs are localized in the cytosol with a catalytic domain inserted into the RH domain, forming an open conformation. After the activation of GPCR, GRKs translocate to the cytoplasmic membrane while undergoing a conformation change. The catalytic domain is liberated from the association with the RH domain, and  $\alpha$ N-helix stabilizes the catalytic domain closure forming and kinase-active state (Boguth, Singh, Huang, & Tesmer, 2010; Singh, Wang, Maeda, Palczewski, & Tesmer, 2008).

Besides the canonical function of GRKs in receptor desensitization, these kinases have a more complex role in terms of the regulation of cell signaling and physiological processes. Using different biochemical methods and yeast two-hybrid screens, it has been shown that the GRK substrates and interaction partners are not confined only to GPCRs, but include molecules like PI3K, MEK, AKT, RKIP, calmodulin, clathrin, and caveolin, actin, heat shock protein 90 or G protein subunits  $G\beta\gamma$  (Cant & Pitcher, 2005; Carman, Lisanti, & Benovic, 1999; Freeman, De La Cruz, Pollard, Lefkowitz, & Pitcher, 1998; Luo & Benovic, 2003; Pitcher et al., 1992; Pronin, Satpaev, Slepak, & Benovic, 1997; Shiina et al., 2001). Such a broad interactome of GRKs points to the ability of these kinases to modulate broad spectra of cellular signaling. However, the ability of GRKs to modulate signaling is not restricted only to their kinase activity, but these enzymes can modify the cellular response in a phosphorylation-independent manner as well. For instance, it has been shown that GRK2/3 are able to sequester  $G\beta\gamma$  subunits of G proteins, thus hindering the interaction of this dimer with its downstream signaling partners (Lodowski, Pitcher, Capel, Lefkowitz, & Tesmer, 2003). While GRKs represent a crucial class of GPCR modulators, the full physiological impact of interactions of these kinases remains to be elucidated.



**Figure 3. The general structure of GRKs.** The structure of the GRK kinase family consists of  $\alpha$ N-helix that helps regulate the kinases by bridging N and C lobes of the catalytic domain, RH domain that is essential for switching the conformational state of kinases between close – inactive form and open–active form, catalytic domain responsible for kinase activity, and C-terminal domain with distinct role based on the GRK subfamily.

### 1.2.10. Arrestins

Arrestins are a small family of scaffold proteins important for regulation of GPCR signal transduction. This family consists of four molecules: arrestin1, arrestin2 (also known as  $\beta$ -arrestin1), arrestin3 (known as  $\beta$ -arrestin2), and arrestin4. Two of them, arrestin1 and arrestin4, are known as visual arrestins as they are uniquely expressed in the rods of retinal tissue, where they regulate GPCR-driven visual perception, while  $\beta$ -arrestin1 and  $\beta$ -arrestin2 are almost ubiquitously expressed in all tissues (Murakami, Yajima, Sakuma, McLaren, & Inana, 1993; Premont & Gainetdinov, 2007).

Arrestins facilitate GPCR signal attenuation by two complementary mechanisms: receptor sequestration and desensitization. G proteins, GRKs, and arrestins compete for the binding site of the activated GPCR. Once kinases phosphorylate a receptor, arrestins are recruited to GPCR. By binding to phosphorylated GPCR, arrestins directly uncouple GPCR from their cognate G protein, thus sterically blocking their further interaction and subsequent signaling (Moore, Milano, & Benovic, 2007).

Besides the key role of arrestins in the desensitization of GPCRs, these proteins are also involved in the process of receptor internalization via the clathrin pathway. Arrestins act as molecular scaffolds, mediating the association of GPCR and proteins involved in clathrin endocytic machinery. Arrestins recruited to GPCR promote the interaction with adaptins (the AP-2 complex), and clathrin, proteins responsible for the internalization of the receptor (Goodman et al., 1996; Laporte et al., 1999). GPCR internalization reduces the number of receptors present on the cellular membrane available for ligand stimulation. Depending on the affinity between the arrestins and the phosphorylated receptors, upon the endocytosis of GPCR, arrestins may dissociate from the receptor or can remain bound to the

receptor as the complex transits through intracellular vesicular compartments (Luttrell & Lefkowitz, 2002).

Beyond the arrestins' roles in GPCR desensitization and internalization, arrestins also regulate multiple signaling processes. Besides serving as molecular scaffolds for endocytic machinery, the interactome of arrestins consists of many proteins involved in intracellular signaling cascades as calmodulin, tubulin, tyrosine kinases of Src family, Mitogen-Activated Protein Kinases (MAPKs), Extracellular signal-regulated kinases 1 and 2 (ERK1/2) or c-Jun N-terminal kinases (JNKs) (Peterson & Luttrell, 2017). Interestingly, the signaling events linked to arrestins are not confined to the plasma membrane but can continue from endosomes of internalized receptor-arrestins complexes (Rozenfeld & Devi, 2008). Arrestins' function as signaling facilitators is dependent on several factors like the type of receptor, ligand, and cellular environment.

Arrestin recruitment to the activated GPCR is not a straightforward process with a single binding outcome. Distinct GPCR phosphorylation patterns mediated by GRKs induce different arrestin conformations with diverse consequences (Sente et al., 2018; Yang et al., 2015). A particular phosphorylation pattern of the receptor can modify the arrestin conformation state in a way that the binding sites for the downstream proteins are exposed while the binding sites for the proteins of clathrin machinery remain masked (Latorraca et al., 2020). In such a case, the receptor would be desensitized but would not be able to be internalized, thus potentially prolonging the arrestin-mediated signaling. Moreover, Ngyuen and colleagues identified an arrestin conformation that induces the interaction that permits the stimulation of G protein signaling while the receptor is being internalized by arrestin (A. H. Nguyen et al., 2019). Furthermore, in the absence of C-terminal phosphorylation, some receptors can recruit arrestins in a unique conformation, further adjusting their functionality and signaling outcomes (Haider et al., 2022). Therefore, modifying the arrestin conformation state presents a promising therapeutic target for modifying GPCR signaling pathways.

### **1.2.11. GPCR internalization**

Desensitization of GPCRs ultimately leads to receptor internalization (endocytosis). However, receptor endocytosis is not used only for a signal termination of ligand-activated receptors but also for a reduction of the population of surface receptors in the process of receptor downregulation. This process has a profound implication for cellular signaling, as

it decreases the number of receptors available for ligand binding, or decreasing expression of the receptor, thus modifying the potency of the signaling response and cellular sensitivity to a molecule. Downregulation is usually a result of prolonged chronic exposure to a particular ligand or an excessive amount of a ligand.

Receptors can be internalized via multiple endocytic pathways, the activation of which depends on several variables like receptor, cellular context, or environmental conditions (Johannes, Parton, Bassereau, & Mayor, 2015). These mechanics include clathrin-mediated endocytosis, caveolae-dependent endocytosis, and nonclathrin/noncaveolae endocytosis. Of these, clathrin-mediated endocytosis (CME) is the best-characterized pathway.

### **1.2.12. Clathrin-mediated endocytosis**

Clathrin-mediated endocytosis (CME) is an evolutionarily conserved mechanism that plays an essential role in cellular interactions as well as signaling and homeostasis. CME is characterized by the formation of a partially invaginated membrane structure with a clathrin-coated cytoplasmic surface, followed by the scission of the invaginated clathrin-coated vesicles by the GTPase dynamin. This process can be divided into four stages: initiation, growth, scission, and internalization, followed by uncoating (Fig. 4).

Upon ligand binding to a receptor, GRKs phosphorylate the C-terminus of the receptor, followed by arrestin binding. This recruitment induces a conformational change in arrestin that exposes its binding motif for the  $\beta$ 2-adaptin subunit of the Adaptor protein complex 2 (AP-2), which leads the receptor-arrestin complexes into maturing clathrin-coated pits (CCPs) (Laporte, Oakley, Holt, Barak, & Caron, 2000). During this process, AP-2 undergoes a conformational change that allows interaction with an array of CME accessory proteins like clathrin, epsin, EGFR pathway substrate 15 (EPS15), amphiphysin, intersectin and FCH domain only 1/2 (FCHO1/2) (Taylor, Perrais, & Merrifield, 2011). AP-2 thus serves as a protein scaffold that concentrates the CME-related proteins to form a nucleation module that marks the membrane for clathrin binding and subsequent vesicle formation. The nucleation module's formation depends on the activity of proteins that bend the membrane such as FCHO1/2, EPS15, or intersectins, as their depletion inhibits the formation of CCP (Henne et al., 2010; Stimpson, Toret, Cheng, Pauly, & Drubin, 2009).

As the membrane starts to curve, clathrin proteins are recruited by AP-2. Consequently, clathrin molecules start polymerizing, stabilizing the membrane curvature and clathrin-coated vesicle assembly (McMahon & Boucrot, 2011).

The forming vesicles are separated from the membrane in the process of scission. This process is catalyzed by GTPase molecule dynamin, which localizes to the neck of CCP. The activity of dynamin constricts the neck of the membrane, ultimately leading to the fission of the vesicle (Antonny et al., 2016). Dynamin is essential not only for the CME but also for caveolae-mediated endocytosis as the pharmacological inhibitors and dominant-negative mutations like DynK44A lead to the inhibition of both endocytic pathways (Henley, Krueger, Oswald, & McNiven, 1998; van der Blik et al., 1993).

After the receptors-containing vesicles are released from the membrane, the clathrin coat is disassembled, and the vesicles are transported and fused with early endosomes, where they are subjected to one of the two trafficking pathways: either the receptors are dephosphorylated and recycled back to the plasma membrane, or they are directed for degradation in lysosomes (Calebiro & Godbole, 2018).

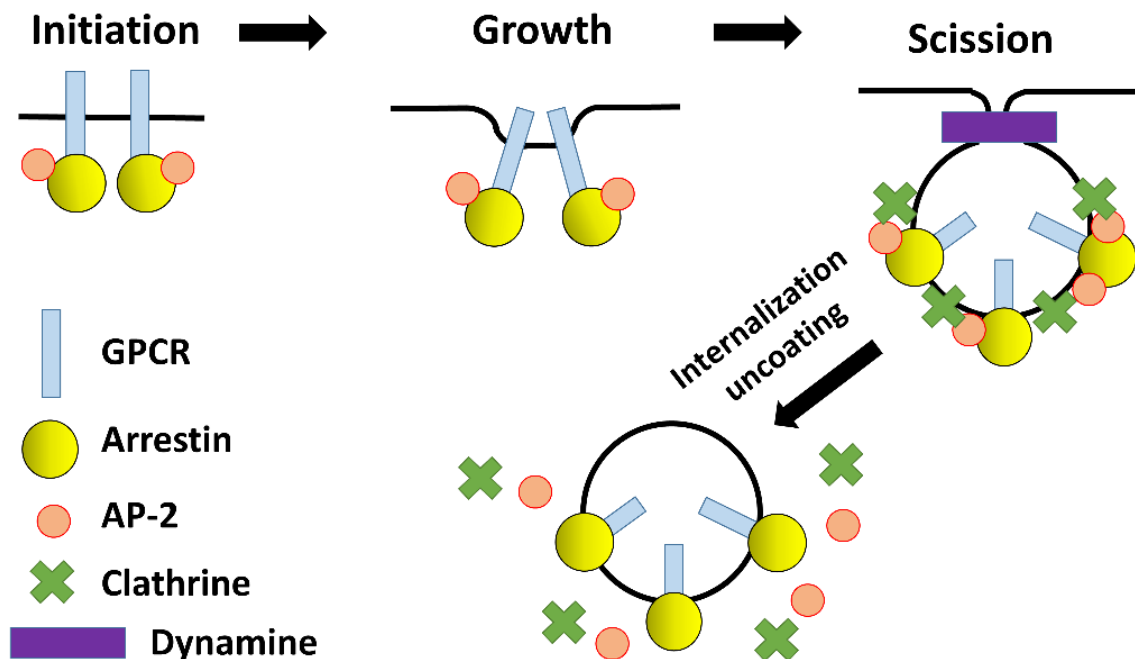


**Figure 4. Model of CCP formation.** Initiation of the formation of CCP starts with the binding of AP-2 to receptor-arrestin complex followed by recruitment of CME accessory proteins (not shown) and clathrin to the site of nucleation. Invagination of CCP requires further CME machinery proteins like FCHO2. Growth of the CCP involves the recruitment of more clathrin and AP-2 molecules as well as endocytic accessory proteins (not shown). Receptor-arrestin complexes accumulate in CCPs via arrestin interaction with clathrin and

AP-2, which additionally stabilizes growing vesicles. Scission of vesicles is performed by dynamin and is followed by the release of AP-2 and clathrin molecules from the internalized vesicles (uncoating).

### **1.3. Endocannabinoid system**

The endocannabinoid system (ECS) is a complex signaling system and an important regulator of synaptic plasticity that plays a crucial role in many functions of the central nervous system (CNS), including neuroprotection and neurogenesis, pain modulation, memory, emotions, but also in physiological processes like appetite and metabolism, immunity, cellular respiration or fertility (Ligresti, Petrosino, & Di Marzo, 2009; Maccarrone, Dainese, & Oddi, 2010). Given the vital role of ECS in many physiological functions, dysregulation of this system is linked with many pathological conditions such as neurodegeneration, epilepsy, stroke, cancer, immune system diseases, inflammation, cardiovascular diseases, diabetes, and obesity (Giacobbe, Marrocu, Di Benedetto, Pariante, & Borsini, 2021; Ilyasov, Milligan, Pharr, & Howlett, 2018; Schulz et al., 2021). ECS consists of cannabinoid receptors, their endogenous lipid ligands called endocannabinoids (eCBs), and enzymes responsible for their synthesis and degradation.

#### **1.3.1. Endocannabinoids**

Endocannabinoids are endogenous signaling lipids that activate cannabinoid receptors. From a chemical perspective, eCBs are derivatives of arachidonic acid often conjugated with ethanolamine or glycerol. The most studied and characterized are N-arachidonylethanolamine, also known as anandamide (AEA), and 2-arachidonoylglycerol (2-AG), yet the family of eCBs also includes molecules like virodhamine and N-arachidonoyldopamine, oleoylethanolamine, palmitoylethanolamine or oleoylglycerol (Grabiec & Dehghani, 2017; Katona & Freund, 2012; Porter et al., 2002; Stella, Schweitzer, & Piomelli, 1997; Sugiura et al., 1995) (Fig. 5).

Although AEA and 2-AG show structural similarity, these molecules have different physiological roles and are synthesized and degraded by distinct enzymatic pathways. 2-AG is a metabolic intermediate in the  $C\beta$ -diacylglycerol lipase pathway, while AEA is a product of the cleavage of membrane phospholipids N-acylphosphatidylethanolamines (Ueda & Tsuboi, 2012). AEA is a partial agonist of two central ECS receptors, cannabinoid receptor 1 (CB1R) and cannabinoid receptor 2 (CB2R), while 2-AG is a full agonist of both (Sugiura,

Kishimoto, Oka, & Gokoh, 2006). Furthermore, the concentration of 2-AG in the mouse brain is 170-fold higher than that of AEA (Stella et al., 1997).

The distinct feature of endocannabinoids, which separates this class of neurotransmitters from the others, is the mechanism of their synthesis. Unlike classic neurotransmitters that are synthesized and stored in the vesicles until their release into the synaptic cleft, eCBs exist in the form of precursors in the membrane and are liberated by the enzymatic activity of lipases “on demand”. After eCBs are synthesized, they are released into extracellular space where they reach presynaptic terminals presumably via molecular carrier proteins fatty acid-binding protein 5, albumins and lipocalins, or eCBs target cannabinoid receptors in the same cells they were formed through diffusion within the cellular membrane (Fauzan et al., 2022; Piomelli, 2003). The termination of eCBs signaling is mediated via the degradation of these molecules by two specific enzymatic systems: the monoacylglycerol lipases (MAGL) and the fatty acid amide hydrolases (FAAH). 2-AG is degraded by MAGL into arachidonic acid and glycerol, while FAAH hydrolyzes AEA into free arachidonic acid and ethanolamine (Cravatt et al., 1996; Dinh et al., 2002).

### **1.3.2. Phytocannabinoids and synthetic cannabinoids**

Besides the eCBs, another group of cannabinoids, called phytocannabinoids, originates from the flowering plants of *Cannabis sativa L.* of the family *Cannabaceae*. Cannabis has been used for thousands of years in traditional medicine and recreational purposes due to its sedative, analgesic, anti-spasmodic, anti-inflammatory, and anti-convulsant effects (Reekie, Scott, & Kassiou, 2018). The aforementioned effects of Cannabis are due to the content of phytocannabinoids that profoundly impact ECS. So far, there have been identified and isolated more than 113 different phytocannabinoids from *C. sativa*. The most abundant and characterized are cannabidiol (CBD) and psychoactive (–)-trans- $\Delta^9$ -tetrahydrocannabinol (THC) (ElSohly & Slade, 2005) (Fig. 5). Currently, phytocannabinoids are extensively studied for their possible therapeutic use.

Since the description of the structure of THC in early 1960, synthetic cannabinoids have been developed to pharmacologically manipulate ECS. While several studies of synthetic cannabinoids have shown that they do not appear to feature therapeutic effects without severe side effects, this group of compounds presents an important pharmacological tool for studying cannabinoid receptors (De Luca & Fattore, 2018). The most used synthetic

cannabinoids in ECS research include CB1R full agonist WIN 55,212-2 (WIN), CB1R antagonist SR-141716A (also known as rimonabant), and CB1R/CB2R full agonist CP 55,940.

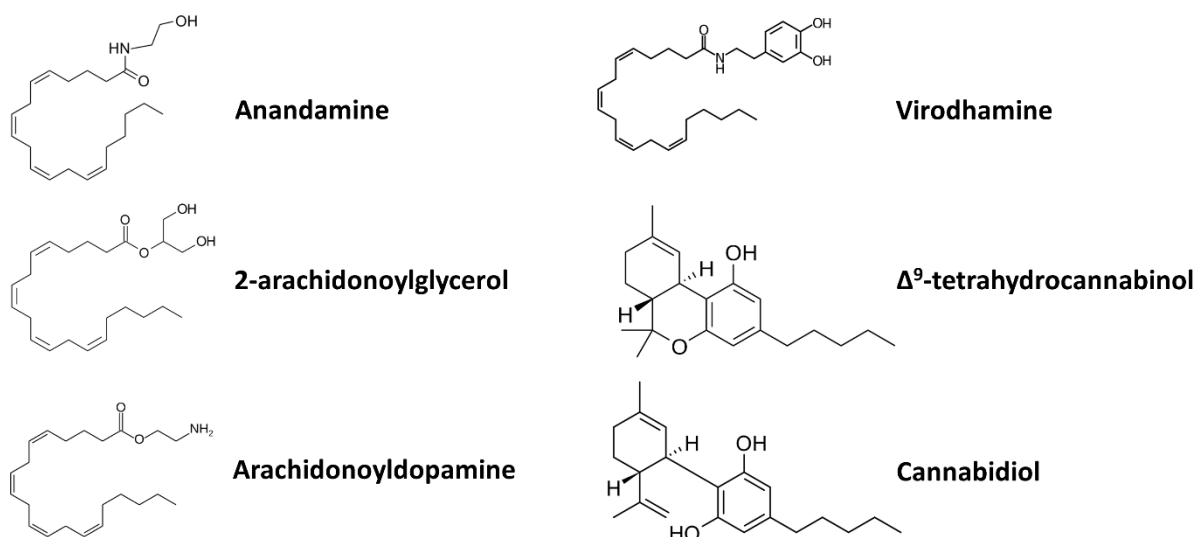


**Figure 5. Chemical structure of selected cannabinoids.** Anandamide, 2-arachidonoylglycerol, arachidonoyldopamine, and virodhamine are endocannabinoids naturally occurring in animal bodies.  $\Delta^9$ -tetrahydrocannabinol and cannabidiol belong to the group of phytocannabinoids, compounds synthesized by the plant *Cannabis sativa L.*

### 1.3.3. Cannabinoid receptors

Cannabinoid receptors, belonging to class A of GPCR receptors, are activated by eCBs, phytocannabinoids, and synthetic cannabinoids. This family consists of CB1R, CB2R, Transient receptor potential cation channel subfamily V member 1 (TRPV1), Peroxisome proliferator-activated receptors  $\alpha$  and  $\gamma$  (PPAR $\alpha$  and PPAR $\gamma$ ), and two orphan receptors GPR55 and GPR18.

The best-characterized receptors of this class are CB1R and CB2R. While these receptors show only 44% protein sequence similarity, they both share several key features, including preferential coupling to inhibitory G proteins, stimulation of MAPK and G protein-coupled inwardly rectifying potassium channels (GIRKs), inhibition of adenylyl cyclase, and specific voltage-sensitive calcium channels (Howlett et al., 2002; Munro, Thomas, & Abushaar, 1993). Despite sharing specific characteristics, these receptors are distinct in both function and localization. CB1R is primarily expressed in CNS, but to a lower extent also in skin, liver, or adipose tissue. On the other hand, CB2R is mainly expressed in immune cells including microglia, spleen, cardiovascular system, reproductive and digestive system, and

to a lower extent in CNS, particularly during pathological states (Atwood & Mackie, 2010; Zou & Kumar, 2018).

TRPV1 is found in GABAergic and glutamatergic terminals and neural somata in hippocampus and cerebellum, where it increases the excitability of central neurons and regulates memory, food intake, visual development, locomotion, mood, especially long-term depression and fear (Cristino et al., 2006; Cristino et al., 2008; Edwards, 2014). This receptor is also expressed in dorsal root ganglia, where is involved in pain processing (Caterina et al., 1997).

PPAR $\alpha$  and PPAR $\gamma$  are localized in neurons, astrocytes, and microglia in the brain, where they exert neuroprotective and anti-inflammatory effects during neuroinflammatory pathologies like ischemia, brain trauma, Alzheimer's disease and multiple sclerosis (Villapol, 2018).

The function of GPR55 as an ECS receptor remains elusive. However, research suggests that its activation by eCBs stimulates excitatory hippocampal neurons and can play a role in epilepsy or other neuropathies linked to glutamate excitotoxicity (Kaplan, Stella, Catterall, & Westenbroek, 2017; Sylantsev, Jensen, Ross, & Rusakov, 2013). It is proposed, that antiepileptic properties of CBD are due to antagonism of GRP55 (Gray & Whalley, 2020).

The role of GPR18 is also unclear. However, as is expressed in microglia, it is suggested that this receptor plays a role in neuroinflammation (Penumarti & Abdel-Rahman, 2014).

#### **1.3.4. Cannabinoid receptor 1**

Cannabinoid receptor 1 is the principal constituent of the ECS and one of the most abundant metabotropic receptors in the brain (Herkenham et al., 1991). CB1R is expressed in all brain compartments that are important for the processing of anxiety, fear, stress, cognitive and motoric functions, namely basal ganglia, hippocampus, cerebellum, prefrontal cortex and amygdala (Herkenham et al., 1990) (Fig. 6).

Neuron-wise, CB1R is located in the presynaptic area of GABAergic interneurons, glutamatergic, cholinergic, serotonergic, and noradrenergic neurons, where it serves as a crucial retrograde messenger that suppress neurotransmitter release (Haring, Marsicano,

Lutz, & Monory, 2007; Kirilly, Hunyady, & Bagdy, 2013; Marsicano & Lutz, 1999). Besides the neurons, CB1R in CNS is also expressed in astrocytes, microglia, and oligodendrocytes, where it facilitates synaptic transmission, metabolism of glucose, and the release of inflammatory molecules (Castillo, Younts, Chavez, & Hashimoto, 2012; Jimenez-Blasco et al., 2020).

In addition to the CNS, CB1R receptor is also present in the peripheral nervous system, as well as in tissues like skeletal muscle, bone, skin, eye, adipose tissue and reproductive system (Maccarrone et al., 2015). Being a member of GPCR, CB1R is primarily localized in the cellular membrane. However, a small pool of CB1Rs is also located in the outer mitochondrial membrane, where it affects the electron transport and respiratory chain, ultimately modifying the brain metabolism and formation of memories (Hebert-Chatelain & Marsicano, 2017).

Given the broad distribution in the body, CB1R modulates a vast spectrum of physiological functions. The eCB, including CB1R, is involved in the processes like appetite stimulation, energy balance and metabolism, learning and memory, pain, neurogenesis and neuroprotection, embryogenesis, and immune response, but also in pathological conditions including schizophrenia, multiple sclerosis, anxiety, depression, epilepsy, Parkinson's disease, Huntington's disease, Alzheimer's disease, addiction, stroke, inflammation, glaucoma, cancer, musculoskeletal and liver disorders (Joshi & Onaivi, 2019; Zou & Kumar, 2018).

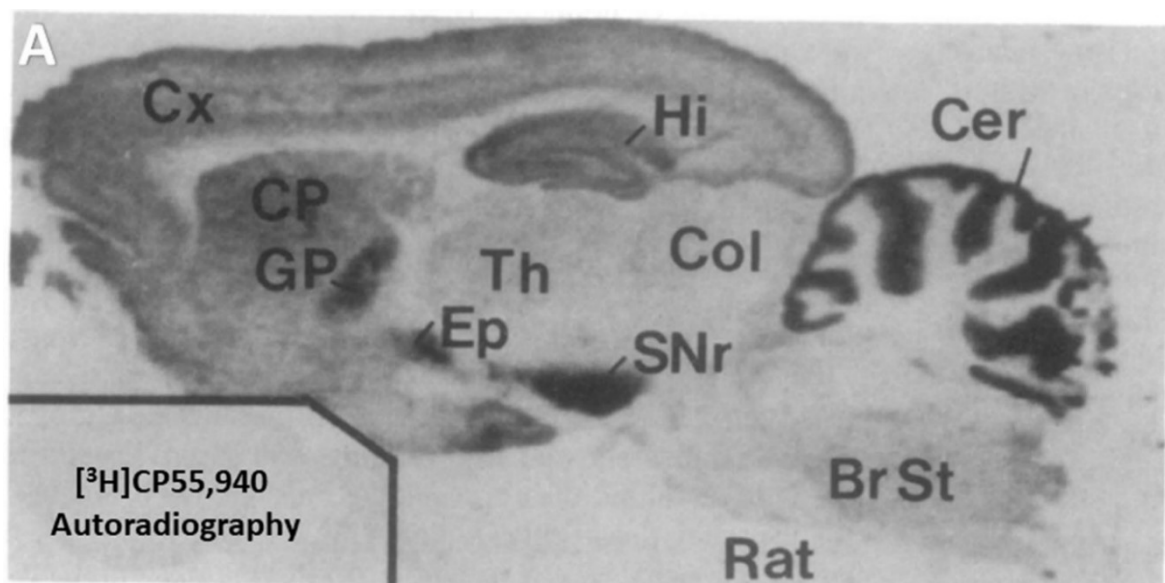


**Figure 6. CB1R distribution in rat brain.** Autoradiography image of CB1R agonist [<sup>35</sup>H]CP55,940 binding shows a CB1R localization in rat brain. Cer - cerebellum, Col - colliculi, CP - caudate-putamen, Cx - Cortex, Ep - entopeduncular nucleus, GP - globus pallidus, Hi - hippocampus, SNr - substantia nigra pars reticulata, Th - thalamus, Br St – Brain stem (Herkenham et al., 1990).

### 1.3.5. Cannabinoid receptor 1 structure

In humans, CB1R is encoded by the gene CNR1 located on chromosome 6. The full human CB1R protein sequence consists of 472 amino acids. However, two splice isoforms differing at the N-terminus hCB1a and hCB1b have been identified (Ryberg et al., 2005; Shire et al., 1995).

Crystallography studies showed that CB1R shares all characteristics of the GPCR receptor family described in the chapter “1.2. G protein-coupled receptors” (Hua et al., 2017; Shao et al., 2016). Interestingly, only crystal structures of CB1R in complexes with synthetic cannabinoids have been published. At the time of writing this thesis, the crystal structure of CB1R in the presence of phytocannabinoid remains unresolved.

Besides having an orthosteric ligand-binding site, CB1R also features an allosteric modulatory binding site (T. Nguyen et al., 2017). However, *In silico* study predicted that CB1R can have as many as three distinct allosteric sites, presenting a potential to pharmacologically modulate the activity of this receptor (Sabatucci, Tortolani, Dainese, & Maccarrone, 2018).

### 1.3.6. Cannabinoid receptor 1 signaling

Activation of CB1R affects a plethora of cellular signaling cascades with distinct outcomes mediated by a broad spectrum of intracellular effector proteins. CB1R signaling is mediated by G proteins and arrestins (Nogueras-Ortiz & Yudowski, 2016). The signaling begins with the activation of CB1R resulting in G proteins activation, followed by signaling mediated by arrestins. The signal transduction culminates in the signaling originating from the intracellular compartments, namely endosomes.

As a member of GPCRs class of receptors, CB1R activates G protein signaling cascades. CB1R couples to  $G\alpha_{i/o}$ , thereby the activation of this receptor induces a cascade of signaling pathways that inhibit adenylyl cyclase, thus reducing the levels of intracellular

cyclic adenosine triphosphate (cAMP) and decreasing the activity of PKA, consequently suppressing PKA-dependent signaling molecules. On the other hand, dissociated G $\beta\gamma$  subunits inhibit voltage-dependent calcium channels, activate GIRKs, as well as induce phosphoinositol 3-kinase (PI3K) and protein kinase B (PKB) pathways, consequently phosphorylating and activating MAPK (Turu & Hunyady, 2010).

The signaling is also mediated by arrestins that are recruited to the activated and phosphorylated CB1R. Arrestins serve as a scaffold for binding a plethora of signaling molecules (discussed in the chapter “1.2.10. Arrestins”), leading to the activation of ERK1/2 and Src signaling pathways (Peterson & Luttrell, 2017).

The signaling can further arise from the receptors present in the endosomes and lysosomes. Following the agonist-induced binding of arrestin to CB1R, the receptor is rapidly internalized and translocated into endosomes, where the stimulation of ERK1/2 pathways occurs, presumably via effectors of both arrestins and G proteins (Nogueras-Ortiz & Yudowski, 2016).

While most studies associate CB1R signaling with plasma membrane, accumulating evidence suggests that CB1R features a large intracellular pool, particularly enriched in the endosomal system and mitochondria (Grimsey, Graham, Dragunow, & Glass, 2010). When HEK293 cells expressing CB1R were intracellularly injected with anandamide, Ca<sup>2+</sup> release from the endoplasmic reticulum and lysosomal calcium stores was observed (Brailoiu, Oprea, Zhao, Abood, & Brailoiu, 2011). In addition, activation of mitochondrial CB1Rs lead to altered enzymatic activity and respiration in neuronal mitochondria (Benard et al., 2012). These findings show that the intracellular CB1R is also involved in cell signaling.

### **1.3.7. Cannabinoid receptor 1 biased signaling**

Distinct ligands can induce and stabilize different conformations of a given GPCR. Consequently, these conformations could preferentially activate a particular signaling cascade over others, in a phenomenon called „biased signaling“. The ligands capable of selectively activating either G protein or arrestin pathway are called biased ligands. In addition, a biased ligand can be an agonist for one signaling cascade and simultaneously an inverse agonist or antagonist for the other signaling cascade. The phenomenon of biased signaling has profound consequences on pharmacology and drug discovery of GPCRs, including cannabinoid receptors.

Several instances of CB1R-biased signaling have been observed and described. As mentioned in chapter “1.3.6. Cannabinoid receptor 1 signaling”, CB1R preferentially couples to  $G\alpha_{i/o}$ . However, depending on the cellular context, protein expression profile, and ligand, CB1R can couple to different  $G\alpha$  (Busquets-Garcia, Bains, & Marsicano, 2018). Stimulation of CB1R with synthetic cannabinoid WIN leads to coupling of  $G\alpha_q$  to the activated receptor, while stimulation with CP55,940 leads to preferential coupling to  $G\alpha_s$  (Laprairie, Bagher, Kelly, & Denovan-Wright, 2016; Lauckner, Hille, & Mackie, 2005). Certain cannabinoids can favor G protein over the arrestin pathway, as in the case of novel compounds PNR-4-20 and PNR-4-02 that selectively activate the  $G\alpha_i$  pathway while significantly inhibiting  $\beta$ -arrestin2 recruitment (Ford et al., 2017). On the other hand, allosteric modulator ORG27569 induces a CB1R conformation state that selectively activates the ERK1/2 cascade via  $\beta$ -arrestin1 (Ahn, Mahmoud, & Kendall, 2012).

CB1R biased signaling is not limited to the effect of ligands and allosteric modulators. Interaction partners of CB1R also play an essential role in the modulation of signaling. For instance, the presence of SH3-containing GRB2-like protein 3-interacting protein 1 (SGIP1) attenuates CB1R-driven ERK1/2 phosphorylation while leaving G protein signaling intact (Hajkova et al., 2016). Contrary, cannabinoid receptor interacting protein 1a (CRIP1a) modifies G protein-driven cAMP levels and ERK1/2 phosphorylation via changing  $G\alpha_{i/o}$  subtypes that CB1R couples to (Blume et al., 2016). In addition, CB1R can form dimers with dopamine receptor 2, and stimulation of these heterodimeric receptors activates the  $G\alpha_s$  pathway leading to the increase of cAMP, thus generating the opposite outcome of CB1R homodimer activation (Jarrahian, Watts, & Barker, 2004).

Cannabinoid receptor 1 and ECS in general have been an interesting area of research due to its therapeutic potential. However, the medical application has been considerably limited due to the pleiotropic nature of ECS. Accordingly, the biased signaling thus represents an attractive target to limit unwanted side effects of future therapies based on ECS.

### **1.3.8. Cannabinoid receptor 1 desensitization and internalization**

Given the vital role of CB1R in various physiological processes including fine-tuning of synaptic transmission, this receptor's activity must be tightly regulated. Attenuation of CB1R signaling follows a common path for GPCRs. Upon the activation of CB1R, the C-

terminal tail is phosphorylated by GRKs, followed by recruitment of arrestins, which sterically prevent receptor activation of signaling effectors, and the receptor is subsequently internalized (Jin et al., 1999; Kouznetsova, Kelley, Shen, & Thayer, 2002; Morgan et al., 2014; Straiker, Wager-Miller, & Mackie, 2012).

Several studies have shed light on the molecular mechanism underlying the desensitization of CB1R. These studies suggest that GRKs and  $\beta$ -arrestins play a central role in agonist-induced CB1R desensitization. Desensitization of CB1R expressed in *Xenopus* oocytes was shown to be dependent on the coexpression of both GRK3 and  $\beta$ -arrestin2 (Jin et al., 1999). Expression of dominant negative GRK or dominant negative  $\beta$ -arrestin2 inhibited desensitization of CB1R at the synapses of rat hippocampal neurons (Kouznetsova et al., 2002). Another demonstration of  $\beta$ -arrestin2 as a central molecule in CB1R desensitization was observed in HEK293 cells. CB1R mutants that were able to recruit  $\beta$ -arrestin2 did undergo desensitization and internalization, while mutants unable to interact with  $\beta$ -arrestin2 had impaired these processes (Daigle, Kwok, & Mackie, 2008). Interestingly, CB1R shows only a marginal interaction with  $\beta$ -arrestin1, suggesting a preference for  $\beta$ -arrestin2 (Ibsen, Connor, & Glass, 2017).

Following the recruitment of  $\beta$ -arrestin2, CB1R is internalized, and afterward, CB1R is either trafficked into early endosomes, where it is subsequently sorted by G protein-coupled receptor associate protein 1 (GASP1) for degradation in lysosomes (Blume et al., 2016; Grimsey et al., 2010; Martini et al., 2007), or the receptor may be recycled back to the cellular membrane, especially in case of short-term ligand stimulation, (Hsieh, Brown, Derleth, & Mackie, 1999).

### **1.3.9. Role of CB1R C-tail in the desensitization and internalization**

C-tail of CB1R consists of 73 amino acid residues (hCB1R: R400-L472, rCB1R: R401-L473) (Fig. 7 A). This region features two putative amphipathic  $\alpha$ -helical domains H8 and H9. H8 is thought to play a role in CB1R biosynthesis and assembly in the endoplasmic reticulum, while the 21-residue long helical H9 domain contributes to the delivery and stabilization of CB1R in axons (Ahn et al., 2010; Stadel et al., 2011; Fletcher-Jones et al., 2023). In addition, the deletion of H9 results in increased agonist-induced internalization and decreased downstream signaling (Fletcher-Jones et al., 2019).

Earlier studies implicated the importance of two regions within the CB1R C-tail in the desensitization and internalization of the CB1R (Blume et al., 2016; Daigle, Kearns, & Mackie, 2008; Jin et al., 1999; Morgan et al., 2014; Straiker et al., 2012). These two regions contain clusters of serine and threonine residues that are phosphorylated during CB1R desensitization and internalization. One motif is situated between residues 425 and 429, namely <sup>425</sup>SMGDS<sup>429</sup>, and another is between residues 460 and 468, <sup>460</sup>TMSVSTDTS<sup>468</sup> of human CB1R (hCB1R) (Fig. 7 B).

Previous observations showed that the mutation of two serine/threonine residues S426/S430 (rat CB1R numbering, corresponding to S425/S429 of hCB1R – Fig. 7 A) in the C-tail of rat CB1R (rCB1R) into alanines blocked GRK3/ $\beta$ -arrestin2-driven desensitization in *Xenopus* oocytes (Daigle, Kearns, et al., 2008). Another indication of the importance of serine/threonine motif in CB1R desensitization comes from the *in vivo* study of mice with alanine mutations in S426/S430 residues of CB1R. These mice showed a phenotype characterized by enhanced responses to THC and delayed development of tolerance to this phytocannabinoid (Morgan et al., 2014).

In addition, WIN-induced desensitization was obliterated in AtT-20 cells expressing CB1R mutant missing the last 55 residues (Jin et al., 1999). While serines of <sup>425</sup>SMGDS<sup>429</sup> are important for CB1R desensitization, phosphorylation of serines/threonines in <sup>460</sup>TMSVSTDTS<sup>468</sup> motif is necessary for receptor internalization. A study performed by Daigle et al. found that mutation of six serine/threonine residues in rCB1R C-tail (461-469) prevented  $\beta$ -arrestin2 recruitment and internalization (Daigle, Kwok, et al., 2008). This is also supported by the study of Straiker et al., in which the authors demonstrated that rCB1R lacking the last 13 residues or mutation of serines/threonines in 461-469 attenuated receptor desensitization (Straiker et al., 2012).

While all these observations suggest an important role of two CB1R C-terminal serine/threonine motives in the desensitization and subsequent internalization, precise roles of these two regions and their relationship with signaling molecules involved has remained unresolved.

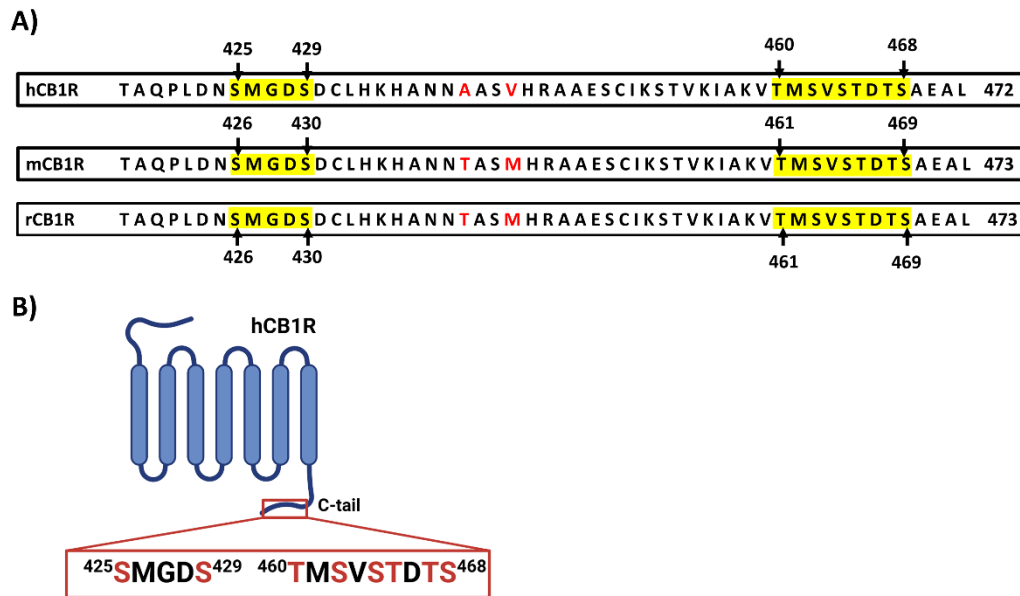


**Figure 7. CB1R C-tail is important for desensitization and internalization.** A) Aligned CB1R protein sequence from different species. In yellow are highlighted regions relevant to desensitization and internalization. hCB1R- human CB1R, mCB1R – mouse CB1R, rCB1R – rat CB1R. Different residues in sequence between human and rodents are colored in red. B) Schematic depiction of human CB1R C-tail. Two regions of CB1R encompass two regions <sup>425</sup>SMGDS<sup>429</sup> and <sup>460</sup>TMSVSTDTS<sup>468</sup>, that contain serine/threonine residues that are important for the desensitization and internalization of CB1R (marked in red).

#### 1.4. Src homology 3-domain growth factor receptor-bound 2-like (endophilin) interacting protein 1 (SGIP1)

SGIP1, as a gene linked to the regulation of energy balance, was first identified in 2005 in Israeli fat sand rat (*Psammomys obesus*) (Trevaskis et al., 2005). In the wild, Israeli fat sand rats maintain a lean phenotype due to feeding on a scarcely-available low-calorie food. However, in the laboratory setting with nutritious food *ad libidum*, *P. obesus* quickly develops metabolic syndrome, including obesity and type 2-like diabetes. Screening of mRNA levels from the hypothalamus (brain compartment linked to the control of appetite and food intake) between lean and obese individuals revealed that obese fat sand rats had elevated levels of mRNA transcripts coding for SGIP1. Upon downregulation of the levels of SGIP1 using siRNA, the food intake was attenuated, and the body weight decreased (Trevaskis et al., 2005). Moreover, human genetic studies suggest that single-nucleotide polymorphisms in SGIP1 are linked to fat mass (Cummings et al., 2012; Yako et al., 2015).

### 1.4.1. SGIP1 structure

Human SGIP1 gene is located on human chromosome 1 (Safran M, 2022). SGIP1 is mainly expressed in the brain in high concentrations and is trafficked into presynaptic boutons (Hajkova et al., 2016; Trevaskis et al., 2005; Wilhelm et al., 2014). SGIP1, together with FCHO1/2 and suppressor of yeast profilin deletion 1 (Syp1), belong to the muniscins, a family of cargo-adaptor proteins involved in CME (Hollopeter et al., 2014) (Fig. 8). The unique feature of SGIP1 that distinguishes it from its orthologues is the presence of unique membrane phospholipid (MP) domain in the place of the Fer-CIP4 homology-BAR (F-BAR) domain typical for the other muniscins (Fig. 8).

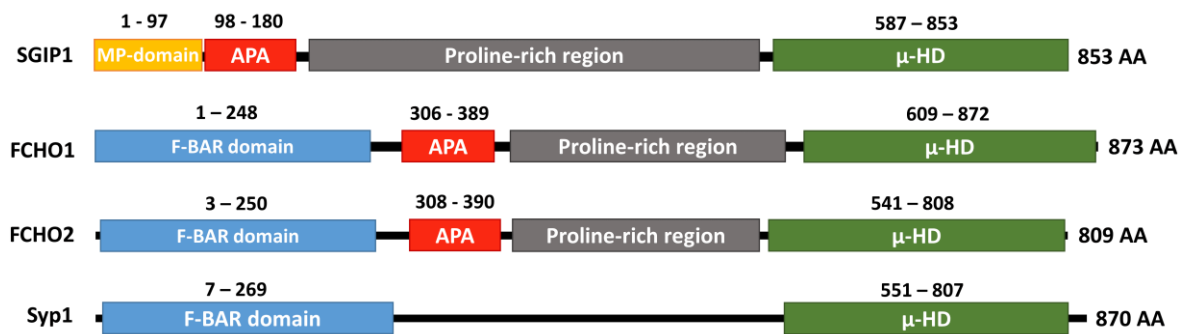


**Figure 8. Structure of proteins belonging to the muniscin family.** Unlike other members of the muniscin family, SGIP1 possesses a unique MP domain.

It was shown that the MP domain interacts with liposomes comprised of phosphatidylserine and phosphoinositides, and deforms membranes by an unknown mechanism (Uezu et al., 2007; Trevaskis et al., 2005). Nevertheless, it is conceivable that the membrane-binding mechanism employed by the MP domain is akin to that of the F-BAR domain, where the membrane binding is facilitated by a positively-charged surface generated by amino acids with positive charges (Henne et al., 2007; Lemmon, 2008). These amino acids - lysine, arginine, and histidine, are also found in the MP domain of SGIP1.

The N-terminal MP domain is followed by the AP2 activator (APA) domain, which can recruit and activate proteins of AP2 complex like  $\alpha$ - and  $\beta$ 2-adaptin subunits, causing clathrin recruitment (Hollopeter et al., 2014).

The central part of SGIP1 is comprised of a proline-rich domain (PRD), which features Src homology 3 (SH3) and Trp-Trp (WW) domain binding motives that mediate interactions with proteins involved in CME like endophilin, intersectin 1 or amphiphysin (Dergai et al., 2010; Trevaskis et al., 2005). This region also contains numerous phosphorylation sites targeted by MAP kinases, with significant physiological implications (Edbauer et al., 2009). For example, dephosphorylation of Ser-149, Ser-169, and Thr-409 was observed during nerve terminals depolarization *in vivo*, and Huntington's disease mice displayed an excessive degree of phosphorylation in SGIP1 (Munton et al., 2007; Craft et al., 2008; Mees et al., 2022).

The final part of SGIP1 consists of the C-terminal  $\mu$  homology domain ( $\mu$ HD), a protein motif highly conserved in muniscins, which facilitates interactions with endocytic adaptors and other proteins involved in clathrin-mediated endocytosis like Eps15 (Uezu et al., 2007).

#### **1.4.2. SGIP1 and CB1R**

Several studies suggested that both SGIP1 and CB1R are involved in the control of energy balance (Di Marzo & Matias, 2005; Hao, Avraham, Mechoulam, & Berry, 2000; Rowland, Mukherjee, & Robertson, 2001; Trevaskis et al., 2005; Williams & Kirkham, 1999). In our laboratory, we detected the association of SGIP1 and CB1R using a yeast two-hybrid system. The extreme C-terminal portion of CB1R following the eighth intracellular alpha-helix of CB1R was used as bait, and, among others, SGIP1 fragment of 99 amino acids was detected (Hajkova et al., 2016). This interaction of CB1R and SGIP1 was further confirmed by co-immunoprecipitation and bioluminescence resonance energy transfer (BRET) assay (Hajkova et al., 2016). In addition, both SGIP1 and CB1R co-localize in cultured cortical neurons with presynaptic marker bassoon (Hajkova et al., 2016).

Functional assays revealed the consequences of SGIP1 on CB1R signaling. The presence of SGIP1 significantly attenuates ligand-induced internalization in transfected human embryonic kidney cells (HEK293) cells (Hajkova et al., 2016). On top of that, SGIP1 affects CB1R signaling in the biased manner: it augments  $\beta$ -arrestin2 interaction with CB1R, decreases ERK1/2 phosphorylation while leaving Gi/o-protein activation and  $\text{Ca}^{2+}$  release unmodified (Hajkova et al., 2016).

The impact of SGIP1 on CB1R signaling was also shown to have *in vivo* consequences. SGIP1 knock-out mice showed an anxiolytic-like phenotype, altered nociception, increased sensitivity to THC and morphine, and prolonged tolerance development while leaving cognitive and motor skills intact (Dvorakova et al., 2021).

### 1.4.3. SGIP1 splice variants

Alternative splicing often yields diverse protein splice variants from a singular gene. This phenomenon encompasses the inclusion or omission of alternative start codons, exons, and polyadenylation sites in the nascent mRNA transcript during the splicing process. The prevalence of alternative splicing is notably higher within the brain, distinguishing it from other tissues and underscoring the intricacy of signaling mechanisms within the brain (Yeo et al., 2004).

The mouse SGIP1 gene consists of 27 exons (Fig. 9 A). This gene's modality permits several potential SGIP1 splicing variants to be possible due to alternative splicing produced by the exclusion of specific exons whose omission does not change the open reading frame, creating frameshift mutation. On top of that, the regulation of SGIP1 expression and alternative splicing is further orchestrated by splicing factors like neuronal Ser-Arg-rich splicing factors 3 and 4 (Srrm3-Srrm4) (Nakano et al., 2012; Nakano et al., 2019). Srrm3-Srrm4 govern the alternative splicing of short exons that are enclosed by highly conserved intronic sequences in neural tissue pre-mRNA. The presence of Srrm3 is crucial for the inclusion of SGIP1 exon 9 and 10 in mRNA, while the Srrm3-Srrm4 regulates the incorporation of exons 9, 10, and 11 (Nakano et al., 2012; Nakano et al., 2019).

While the NCBI Gene database predicts as many as 20 possible mouse SGIP1 variants (Fig. 9 B) (NCBI, 2022), only four have been reported so far. Given the structure of SGIP1 exons, which allows deletions without frameshifting in alternative splicing-type exon-skipping, and splicing factors that regulate signal recognition during splicing, SGIP1 splice variants with distinct protein sequences may have different properties with diverse functional consequences. Indeed, the aforementioned four reported SGIP1 splice isoforms feature unique properties. The first SGIP1 variant with a length of 806 amino acids was shown to interact with CB1R and have profound effects on its signaling properties (Hajkova et al., 2016). Moreover, 854 amino acids long SGIP1 (in some studies named SGIP1 $\alpha$ ) promotes the internalization and recycling of synaptotagmin, while SGIP1 of 826 amino

acids forms complexes with calnexin and Sgip1 660 increases CB1R expression in axons (Lee, Jeong, Lee, & Chang, 2019; Li, Liu, & Michalak, 2011; Fletcher-Jones et al., 2023). In light of these observations, it is conceivable that other potential SGIP1 splice isoforms may differ in their functionality.

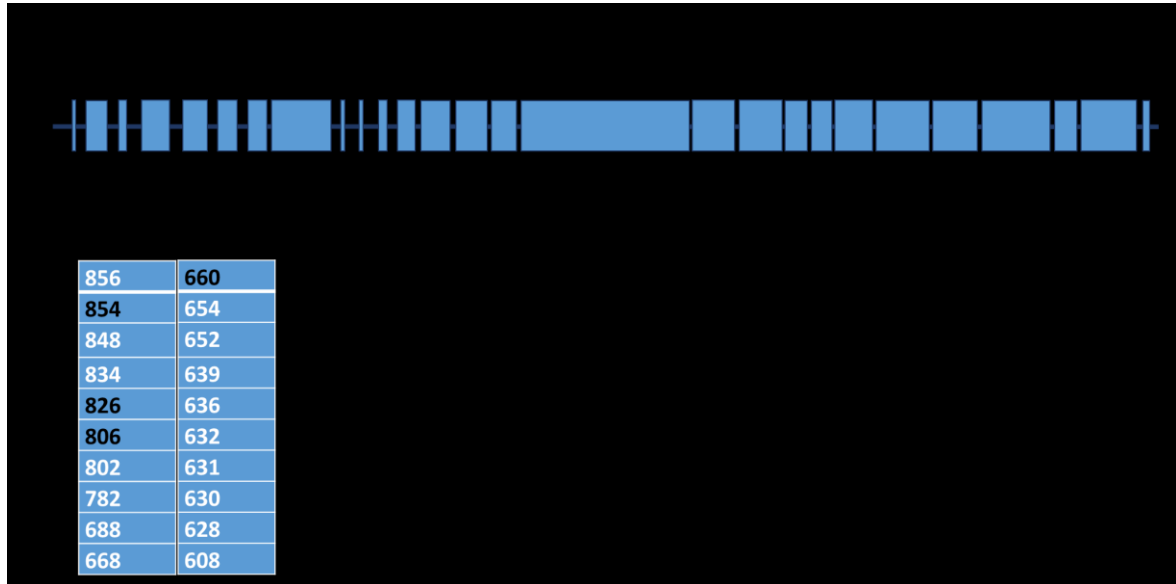


**Figure 9. Schematic depiction of SGIP1 exons.** A) SGIP1 gene consists of 27 exons. Several exons encode the number of amino acids divisible by three thus, they could be omitted during alternative splicing without changing the open reading frame. B) SGIP1 variants predicted by NCBI database. SGIP1 variants characterized in previous studies are marked in black.

## 2. Aims and hypotheses

**Hypothesis 1:** Two regions within the CB1R C-tail contain clusters of serine and threonine residues that can be phosphorylated and collectively play an essential role in the desensitization and internalization of activated CB1R. One motif is between residues 425 and 429, namely <sup>425</sup>SMGDS<sup>429</sup>, and another is between residues 460 and 468, <sup>460</sup>TMSVSTDTS<sup>468</sup>. Previous studies suggest that GRK3 and  $\beta$ -arrestin2 are molecules that play a central role in CB1R desensitization and internalization. Nevertheless, the relationship between the phosphorylation within these two sites in the recruitment of GRK3 and  $\beta$ -arrestin2 is unknown.

**Aim 1:** To investigate the role of the <sup>425</sup>SMGDS<sup>429</sup> and <sup>460</sup>TMSVSTDTS<sup>468</sup> phosphorylation sites of CB1R in the recruitment of GRK3 and  $\beta$ -arrestin2.

**Aim 2:** To characterize the role of GRK3 in facilitating interactions of molecules following activation of the CB1R as it undergoes desensitization.

**Hypothesis 2:** The dynamics of CB1R- $\beta$ -arrestin2 interaction are modified in the presence of SGIP1 (Hajkova et al., 2016). We hypothesize that interactions between CB1R, GRK3 and G proteins might be affected by SGIP1 as well.

**Aim 3:** To test the GRK3-CB1R, and GRK3-G protein interactions in the presence of SGIP1.

**Hypothesis 3:** Mouse SGIP1 is coded by 27 exons, which allow the expression of SGIP1 variants of different lengths via alternative splicing. According to the NCBI Gene database, alternative splicing can hypothetically produce 20 possible mouse SGIP1 variants. However, only four have been described so far. In our laboratory, we have identified several SGIP1 mRNA, derived from the mouse brain, coding potential novel splice variants. We hypothesize that these splice variants can differ in the ability to inhibit CB1R internalization as previously described for 806 amino acids long SGIP1 (Hajkova et al., 2016).

**Aim 4:** To analyze the detected SGIP1 splice variants by testing their expression and the effect on the CB1R internalization.

### 3. Material and methods

#### 3.1. Chemicals, enzymes and kits

	<b>Producer</b>
6x gel loading dye	NEB, USA
Acrylamide	Sigma-Aldrich, Czechia
Agarose	Sigma-Aldrich, Czechia
Ammonium persulfate	Sigma-Aldrich, Czechia
Bradford Reagent	Sigma-Aldrich, Czechia
Bromophenol blue	Sigma-Aldrich, Czechia
Coelenterazine h	NanoLight, USA
cOmplete™ Protease Inhibitor Cocktail tablet	Merck, Germany
Cmpd101	Hello Bio, Ireland
Dithiothreitol	Sigma-Aldrich, Czechia
Dimethyl sulfoxide	Sigma-Aldrich, Czechia
Dulbecco's Modified Eagle Medium	Thermo Fisher Scientific, USA
Ethidium bromide	Top Bio, Czechia
Ethanol absolute	Penta, Czechia
Fetal bovine serum	Gibco, USA
Fluorescein	Merck, Germany
GeneRuler 1 kb Plus DNA ladder	Thermo Fisher Scientific, USA
Glycerol	Sigma-Aldrich, USA
IPOne HTRF kit	Cisbio Bioassays, France
Isopropanol	Penta, Czechia
Lipofectamine™ 2000	Thermo Fisher Scientific, USA
Nitrocellulose membrane	Pall Corporation, USA
N,N'-Methylenebisacrylamide	Sigma-Aldrich, Czechia
Opti-MEM®	Thermo Fisher Scientific, USA
Polyethylenimine	Sigma-Aldrich, Czechia
Poly-l-ornithine	Merck, Germany
Powdered milk - blotting-grade	Carl Roth, Germany
QIAGEN Plasmid Midi Kit	Qiagen, Germany
QIAprep Spin Miniprep kit	Qiagen, Germany
Sodium dodecyl sulfate	Sigma-Aldrich, USA

SuperSignal West PICO chemiluminescent substrate	Thermo Fisher Scientific, USA
SNAP-Lumi4-Tb	PerkinElmer - CisBio, France
TAE	Thermo Fisher Scientific, USA
Tag-lite labeling medium	PerkinElmer - CisBio, France
Tris-HCL	Serva, Germany
Trypsin	Sigma-Aldrich, Czechia
WIN 55,212-2	Tocris, UK

### 3.2. Antibodies

	Producer
anti-actin (rabbit) - 1:500	Sigma-Aldrich, Czechia
anti-GFP (mouse) - 1:400	Roche, Switzerland
anti-mouse IgG-HRP (goat) - 1:10,000	Promega, USA
anti-rabbit IgG-HRP (goat) - 1:10,000	Promega, USA

### 3.3. Expression vectors

Expression vectors for  $G\alpha_{i1}$ -Rluc8,  $G\beta$ -Flag,  $G\gamma_2$ -YFP,  $G\alpha_{q9}$ ,  $\beta$ -arrestin2-Rluc, GRK3-Rluc8, mGluR1a-YFP were kindly provided by Laurent Prezeau (Institut de Génomique Fonctionnelle, Montpellier, France).

Mutant human CB1R variants were prepared by molecular cloning methods from the plasmid coding full-length CB1R S425A, S429A. This plasmid was kindly gifted by Ken Mackie (Indiana University, Bloomington, USA). CB1R variants were fused with either SNAP-Tag (N-terminal) or YFP (C-terminal).

SGIP1-mCherry was constructed in our laboratory from the previously characterized plasmid SGIP1-Flag (Hajkova et al., 2016) by molecular cloning methods. SGIP1 splice variants were cloned by Oleh Durydivka.

All constructs were sequenced prior to their use.

### 3.4. Laboratory devices

	Manufacturer
BioRad Trans-blot Turbo	Bio-Rad Laboratories, USA
Biorad Universal Hood II Gel Doc System	Bio-Rad Laboratories, USA
Mithras LB 940 microplate reader	Berthold Technologies, Germany

Mitre 4000 series incubator	Contherm, UK
MultiSUB horizontal gel electrophoresis	Claever scientific, UK
LAS-300 system	Fujifilm, Japan
OSP-105 power supply	Owl scientific, USA
PHERASTAR plate reader	BMG Labtechnologies, Germany
Telstar BIO II A safety cabinet	Telstar, Spain
TW12 Water bath	Julabo, USA
Ultrasonicator U50	IKA, Germany

**Software**

ImageJ  
 Microwin 2000  
 Prism GraphPad v.8  
 SnapGene

**Producer**

NIH, USA  
 Labsis, Germany  
 GraphPad Software, USA  
 GSL Biotech LLC, USA

### **3.5. Transformation of competent *E. coli***

Firstly, 50 µl aliquot of chemically competent DH $\alpha$  was thawed on ice and transferred into a sterile test tube. Next, 1 µl of circular purified DNA (or 5 µl of ligation mixture in the case of DNA cloning) was added to bacteria, mixed by gentle tube flickering, and left incubating on ice for 30 minutes. Afterward, the competent *E. coli* were heat shocked at 42°C for 45 seconds and immediately returned to ice for further 2 minute incubation. 100 µl of warm Y2T media was added to the bacterial mixture. For kanamycin-resistant plasmids, transformed bacteria were incubated for 1 hour at 37°C before plating on kanamycin-containing LB plates. In the case of ampicillin-resistant vectors, transformed *E. coli* were incubated for 30 minutes at 37°C and subsequently plated on LB plates containing ampicillin. The plates were incubated at 37°C overnight.

### **3.6. Bacterial glycerol stock**

For long-term storage of bacteria and plasmids, bacterial glycerol stocks were made. A culture of 700 µl of transformed bacteria was mixed with 300 µl sterile 50% glycerol solution and transferred into a sterile microcentrifuge tube. The tubes containing the bacterial mix were frozen at -70°C. To recover the bacteria, a sterile inoculating loop was used to scrape a small quantity of frozen bacteria mix and subsequently transferred into fresh LB media with corresponding antibacterial resistance.

### **3.7. Agarose gel electrophoresis**

DNA molecules were resolved in agarose gel electrophoresis. Gel was prepared using 1x TAE buffer with 0.5 µg/mL of ethidium bromide. The agarose concentration in gel ranged from 1% to 1.5%, based on the length of DNA fragments. The DNA samples were mixed with 6x gel loading dye and loaded into gel parallel to 5 µl of GeneRuler 1 kb Plus DNA ladder DNA molecular weight standard. The samples were run at 90V in 1x TAE buffer using OSP-105 power supply (Owl scientific, USA) and multiSUB horizontal gel electrophoresis (Claevery scientific, UK). Gels were visualized on Biorad Universal Hood II Gel Doc System (Bio-Rad Laboratories, USA).

### **3.8. DNA Mini Prep**

Single colonies were picked from the plate and used to inoculate tubes containing 2 ml LB medium with corresponding antibiotic and incubated overnight at 37°C in a shaking incubator. The following morning, the plasmids were isolated using the QIAprep Spin Miniprep kit (Qiagen, Germany) according to the manufacturer's instructions. Isolated plasmids were checked by restriction enzyme digestion and/or by DNA sequencing.

### **3.9. DNA Midi Prep**

Single colonies or bacteria from glycerol stock were used to inoculate an overnight culture in an Erlenmeyer flask containing 100 ml LB medium with corresponding antibiotic resistance. Cultures were incubated overnight at 37°C in a shaking incubator. The next day, the plasmids were isolated using the QIAGEN Plasmid Midi Kit (Qiagen, Germany) according to the manufacturer's instructions. Isolated plasmids were checked by restriction enzyme digestion and/or by DNA sequencing.

### **3.10. DNA sequencing**

Plasmids were sequenced by using the LightRun service of Eurofins Genomics Company. 400 – 500 ng of purified plasmid DNA was mixed with 25 pmol of primer and brought up to the total volume of 20 µl by adding sterile water. The sequences were analyzed using SnapGene software. Plasmids with correct sequences were either used for further experiments or amplified, and midi prepped.

### **3.11. Cell culture and transient transfection**

Human embryonic kidney 293 (HEK293) cells were grown in Dulbecco's Modified Eagle Medium containing 10% fetal bovine serum (FBS) and cultivated at 37°C, 95% humidity, and 5% CO<sub>2</sub>. HEK293 cell line was maintained by passaging every 3<sup>rd</sup> and 4<sup>th</sup> day. The split ratio used to passage cells was 1:12. Cell line was used up to the 30th passage.

For BRET assays, Lipofectamine 2000 transfection was used. Twenty-four hours before the experiment, 150 ng DNA/well was used to transiently transfect 5×10<sup>4</sup> cells/well

in 96-well plates coated with poly-l- using Lipofectamine™ 2000 according to the manufacturer's instructions.

For western blot and microscopy experiments, cells were transfected by polyethyleneimine. Briefly, 48 hours before the experiment,  $5 \times 10^6$  cells were seeded into 10 cm plates. Four hours after, cells were treated with a transfection reaction consisting of two solutions mixed together: 5 µg DNA + 500 µl OMEM and 30 µl polyethyleneimine + 500 µl OMEM.

### **3.12. Long-term storage and thawing of cell lines**

Aliquots of HEK293 cells mixed with freezing medium (DMEM + 40% FBS, 20% DMSO) were stored in liquid nitrogen. For the thawing of the new cell line, the aliquot of cells was removed from the liquid nitrogen container and transferred into dry ice. Next, the aliquot was thawed in a 37°C water bath until all the external ice melted. The aliquot was then resuspended in a small plate containing 10 ml DMEM + 10% FBS. Subsequently, the plate's content was transferred into a 15 ml Falcon tube and pelleted at 1000 RPM for 5 minutes. The supernatant was discarded, and the pellet was resuspended in 5 ml fresh media. Cells were seeded on 100 mm plates containing 10 ml of fresh media and cultivated overnight at 37°C, 95% humidity, and 5% CO<sub>2</sub>. The next day, the cells were checked and passaged if needed. HEK293 cell lines were cultivated for at least 5 passages before they were used in the experiments.

### **3.13. Bioluminescence resonance energy transfer assays**

To investigate the interactions between studied molecules, the bioluminescence resonance energy transfer (BRET) assay was used. BRET assay utilizes a phenomenon called Förster resonance energy transfer between two molecules – luciferase and yellow fluorescein protein (YFP). The bioluminescent enzyme luciferase (Rluc), delivered from *Renilla reniformis*, in the presence of substrate coelenterazine h, emits photons that are absorbed by YFP, resulting in excitation and subsequent emission of photons of different wave-length. This phenomenon occurs only when luciferase and YFP are close to each other. To study the interaction of two proteins, each is tagged with YFP or luciferase. The BRET pairs used in this thesis are schematically depicted in Figure 10 A-D.

Cells were seeded and transiently transfected as described in chapter “3.11. Cell culture and transfections”. Twenty-four hours after transfection, cells were washed with PBS, and coelenterazine h was added to a final concentration of 5  $\mu$ M. The stimulation of the cells by agonist was performed 5 min later. BRET signal detection was performed using Mithras LB 940 microplate reader (Berthold Technologies, Germany) equipped with donor (480  $\pm$  20 nm) and acceptor (540  $\pm$  40 nm) filters. The BRET signal ratio was calculated as the emission of the energy acceptor molecules (540  $\pm$  40 nm) divided by the emission of the energy donor molecules (480  $\pm$  20 nm). The data are presented as the agonist-promoted milliBRET (mBRET) change calculated by subtracting the BRET ratio obtained in the absence of an agonist from the one obtained following agonist application and multiplied by 1000 (Figure 10 E).

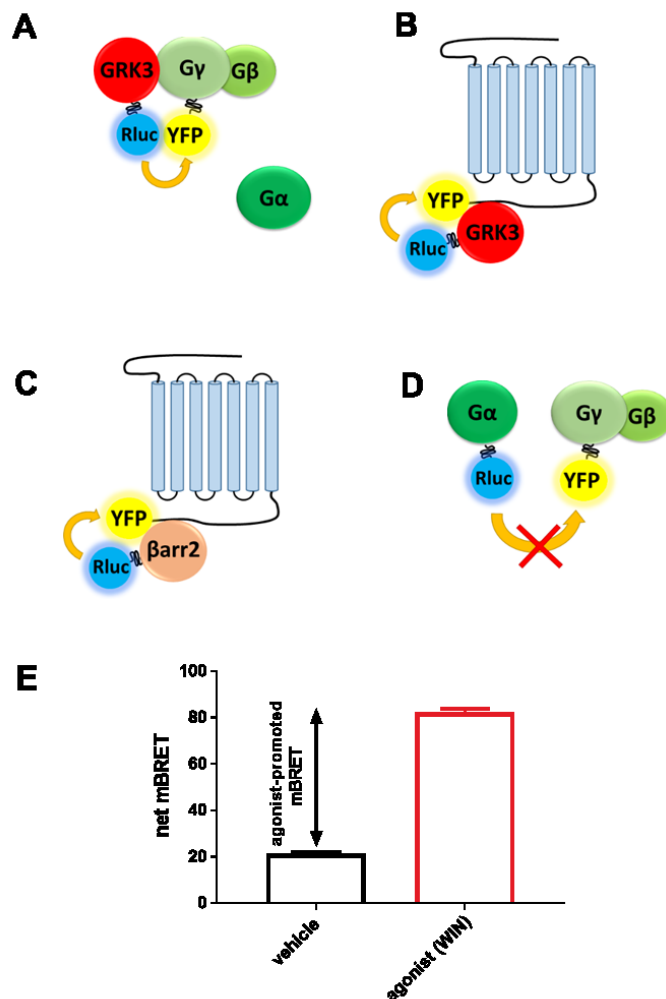


**Figure 10. BRET-based sensors that were used to study protein-protein interactions. mBRET calculation.** A) Schematic representation of GRK3-RLuc8 recruitment to CB1-YFP upon CB1R activation. The formation of GRK3-CB1R complexes is observed as an increase in BRET signal efficiency. B) Schematic representation of GRK3-RLuc8 with G $\gamma$ -YFP complexes formation generating an increase of BRET signal. C) Schematic

representation of the recruitment of  $\beta$ -arrestin2-Rluc by the activated CB1R-YFP generating an increase of BRET signal. **D)** Schematic representation of the activation of heterotrimeric G-proteins, which is observed as a decrease in BRET signal due to dissociation of  $G\alpha_i$  from  $G\beta\gamma$  subunits. **mBRET calculation.** **E)** Agonist-promoted mBRET was calculated by subtracting the BRET ratio obtained in the absence of agonist from the one obtained following agonist application and multiplied by 1000.

### **3.14. Microscopy**

Cells were seeded onto culture dishes dedicated for microscopy and transfected by correspondent plasmids using polyethyleneimine. Live cells were imaged at 37°C using an inverted fluorescent microscope Leica DMI6000 with confocal extension Leica TCS SP5 AOBs TANDEM confocal superfast scanner, objective 63 × 1.4 oil (Leica Microsystems, Germany). Samples were excited with an argon laser 514 nm and detected with a HyD 4 detector in 535–545 nm range. Microscopic images were processed in ImageJ.

### **3.15. SDS-PAGE and Western blot**

Expression levels of CB1R-YFP mutant variants were characterized using the SDS page and subsequent western blot analysis of cell lysates. Briefly, HEK293 cells transfected with a particular CB1R variant or empty plasmid pRK6 (mock) were washed with ice-cold PBS and harvested in PBS complemented with cOmplete™ EDTA-free Protease Inhibitor Cocktail tablet followed by centrifugation 13,000 g for 10 min at 4 °C. Supernatants were decanted, and the pellets were resuspended in cold PBS with protease inhibitor. Afterward, the cells were disrupted by ultrasonication, and the total amount of protein in each lysate was determined using Bradford Reagent-based assay following the manufacturer's instructions. The samples were resuspended in SDS–PAGE treatment buffer (0.25 M Tris-Cl, 8% SDS, 20% glycerol, 0.02% bromophenol blue, 0.04 M DTT, pH 6.8) and boiled for 10 min at 85°C. Lysates were separated by 10% SDS–PAGE.

Subsequently, the proteins were transferred to the nitrocellulose membrane using BioRad Trans-blot Turbo transfer system (semi-wet transfer) according to the manufacturer's instructions.

The membrane was blocked in 5% blotting-grade powdered milk in PBST buffer. Afterward, the membrane was cut into two pieces and labeled either with primary antibody mouse anti-GFP (1:400) followed by secondary antibody labeling goat anti-mouse IgG-HRP

antibody (1:10,000) for detection of CB1R-YFP variants or with primary antibody rabbit anti-actin (1:500) followed by secondary goat anti-rabbit IgG-HRP antibody (1:10,000) for the detection of actin to check the equal loading and protein transfer. The proteins of interest were visualized by chemiluminescence using the SuperSignal West PICO chemiluminescent substrate and detected on the LAS-300 system (Fujifilm, Japan).

### **3.16. Animals**

Mice were bred and group-housed in accordance with animal welfare rules. The animal care and experimental procedures used in this study complied with applicable laws, Guidelines of the National Institutes of Health on the Care and Use of Animals and to Directive 2010/63/EU. All animal models and experiments in this study were ethically reviewed and approved by the Institute of Molecular Genetics.

### **3.17. Inositol monophosphate accumulation**

To measure the inositol monophosphate (IP1) release, IPOne HTRF kit (PerkinElmer - CisBio, France) was utilized accordingly to the manufacturer's recommendations. Briefly, cells were seeded and transiently co-transfected with CB1R variant and chimeric G protein  $G\alpha_{q19}$  (1:1 ratio), which permits  $G_{i/o}$ -coupled GPCRs to couple to  $G\alpha_q$  and produce IP1 (Brule et al., 2014). 24 hours after the transfection, cells were incubated in the presence of receptor agonist for 20 min at 37°C, and then cryptate-labeled anti-IP1 and D2-labeled IP1 antibodies were added for 1 h at the 21°C. Native IP1 produced by cells compete with d2-labeled IP1 (acceptor of energy) for binding of anti-IP1-Cryptate (donor of energy). The fluorescence was detected at 665 and 620 nm using a PHERAstar plate reader (BMG Labtechnologies, Germany). The HTRF signal was calculated as the 665/620 nm emission ratio multiplied by 10,000. The specific measured HTRF signal (energy transfer) is inversely proportional to the concentration of IP1 in the cells. The data were normalized against the minimal and maximal IP1 accumulation in cells driven by specific CB1R variant.

### **3.18. Internalization assay**

The Homogenous Time-Resolved FRET (HTRF) technology was used to assess the cell surface receptor internalization rate as described previously (Levoye et al., 2015).

Briefly, HEK293 cells were seeded on 96-well plate and transiently transfected with SNAP-tagged CB1R plasmid and either with empty plasmid (pRK6) or SGIP1 splice variant (1:2 DNA mass ratio) using Lipofectamine™ 2000 according to the manufacturer's protocol. Twenty-four hours after the transfection, the cell culture medium was removed, and the cells were labeled with 100 nM SNAP-Lumi4-Tb, diluted in Tag-lite labeling medium, and incubated for 1 h at 37°C, 5% CO<sub>2</sub>. Afterward, cells were washed four times with Tag-Lite buffer solution. The receptor internalization experiment was performed by adding Tag-lite buffer containing 24 μM fluorescein and agonist WIN 55,212-2 mesylate (WIN) or vehicle dimethyl sulfoxide (DMSO). HTRF signal was recorded over the course of 90 minutes at 37°C using Mithras LB 940 microplate reader equipped with HTRF module with relevant filters. After the donor (terbium cryptate) was excited at 340 ± 26 nm, the donor emission was measured at 520 ± 10 nm, and the acceptor (fluorescein) emission was measured at 620 ± 10 nm. The HTRF ratio was calculated as the donor emission divided by the acceptor emission multiplied by 10,000. Then, the ratios were normalized to maximal CB1R internalization values in the absence of SGIP1.

### **3.19. Statistical analysis**

To determine statistical significance analysis was performed using two-way ANOVA followed by Sidak's multiple comparisons test using GraphPad Prism 7 (GraphPad Software, Inc.). Full results of the statistical analysis are disclosed in tables in appendices. Data are presented as means ± SEM. The statistical confidence thresholds is: \*  $p \leq 0.05$ .

## 4. Results

### 4.1. Activation of GRK3 is necessary for its optimal association with G $\beta\gamma$

The first step of CB1R desensitization is the phosphorylation of its C-terminal tail by the kinase activity of GRKs. GRK3, in its inactive form, is a cytosolic protein. However, GPCR-mediated activation of G proteins translocates GRK3 to the membrane and close proximity of the receptor via interaction with G protein G $\beta\gamma$  dimer (Carman et al., 2000; Lodowski et al., 2005).

To test whether GRK3 requires active conformation to interact with G $\beta\gamma$ , I used compd101, a pharmacological inhibitor that binds to the GRK2/3 active site and renders the kinase catalytically inactive (Ikeda S, 2007; Thal, Yeow, Schoenau, Huber, & Tesmer, 2011), together with a BRET-based sensor. In this assay, the G $\gamma_2$  subunit of G protein fused with a YFP (G $\gamma_2$ -YFP) was co-expressed in HEK293 cells with CB1R-SNAP and GRK3 fused with a bioluminescence enzyme luciferase 8 (GRK3-Rluc8). The interaction of G $\gamma_2$ -YFP and GRK3 is observed as an increase in the BRET signal. The CB1R-induced G $\gamma_2$ -YFP-GRK3-Rluc8 interaction was tested in cells pretreated or not with GRK2/3 inhibitor compd101. Application of the CB1R agonist WIN resulted in a rapid GRK3-Rluc8-G $\gamma_2$ -YFP association, as observed by the increase of the BRET signal (Figure 11 A). The pretreatment of cells with of compd101 significantly reduced the interaction between GRK3-Rluc8 and G $\gamma_2$ -YFP upon WIN stimulation (mBRET values  $\pm$  SEM in 15 min: CB1R =  $161 \pm 7.34$ ; CB1R + compd101 =  $49.1 \pm 3.24$ ). The application of compd101 did not alter the amount of CB1R (Figure 11 B).

WIN-dose response assay in cells untreated and pretreated cells with compd101 was performed to verify that compd101 does not affect the potency of WIN. As shown in Fig. 11 C, WIN potency was not modified in the presence of compd101.

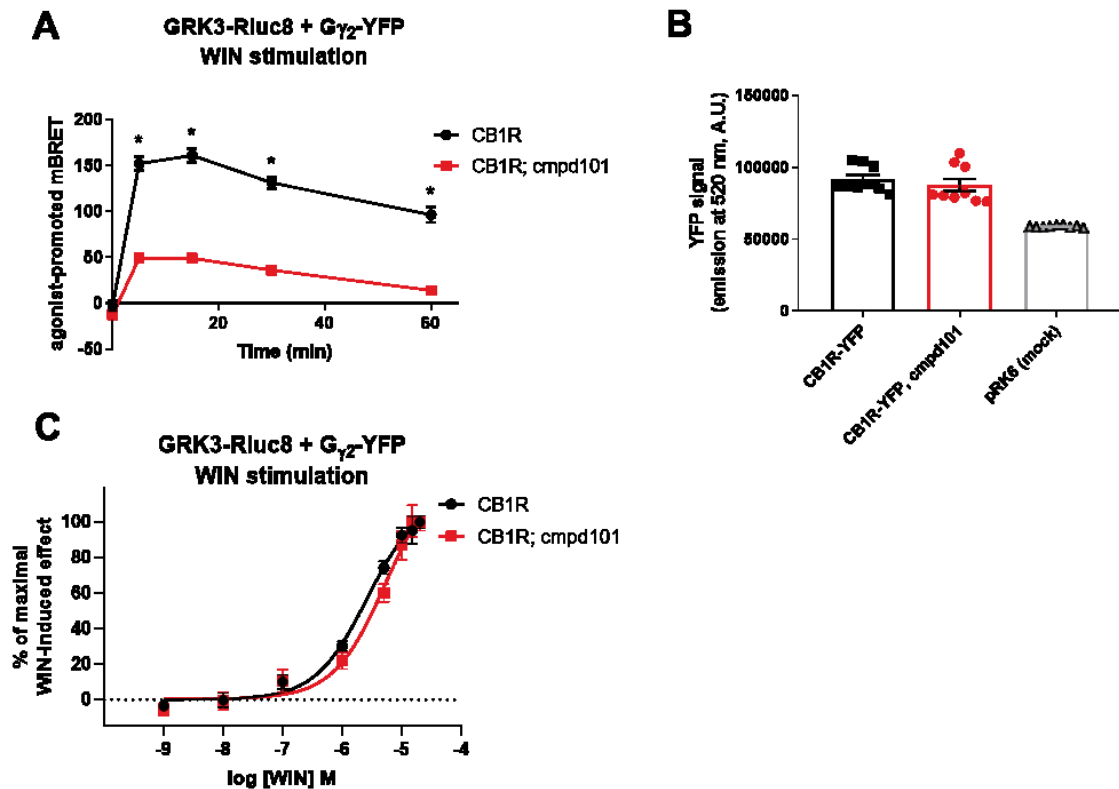


**Figure 11. Inhibitor of GRK3 catalytic activity cmpd101 attenuates GRK3 interaction with G $\gamma$ <sub>2</sub>.** **A)** Kinetic profiles of GRK3-RLuc8 and G $\gamma$ <sub>2</sub>-YFP association dynamics in cmpd101 treated and nontreated cells. HEK293 cells were transiently cotransfected with CB1R-SNAP + GRK3-Rluc8 + G $\beta$ -flag + G $\gamma$ <sub>2</sub>-YFP (2:1:1:2 ratio). After 24 h, cells were pretreated for 30 min with cmpd101 (30  $\mu$ M) before the stimulation with the CB1R agonist 1  $\mu$ M WIN. **B)** cmpd101 does not affect the expression of CB1R-YFP. HEK293 cells were transiently cotransfected with CB1R-SNAP + GRK3-Rluc8 + G $\beta$ -flag + G $\gamma$ <sub>2</sub>-YFP (2:1:1:2 ratio). After 24 h, the expression level of CB1R-YFP in the presence/absence of cmpd101 was assessed by measuring the emission of CB1R-YFP at 520 nm on Mithras LB 940 microplate reader after excitation at 485 nm. **C)** cmpd101 does not alter WIN potency. Dose-response curves of GRK3-RLuc8 and G $\gamma$ <sub>2</sub>-YFP association dynamics in cmpd101 treated and nontreated cells after CB1R stimulation with increasing concentrations of WIN. Twenty-four hours after transfection, 5  $\mu$ M coelenterazine h was added, cells were stimulated with increasing concentrations of WIN and the increase in BRET signal was measured 15 min after WIN application. All data represent the mean  $\pm$  SEM of three experiments of independent cell preparations performed in three technical replicates. \* $p \leq 0.05$ .

#### 4.2. GRK3 has to be in active form to interact with CB1R

To test whether activation of GRK3 is required for the interaction with CB1R, HEK293 transiently expressing CB1R-YFP and GRK3-RLuc8 were used to study their association using BRET method. Stimulation of CB1R by WIN resulted in a rapid increase in BRET signal, implying a formation of CB1R-GRK3 complexes (Fig. 12 A). In contrast, pretreatment of cells with GRK2/3 activity blocker cmpd101 resulted in inhibited CB1R-

GRK3 complex formation, as observed by decreased BRET signal (mBRET values  $\pm$  SEM in 5 min: CB1R =  $22.45 \pm 1.57$ ; CB1R + cmpd101 =  $3.88 \pm 1.73$ ) (Fig. 12 A). This finding suggests that GRK3 has to be in active form to interact with CB1R.

To verify that the GRK3-CB1R association is driven by WIN-induced CB1R activation, WIN was applied to mGluR1a-expressing cells. In this case, no change in BRET signal was observed (Fig. 12 B). In addition, pretreatment of cells with the CB1R selective inverse agonist rimonabant (SR141716) completely suppressed WIN-driven CB1R-GRK3 complex formation (Fig. 12 B). These results confirm that the WIN activation of CB1R truly drives GRK3 recruitment to CB1R.

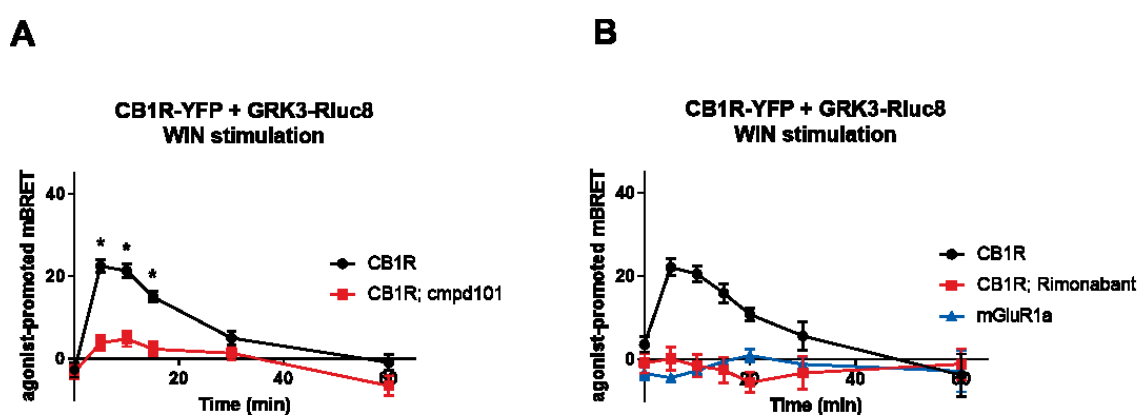


**Figure 12. GRK3 catalytic activity is required for its association with the activated CB1R.** **A)** Kinetic profiles of GRK3-RLuc8 recruitment by WIN-activated CB1R-YFP in HEK293 cells pretreated or not treated with cmpd101. HEK293 cells were transiently co-transfected with CB1R-YFP + GRK3-RLuc8 + empty plasmid pRK6 (2:1:2 ratio). **B)** GRK3 recruitment to CB1R is driven by WIN stimulation of CB1R. Kinetic profiles of GRK3-RLuc8 recruitment by WIN-activated CB1R-YFP/mGluR1a-YFP in HEK293 cells pretreated or not with rimonabant. HEK293 cells were transiently co-transfected with the plasmid coding for CB1R-YFP or mGluR1a-YFP and GRK3-RLuc8. After 16 hours, cells were pretreated or not for 30 minutes with 45  $\mu$ M rimonabant prior to the stimulation with 1  $\mu$ M WIN. Data represent the mean  $\pm$  SEM of three experiments of independent cell preparations performed in three technical replicates. \* $p \leq 0.05$ .

#### 4.3. GRK2/3 inhibitor cmpd101 impedes CB1R-driven recruitment of $\beta$ -arrestin2

Phosphorylation of GPCRs results in  $\beta$ -arrestin recruitment and subsequent receptor desensitization. I investigated if  $\beta$ -arrestin2 binding to CB1R is dependent on the kinase activity of GRK2/3. HEK293 cells transfected with plasmids coding  $\beta$ -arrestin2-RLuc and CB1R-YFP were treated or not with cmpd101. Upon activation of CB1R by WIN, an apparent increase in BRET signal was recorded due to formation of CB1R- $\beta$ -arrestin2

complexes whereas application of cmpd101 resulted in inhibited  $\beta$ -arrestin2 recruitment (mBRET values  $\pm$  SEM in 10 min: CB1R =  $29.72 \pm 3.57$ ; CB1R + cmpd101 =  $5.46 \pm 2.08$ ) (Fig. 13). This experiment confirms that recruitment of  $\beta$ -arrestin2 to WIN-stimulated CB1R depends on the catalytic activity of GRK2/3.

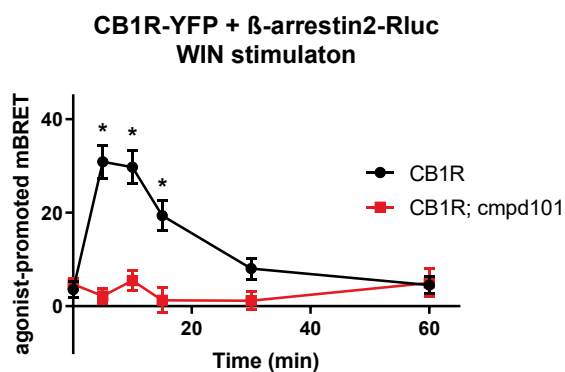


**Figure 13.  $\beta$ -arrestin2 recruitment to CB1R is dependent on the activity of GRK2/3.**  $\beta$ -arrestin2-Rluc recruitment by activated CB1R-YFP in cmpd101 pretreated and non-pretreated cells. HEK293 cells were transiently co-transfected with CB1R-YFP +  $\beta$ -arrestin2-Rluc + empty plasmid pRK6 (2:1:2 ratio). After 16 h, cells were pretreated for 30 min with 30  $\mu$ M cmpd101 before stimulation with 1  $\mu$ M WIN. Data represent the mean  $\pm$  SEM of three experiments of independent cell preparations performed in three technical replicates. \* $p \leq 0.05$ .

#### 4.4. Mutagenesis and characterization of CB1R C-tail phosphorylation mutants

To study the role of CB1R C-tail phosphorylation in mediating interactions with molecules involved in receptor signaling and desensitization, a set of CB1Rs mutated within the  $^{425}$ SMGDS $^{429}$  and  $^{460}$ TMSVSTDTS $^{468}$  was created. Using molecular biology techniques, serine and threonine residues were mutated either into alanine residues, which cannot be phosphorylated, or into negatively charged aspartic acid, which partially mimics a phosphorylated state (Fig. 14). CB1R variants with mutations within  $^{425}$ SMGDS $^{429}$  region are termed as CB1R\_2X, mutants in  $^{460}$ TMSVSTDTS $^{468}$  region as CB1R\_6X. Receptors simultaneously mutated in both regions are labeled as CB1R\_8X. Based on the amino acid substitution, X is either A (mutation into alanine) or D (aspartic acid mutations). Each CB1R variant was created in two versions: C-terminally fused YFP or N-terminally fused SNAP-Flag tag. The sequences of all plasmids were verified by sequencing.

The expression level of mutant CB1Rs was analyzed by western blot. Protein samples were prepared from lysates of HEK293 cells expressing mutant CB1R-YFP variants. For the receptor detection, an antibody against green fluorescent protein was used (the green fluorescent protein recognition epitope is identical to YFP). As control of protein loading and transfer, samples were also visualized using an anti-actin antibody. The western blot analysis showed that all mutant receptors have similar expression levels to wild type CB1R (Fig. 15 A). Additionally, imaging by confocal fluorescent microscopy confirmed the proper receptor localization on the cellular membrane (Fig 15. B).

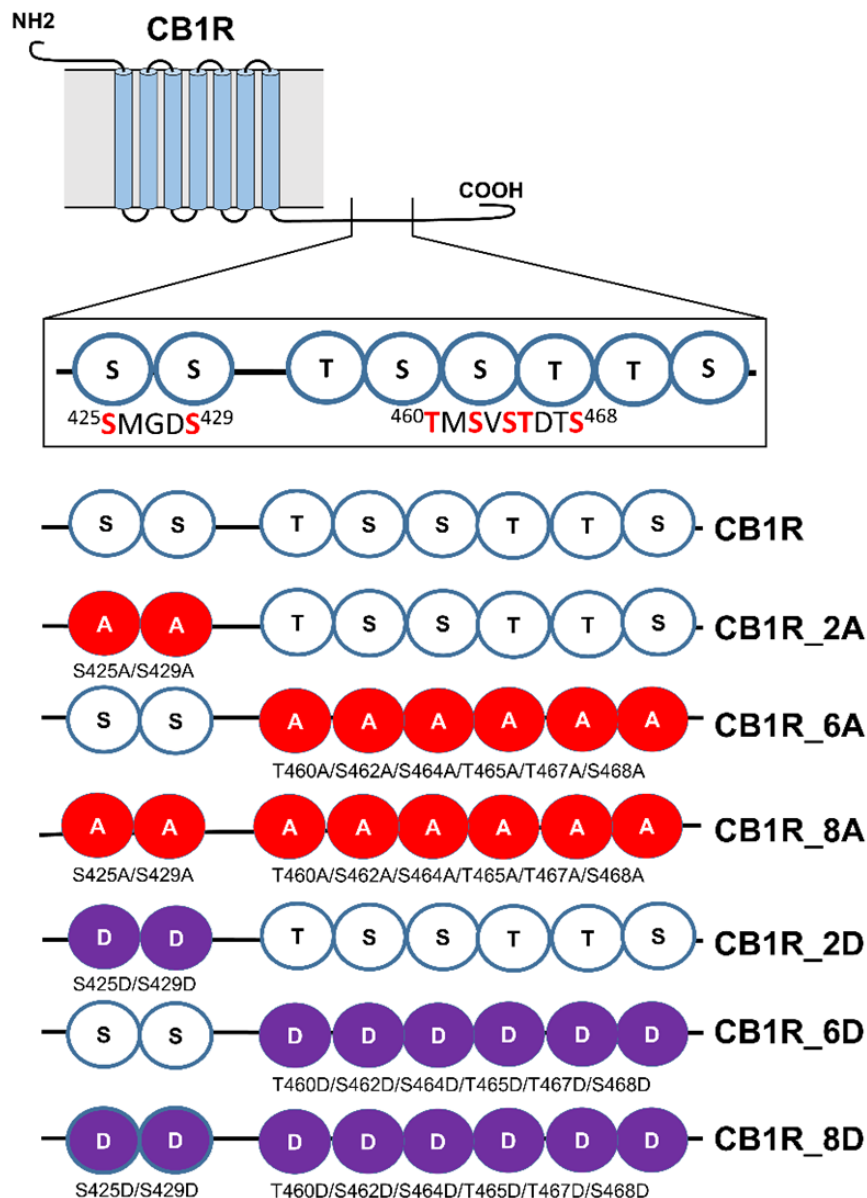


**Figure 14. List of constructed CB1R variants mutated within the C-tail.** Schematic depiction of CB1R mutants with corresponding sequences. Two regions of CB1R contain serine/threonine residues that are possibly phosphorylated during the desensitization of CB1R. CB1R C-tail phosphorylation mutants were constructed according to the following scheme: A - alanine mutation, D - aspartic acid mutation.

Finally, the functionality of mutant CB1Rs was tested by examining their ability to activate G proteins using BRET method. In this assay, the  $G\gamma_2$  subunit of G protein was fused with YFP ( $G\gamma_2$ -YFP) and co-expressed in HEK293 cells with mutant CB1R-SNAP and  $G\alpha_{i1}$  fused with a luciferase 8 ( $G\alpha_{i1}$ -Rluc8). The activation of G proteins results in the dissociation of  $G\alpha_{i1}$  and  $G\beta\gamma$  subunits, which can be observed as a decreased BRET signal. Stimulation of all CB1R variants by WIN resulted in a decrease of the BRET signal due to the activation of G proteins (Fig. 16). This confirms that CB1R C-tail phosphorylation mutants are functional and maintain the ability to activate the  $G\alpha_{i1}$  protein signaling pathway.

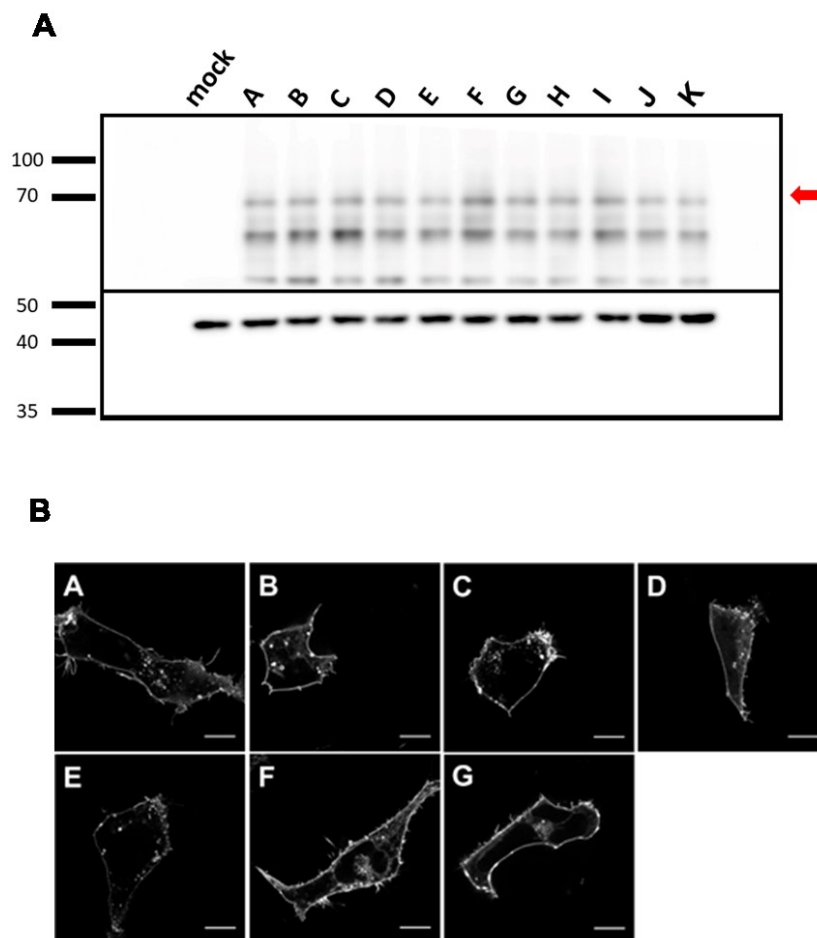


**Figure 15. Mutant CB1Rs variants have similar levels of expression and cellular localization as wild type CB1R.** A) Mutant CB1Rs variants have similar levels of expression to wild type CB1R. HEK293 cells were transfected with the indicated CB1R variant or empty plasmid pRK6 (mock). Cell lysates were separated by SDS-PAGE and subjected to Western blotting. Membranes were stained with either anti-GFP antibody for detection of CB1R-YFP variants (top blot) or anti-Actin antibody (actin) to normalize for loading and transfer of proteins (bottom blot). Legend: mock (pRK6 empty vector transfection), A) CB1R, B) CB1R\_2A, C) CB1R\_6A, D) CB1R\_8A, E) CB1R\_2D, F) CB1R\_6D, G) CB1R\_8D, H) CB1R<sub>425</sub>SMGDS<sup>429-460</sup>TMAVATDTA<sup>468</sup>, I)

CB1R<sup>425</sup>AMGDA<sup>429-460</sup>TMAVATDTA<sup>468</sup>, J) CB1R<sup>425</sup>SMGDS<sup>429-460</sup>AMSVSADAS<sup>468</sup>, K) CB1R<sup>425</sup>AMGDA<sup>429-460</sup>AMSVSADAS<sup>468</sup>. **B)** CB1R and mutant CB1Rs are predominantly localized on the cellular membrane. HEK293 cells were transiently transfected with CB1R-YFP variant. Twenty-four hours after transfection, cells were visualized using a fluorescent microscope. A single confocal section through the equatorial plane of the cells is shown. Legend: (A) CB1R, (B) CB1R\_2A, (C) CB1R\_6A, (D) CB1R\_8A, (E) CB1R\_2D, (F) CB1R\_6D, (G) CB1R\_8D. The scale bar represents 10  $\mu$ m.

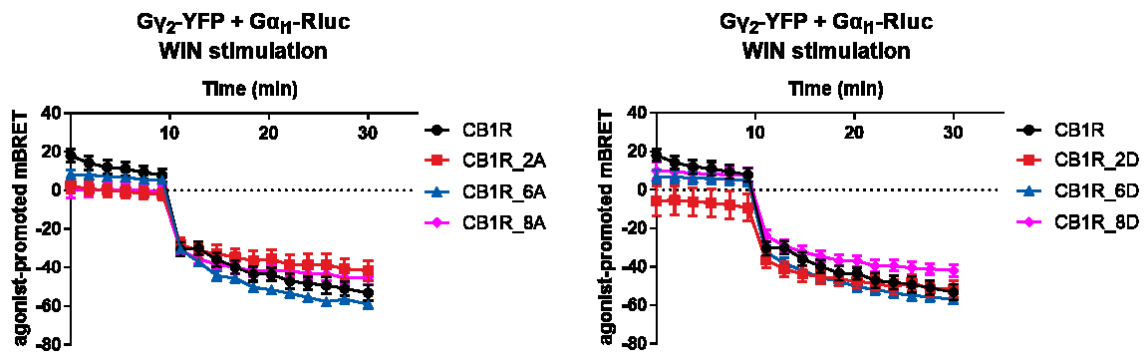


**Figure 16. CB1Rs mutated in C-tail preserve the ability to activate G proteins.** HEK293 cells were transiently co-transfected with CB1R-SNAP variant,  $G\alpha_{i1}$ -Rluc8,  $G\beta$ -Flag,  $G\gamma_2$ -YFP (2:1:1:1 ratio). Firstly, basal BRET was measured for 10 minutes. Afterward, cells were stimulated by 1  $\mu$ M WIN. Data represent the mean  $\pm$  SEM of three experiments of independent cell preparations performed in three technical replicates

#### 4.5. G protein activation and signaling are not altered in CB1R phosphorylation mutants

To study the impact of CB1R C-terminal tail mutations on signaling, two different G protein-activation assays were employed. The first BRET-based assay utilized  $G\alpha_{i1}$ -Rluc8 and  $G\gamma_2$ -YFP sensors to monitor G protein activation. The second assay measured the levels of inositol monophosphate (IP1) release via CB1R-driven activation of  $G\alpha_{q19}$ . Chimeric  $G\alpha_{q19}$  allows  $G\alpha_q$ -coupled GPCRs to produce IP1 (Brule et al., 2014). Both assays assessed the CB1R response on gradually increasing WIN concentrations (WIN dose-response).

The extent and potency of  $G\alpha_{i1}$  activation was similar in all tested CB1R variants (logEC<sub>50</sub> for  $G\alpha_{i1}$  activation; CB1R = -7.169; CB1R\_2A = -7.128; CB1R\_6A = -7.007; CB1R\_8A = -7.146) (Fig. 17 A). Similarly, the production of IP1 by  $G\alpha_{q19}$  driven CB1R mutants was not changed (logEC<sub>50</sub> for  $G\alpha_{q19}$  activation; CB1R = -6.202; CB1R\_2A = -6.353; CB1R\_6A = -6.311; CB1R\_8A = -6.170) (Fig. 17 B). Taken together, these observations show that an inability to phosphorylate serines and threonines within CB1R C-tail regions <sup>425</sup>SMGDS<sup>429</sup> and <sup>460</sup>TMSVSTDT<sup>S468</sup> does not affect G protein signaling.

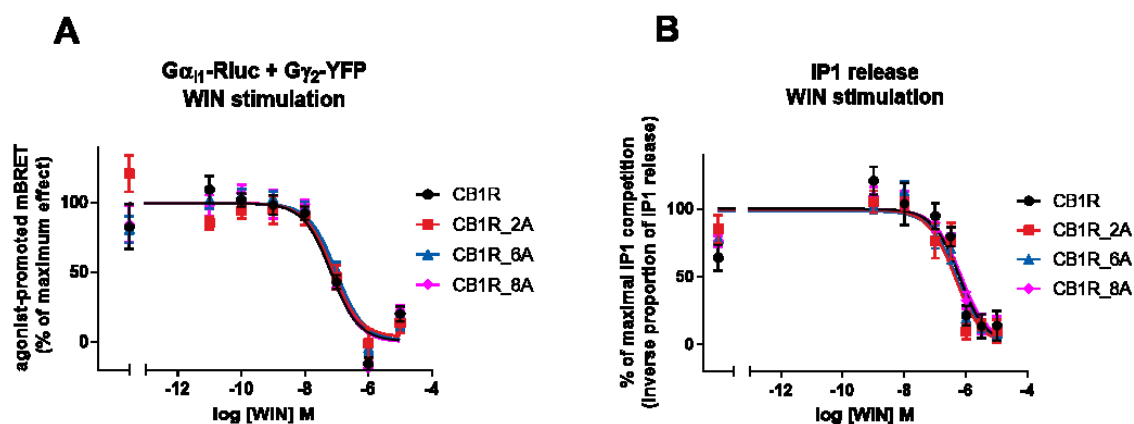


**Figure 17. CB1R mutants do not cause altered G protein signaling.** **A)** C-tail mutations do not influence CB1R mediated  $G\alpha_{i1}$  protein activation. HEK293 cells were transiently co-transfected with CB1R-SNAP variant,  $G\alpha_{i1}$ -Rluc8,  $G\beta$ -Flag,  $G\gamma_2$ -YFP (2:1:1:1 ratio). Twenty-four hours after transfection, 5  $\mu$ M coelenterazine h was added, cells were stimulated with increasing concentrations of WIN and the decrease in BRET signal was measured 15 min after WIN application. **B)** CB1R mutants release comparable levels of IP1 as WT CB1R. HEK293 cells were transiently co-transfected with CB1R-SNAP variant and chimeric G protein  $G\alpha_{q19}$ . Twenty-four hours after transfection, cells were stimulated with increasing concentrations of WIN. The extent of IP1 accumulation was measured 20 min after WIN application. Data represent the mean  $\pm$  SEM of three experiments of independent cell preparations performed in three technical replicates. Data were normalized against the maximal WIN-induced response.

#### 4.6. CB1R phosphorylation state partially affects the formation of GRK3- $G\beta\gamma$ complexes

To investigate whether phosphorylation of the C tail affects the interaction of the GRK3 with  $G\beta\gamma$  subunits, the BRET assay with GRK3-Rluc8 and  $G\gamma_2$ -YFP was used. Stimulation of WT CB1R with 1  $\mu$ M WIN resulted in the rapid formation of GRK3-Rluc8- $G\gamma_2$ -YFP complexes, as illustrated by the increase in BRET signal (Fig. 18 A). WIN stimulation of the CB1R\_2A also induced increase in BRET signal (mBRET values  $\pm$  SEM at 5 min CB1R =  $138.3 \pm 1.93$ ; CB1R\_2A =  $157.5 \pm 7.42$ ) (Fig. 18 B). Contrary, the activation of CB1R\_6A and CB1R\_8A lead to lower BRET efficiency in comparison to WT CB1R response (mBRET values  $\pm$  SEM at 5 min: CB1R =  $138.3 \pm 1.93$ ; CB1R\_6A =  $91.77 \pm 2.90$ , CB1R\_8A =  $83.82 \pm 10.57$ ) (Fig. 18 C & D). All tested CB1R mutants were able to initiate recruitment of GRK3-Rluc8 to  $G\gamma$ -YFP, albeit with different efficiency.

Consequently, the phosphorylation of the CB1R C-terminal motif is not required for GRK3-G $\beta\gamma$  interaction but is partially affected by it.

#### 4.7. SGIP1 augments and prolongs GRK3-G $\beta\gamma$ coupling

Previous study demonstrated that SGIP1 enhanced CB1R and  $\beta$ -arrestin2 interaction (Hajkova et al., 2016). Therefore I hypothesized that GRK3-G $\beta\gamma$  association could also be affected by SGIP1. To analyze this, I co-expressed GRK3-Rluc8, G $\gamma_2$ -YFP, and CB1R-SNAP in HEK293 cells expressing or not SGIP1. Indeed, CB1R-induced interaction of GRK3-Rluc8 and G $\gamma_2$ -YFP was significantly augmented and prolonged in presence of SGIP1 (mBRET values  $\pm$  SEM in 30 min: CB1R =  $107.6 \pm 9.73$ ; CB1R + SGIP1 =  $160.3 \pm 13.91$ ) (Fig. 18 A).

Next, the effect of SGIP1 on GRK3-G $\beta\gamma$  complex formation driven by CB1R phosphorylation mutants was examined. Co-expression of SGIP1 resulted in enhanced BRET signal in CB1R\_2A and CB1R\_6A mutants (mBRET values  $\pm$  SEM in 60 min: CB1R\_2A =  $101.1 \pm 5.92$ ; CB1R\_2A + SGIP1 =  $185.3 \pm 10.76$ ; mBRET values  $\pm$  SEM in 5 min: CB1R\_6A =  $99.04 \pm 12.50$ ; CB1R\_6A + SGIP1 =  $162.6 \pm 10.40$ ) (Fig. 18 B & C). On the other hand, activation of CB1R\_8A in the presence of SGIP1 resulted in similar GRK3-G $\beta\gamma$  interaction as in the cells without SGIP1 (Fig. 18 D).

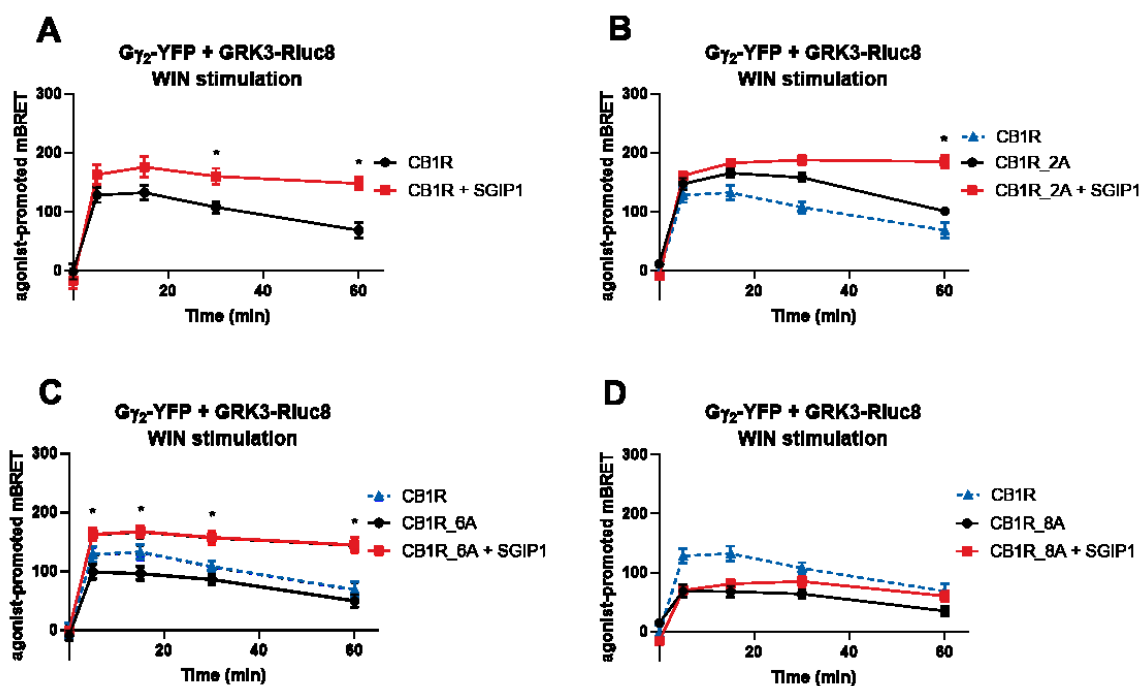


**Figure 18. GRK3-G $\beta\gamma$  association is partially affected by CB1R C-tail phosphorylation. The interaction of GRK3 and G $\beta\gamma$  induced by the mutant receptors is modified by SGIP1.** HEK293 were transiently co-transfected with CB1R-SNAP, GRK3-Rluc8, G $\gamma_2$ -YFP, G $\beta$ , and empty vector or SGIP1-mCherry (1:1:2:1:2 ratio). 24 hours after transfection,

cells were stimulated by 1  $\mu$ M WIN. **A)** Kinetic profile of GRK3 recruitment to  $G\gamma_2$  in CB1R in cell expressing WT CB1R and WT CB1R + SGIP1. **B)** Kinetic profile of GRK3 recruitment to  $G\gamma_2$  driven by CB1R, CB1R\_2A, and CB1R\_2A + SGIP1. **C)** Kinetic profile of GRK3 recruitment to v driven in CB1R and CB1R\_6A in the presence/absence of SGIP1. **D)** Kinetic profile of GRK3 recruitment to  $G\gamma_2$  driven by CB1R and CB1R\_8A in the presence/absence of SGIP1. Data represent the mean  $\pm$  SEM of three experiments of independent cell preparations performed in three technical replicates. \* $p \leq 0.05$ .

#### 4.8. The two CB1R C tail motifs control dynamics of the CB1R-GRK3 association

Phosphorylation of serine/threonine residues within the receptor's third intracellular loop and C-tail by GRKs represents an important step in the desensitization of GPCR. Therefore, the relationship between the phosphorylation pattern of CB1R and the recruitment of GRK3 was examined using HEK293 cells expressing mutant CB1R-YFP variants and GRK3-Rluc8.

Stimulation of WT CB1R by WIN resulted in an increase in BRET signal that peaked at around 10 minutes and then gradually diminished (Fig. 19 A). Activation of CB1R\_2A-YFP, which cannot be phosphorylated in the  $^{425}\text{SMGDS}^{429}$  region, induced increased and prolonged interaction (mBRET values  $\pm$  SEM in 5 min: CB1R =  $23.62 \pm 3.54$ ; CB1R\_2A =  $63.56 \pm 6.28$ ) (Fig. 19 B) while stimulation of phosphomimetic mutant CB1R\_2D lead to similar CB1R-GRK3 interaction as in a case of WT CB1R (mBRET values  $\pm$  SEM in 5 min: CB1R =  $23.62 \pm 3.54$ ; CB1R\_2D =  $31.69 \pm 3.75$ ) (Fig. 19 E). These observations suggest that the phosphorylation of serines in  $^{425}\text{SMGDS}^{429}$  decreases GRK3 interaction with CB1R by limiting association or catalyzing dissociation.

Contrary to previous results, WIN application to CB1R\_6A (mutation of the serine/threonine residues of the motif  $^{460}\text{TMSVSTDTS}^{468}$ ) produced significantly lower BRET signal (mBRET values  $\pm$  SEM in 5 min: CB1R =  $23.62 \pm 3.54$ ; CB1R\_6A =  $9.88 \pm 1.709$ ) (Fig. 19 C). CB1R\_8A, alanine mutant in both regions, did not induce BRET signal increase, pointing at an impaired ability to recruit GRK3 (Fig. 19 D). Both aspartic acid mutants CB1R\_6D and CB1R\_8D exhibited similar GRK3 recruitment dynamics as WT CB1R (mBRET values  $\pm$  SEM in 5 min: CB1R =  $35.54 \pm 2.26$ ; CB1R\_6D =  $27.50 \pm 2.68$ ; CB1R\_8D =  $18.62 \pm 2.16$ ) (Fig. 19 E). The outcomes of these experiments imply that the phosphorylatable serines/threonines of the long motif of  $^{460}\text{TMSVSTDTS}^{468}$  are essential for proper GRK3–CB1R interaction.

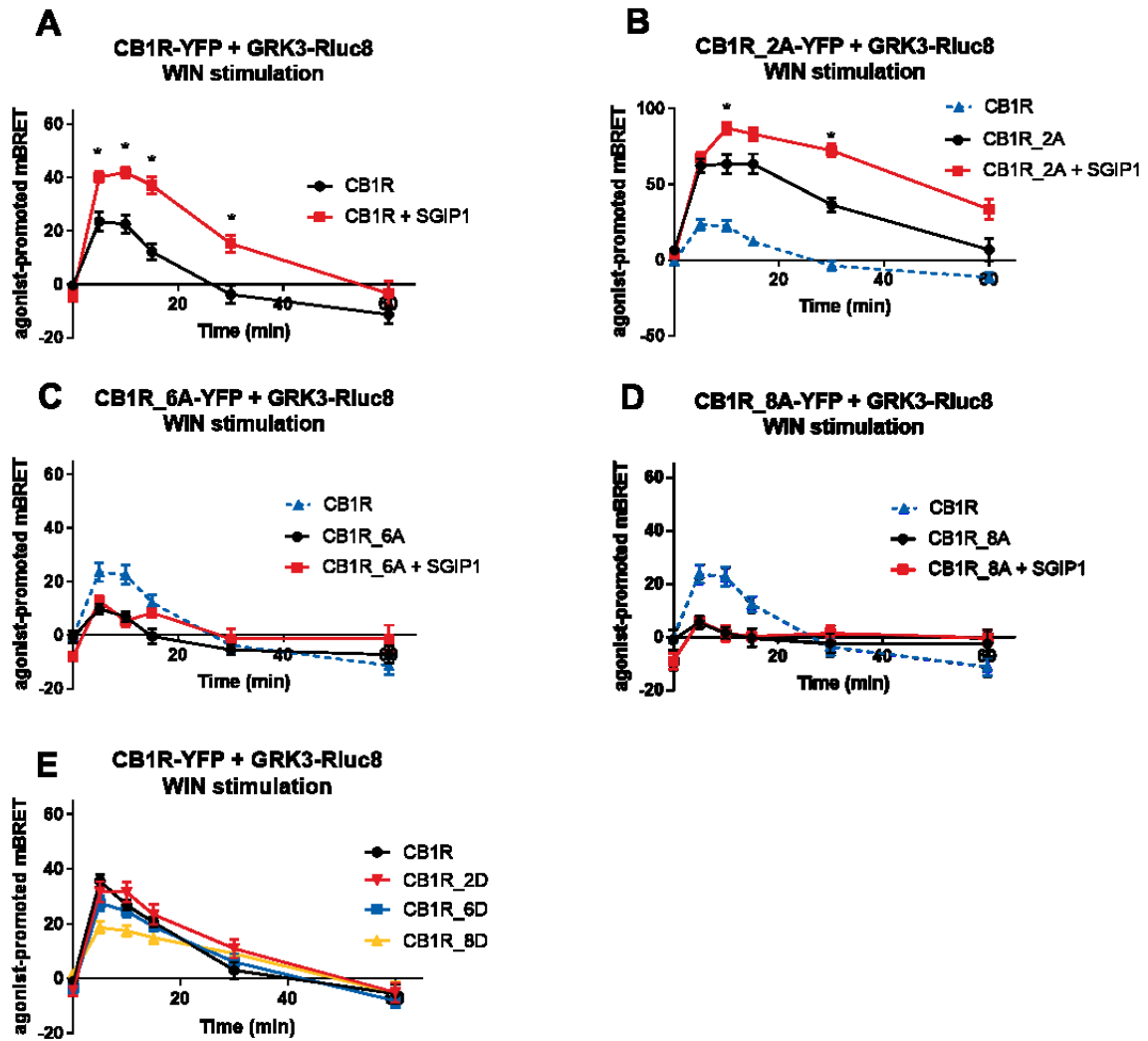


**Figure 19. CB1R C tail multisite phosphorylation is pivotal for GRK3 recruitment and dissociation. SGIP1 increases the association of CB1R-GRK3 in CB1R mutants that interact with GRK3.** HEK293 cells were transiently co-transfected with the plasmids coding CB1R-YFP variant + GRK3-RLuc8 + empty plasmid pRK6/SGIP1-mCherry (2:1:2 ratio). Cells were stimulated by 1  $\mu$ M WIN. **A)** Kinetics of GRK3 recruitment to CB1R in the presence and absence of SGIP1. **B)** Kinetics of GRK3 recruitment to CB1R, CB1R\_2A, and CB1R\_2A + SGIP1. **C)** Kinetic profile of GRK3 recruitment to CB1R and CB1R\_6A in the presence or absence of SGIP1. **D)** Kinetics of GRK3 recruitment to CB1R, CB1R\_8A, and CB1R\_8A + SGIP1. **E)** Kinetic profiles of GRK3 recruitment to CB1R, CB1R\_2D, CB1R\_6D, CB1R\_8D. Data represent the mean  $\pm$  SEM of three experiments of independent cell preparations performed in three technical replicates. \* $p \leq 0.05$ .

#### 4.9. SGIP1 enhances CB1R-GRK3 association

As SGIP1 has a profound impact on CB1R interaction with  $\beta$ -arrestin2 (Hajkova et al., 2016), the recruitment dynamics of GRK3 in the presence of SGIP1 was also studied.

Co-expression of SGIP1 lead to significantly stronger and prolonged GRK3 recruitment by WIN-activated CB1R (mBRET values  $\pm$  SEM in 5 min: CB1R =  $23.62 \pm 3.54$ ; CB1R + SGIP1 =  $40.16 \pm 2.01$ ) (Fig. 19 A). The interaction-enhancing effect of SGIP1 was also observed in CB1R\_2A (mBRET values  $\pm$  SEM in 10 min: CB1R\_2A =  $63.56 \pm 6.28$ ; CB1R\_2A + SGIP1 =  $87.26 \pm 3.92$ ) (Fig. 19 B). On the other hand, SGIP1 did not affect the interaction between either CB1R\_6A or CB1R\_8A and GRK3 (Fig. 19 C & D).

SGIP1 strengthens and prolongs GRK3 recruitment to the receptors interacting with GRK3 (CB1R, CB1R\_2A). Nevertheless, SGIP1 alone was insufficient to rescue this interaction in mutant receptors (CB1R\_6A and CB1R\_8A) that could not recruit GRK3 regardless of SGIP1 presence.

#### 4.10. CB1R C-tail phosphorylation is crucial for $\beta$ -arrestin2 recruitment

Upon WIN-stimulation of WT CB1R,  $\beta$ -arrestin2 is rapidly recruited to the receptor, as observed by the BRET increase that peaked between the 5<sup>th</sup> and 10<sup>th</sup> minute, then progressively reduced (Fig. 20 A).

Moreover, the activation of CB1R\_2A showed decreased recruitment of  $\beta$ -arrestin2, as observed by the lower BRET efficiencies in comparison with WT CB1R (mBRET values  $\pm$  SEM in 5 min: CB1R =  $29.33 \pm 1.93$ ; CB1R\_2A =  $15.53 \pm 3.28$ ) (Fig. 20 B). This interaction was completely abrogated in CB1R\_6A and CB1R\_8A mutants, as their activation did not produce increase in BRET signal (mBRET values  $\pm$  SEM in 5 min: CB1R =  $29.33 \pm 1.93$ ; CB1R\_6A =  $3.49 \pm 2.77$ ; CB1R\_8A =  $4.28 \pm 2.24$ ) (Fig. 20 C & D).

These observations show that <sup>425</sup>SMGDS<sup>429</sup> region is not imperative for the  $\beta$ -arrestin2 recruitment. Nevertheless, it plays an important role as its alanine mutation clearly decreases recruitment efficiency. On the contrary, the serine/threonine residues in <sup>460</sup>TMSVSTDTS<sup>468</sup> motif are essential for  $\beta$ -arrestin2 recruitment to the activated CB1R, as their alanine-mutation completely inhibits  $\beta$ -arrestin2-CB1R interaction.

Interestingly, all aspartic acid mutants exhibited similar diminished  $\beta$ -arrestin2-recruitment dynamics compared to WT CB1R (mBRET values  $\pm$  SEM in 5 min: CB1R =

29.93 ± 1.51; CB1R\_2D = 18.48 ± 2.96; CB1R\_6D = 5.7 ± 1.97; CB1R\_8D = 7.17 ± 1.95)  
 (Fig. 20 E).

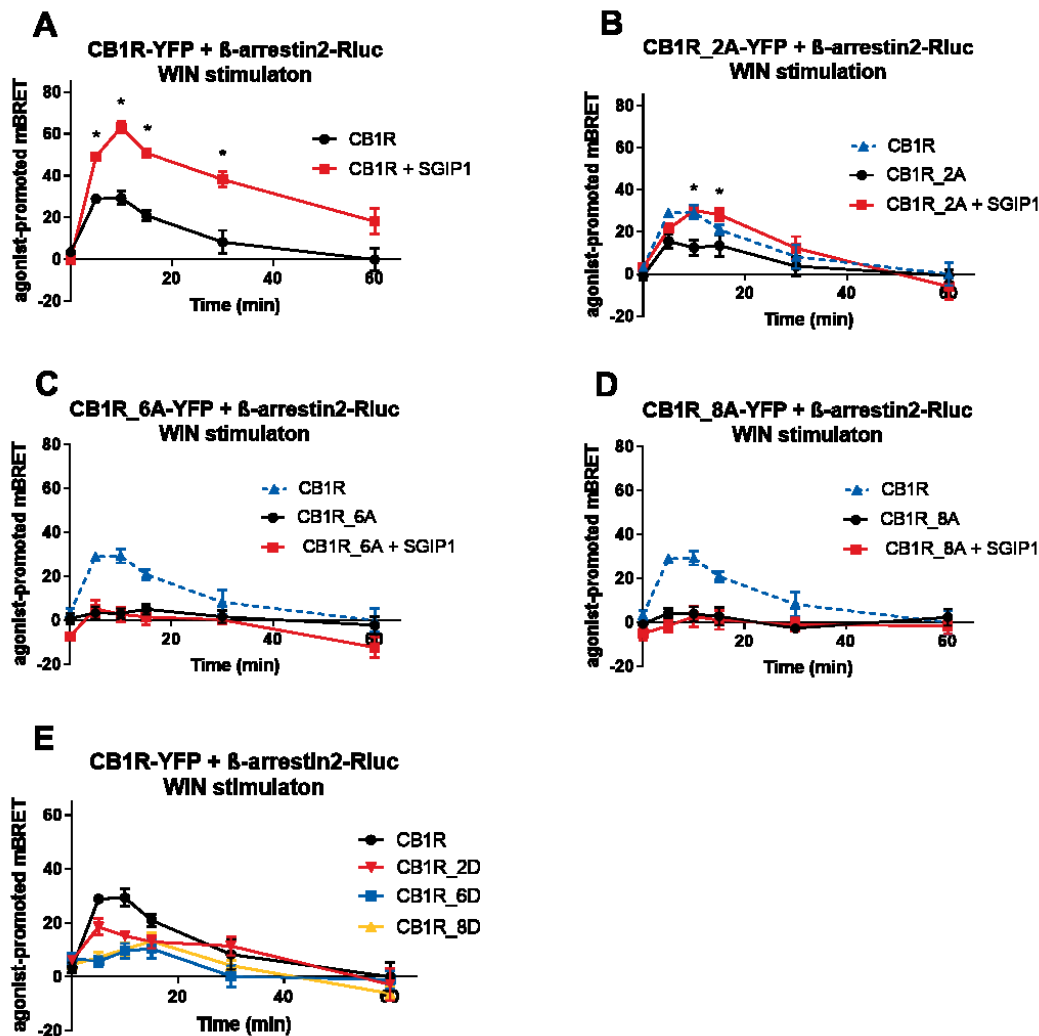


**Figure 20. CB1R C tail multisite phosphorylation is important  $\beta$ -arrestin2 recruitment. SGIP1 strengthens the formation of CB1R- $\beta$ -arrestin2 complexes in  $\beta$ -arrestin2-interacting receptors.** HEK293 cells were transiently co-transfected with the CB1R-YFP variants,  $\beta$ -arrestin2-Rluc, and empty vector/SGIP1-mCherry (2:1:2 ratio). Cells were stimulated by 1  $\mu$ M WIN. **A)** Interaction dynamics of  $\beta$ -arrestin2 recruitment to CB1R in the presence/absence of SGIP1. **B)** Interaction dynamics of  $\beta$ -arrestin2 recruitment to CB1R, CB1R\_2A, and CB1R\_2A + SGIP1. **C)** Interaction dynamics of  $\beta$ -arrestin2 recruitment to CB1R and CB1R\_6A in the presence/absence of SGIP1. **D)** Interaction dynamics of  $\beta$ -arrestin2 recruitment to CB1R, CB1R\_8A, and CB1R\_8A + SGIP1. **E)**  $\beta$ -arrestin2 recruitment to phosphomimetic CB1R mutants. Data represent the mean  $\pm$  SEM from three experiments of independent cell preparations performed in triplicate. \*Represents  $p \leq 0.05$ .

#### **4.11. The presence of SGIP1 increases CB1R- $\beta$ -arrestin2 association in $\beta$ -arrestin2-interacting CB1R phosphorylation mutants**

As it was previously described, SGIP1 strengthens and prolongs CB1R- $\beta$ -arrestin2 complex formation upon WIN treatment (mBRET values  $\pm$  SEM in 10 min: CB1R =  $26.59 \pm 7.08$ ; CB1R + SGIP1 =  $60.39 \pm 3.53$ ) (Fig. 20 A). This effect was also observed when serine/threonine residues in  $^{425}\text{SMGDS}^{429}$  motif are mutated (mBRET values  $\pm$  SEM in 10 min: CB1R\_2A =  $12.6 \pm 3.60$ ; CB1R\_2A + SGIP1 =  $30.30 \pm 1.651$ ) (Fig. 20 B). On the contrary, I did not detect any effect of SGIP1 on  $\beta$ -arrestin2 recruitment in CB1R\_6A and CB1R\_8A mutants (Fig. 20 C & D).

Although SGIP1 augments  $\beta$ -arrestin2 association with the receptors that interact with  $\beta$ -arrestin2 (WT CB1R, CB1R\_2A), the presence of SGIP1 alone is incapable of rescuing this interaction in mutants (CB1R\_6A, CB1R\_8A), that cannot recruit  $\beta$ -arrestin2.

#### **4.12. Unique phosphorylation patterns mediate GRK3 and $\beta$ -arrestin2 interactions with CB1R**

Different ligands induce distinct receptor conformations and patterns of receptor phosphorylation. Thus, we decided to create additional CB1R mutants with several combinations of alanine replacements within both studied regions to closely identify the residues mediating GRK3 and  $\beta$ -arrestin2 recruitment.

Using molecular biology techniques, an additional set of CB1R mutants was constructed (Fig. 21 A). The expression and correct localization of these new mutants was verified by western blot (Fig. 15) and fluorescent confocal microscopy (Fig. 21 B).

The first five minutes of WIN-activated mutant CB1R\_  $^{425}\text{SMGDS}^{429}_{-460}\text{AMSVSADAS}^{468}$  (with all threonines in long motif mutated into alanine residues) showed a comparable kinetic profile with WT CB1R. However at later points, the interaction in the mutant variant was prolonged (mBRET values  $\pm$  SEM in 30 min: CB1R =  $8.82 \pm 4.03$ ; CB1R\_  $^{425}\text{SMGDS}^{429}_{-460}\text{AMSVSADAS}^{468}$  =  $27.11 \pm 3.71$ ) (Fig. 21 C). When additional mutation of serines in the short motif was introduced (CB1R\_  $^{425}\text{AMGDA}^{429}_{-460}\text{AMSVSADAS}^{468}$ ), the augmentation was even more pronounced, and the receptor exhibited enhanced GRK3 interaction immediately after the stimulation (mBRET values  $\pm$  SEM in 30 min: CB1R =  $8.82 \pm 4.03$ ; CB1R\_425AMGDA42

9\_460AMSVSADAS468 =  $48.58 \pm 2.34$ ) (Fig. 21 C). These results confirm our previous observation that phosphorylation within  $^{425}\text{SMGDS}^{429}$  is vital for GRK3 dissociation. In addition, threonines of  $^{460}\text{TMSVSTDTS}^{468}$  are likely to play a role in GRK3 dissociation as well.

In contrast with the previous results, the mutation of serines in the long motif (CB1R\_ $^{425}\text{SMGDS}^{429}$ \_ $^{460}\text{TMAVATDTA}^{468}$ ) reduced the ability to recruit GRK3 (mBRET values  $\pm$  SEM in 5 min: CB1R =  $51.69 \pm 2.04$ ; CB1R\_ $^{425}\text{SMGDS}^{429}$ \_ $^{460}\text{TMAVATDTA}^{468}$  =  $28.95 \pm 2.18$ ). The reduction of GRK3 recruitment was even more evident, when serines in short motif were mutated as well (mBRET values  $\pm$  SEM in 5 min: CB1R =  $51.69 \pm 2.04$ ; CB1R\_ $^{425}\text{AMGDA}^{429}$ \_ $^{460}\text{TMAVATDTA}^{468}$  =  $13.81 \pm 2.03$ ). These observations suggest that threonines in the long motif are essential for optimal GRK3 binding to CB1R.

When I tested these four aforementioned mutants for  $\beta$ -arrestin2 recruitment, only a minor formation of complexes was seen (Fig. 21 D). This indicates that precise multisite phosphorylation of residues in both motifs is necessary for the optimal interaction of  $\beta$ -arrestin2 with CB1R.

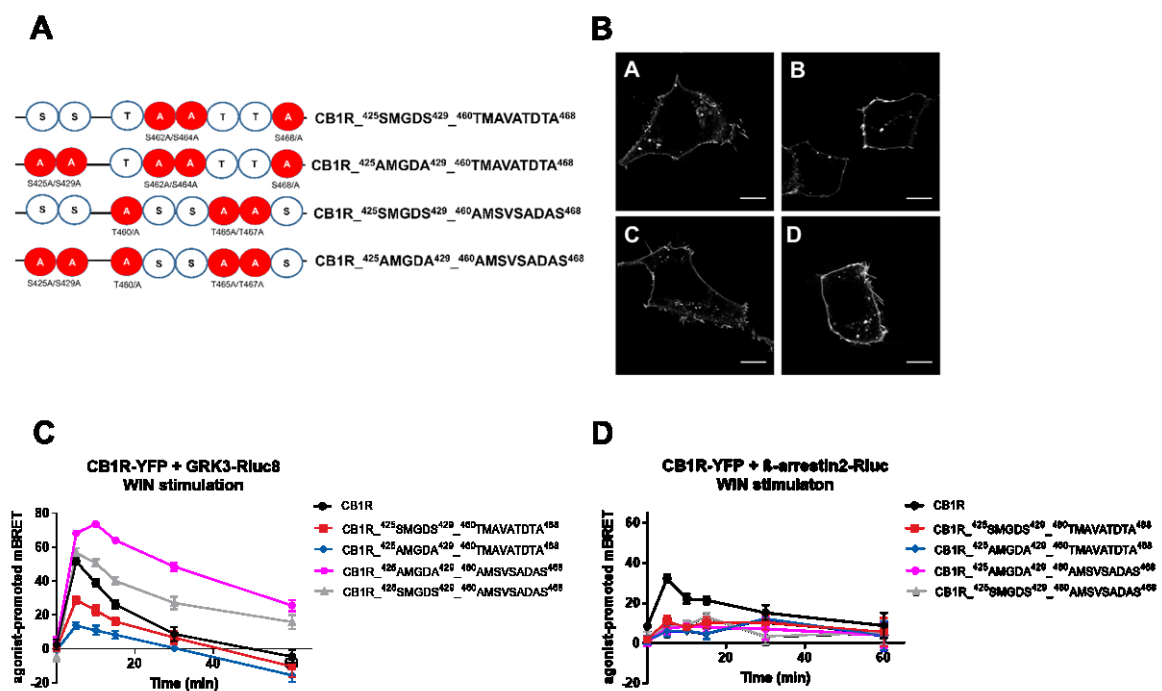


**Figure 21. GRK3 and  $\beta$ -arrestin2 interactions with CB1R depend on distinct phosphorylation patterns.** A) Schematic depiction of additional constructed CB1R mutants. A—mutation into alanine. B) Mutant CB1Rs and WT CB1R are similarly localized on the cellular membrane. A) CB1R\_ $^{425}\text{SMGDS}^{429}$ \_ $^{460}\text{TMAVATDTA}^{468}$ , B) CB1R\_ $^{425}\text{AMGDA}^{429}$ \_ $^{460}\text{TMAVATDTA}^{468}$ , C) CB1R\_ $^{425}\text{SMGDS}^{429}$ \_ $^{460}\text{AMSVSADAS}^{468}$ , D) CB1R\_ $^{425}\text{AMGDA}^{429}$ \_ $^{460}\text{AMSVSADAS}^{468}$ . HEK293 cells were transiently transfected

with CB1R-YFP variant. Twenty-four hours after transfection, cells were visualized using a fluorescent microscope. A single confocal section through the equatorial plane of the cells is shown. The scale bar represents 10  $\mu\text{m}$ . C) Kinetic profile of GRK3 recruitment to CB1R and CB1R mutants. D) Kinetic profile of  $\beta$ -arrestin2 recruitment to CB1R and CB1R mutants. Data represent the mean  $\pm$  SEM from three independent cell preparations experiments performed in triplicate.

#### **4.13. Expression of new SGIP1 splice variants in HEK293 cells**

According to the NCBI Gene database, SGIP1 gene might produce as many as 20 SGIP1 variants due to alternative splicing. However, only 4 splice variants have been identified so far. By isolating mRNA from three different mouse brain regions and subsequent transcription into cDNA by reverse transcriptase, we have identified 12 new, previously undescribed SGIP1 splice variants (Fig. 22 A). Subsequent analysis of sequences of the SGIP1 variants revealed that splicing takes place in N-terminus (exons 4 and 5) and central region (exons 16 to 20). To cover the sequence variability of these regions, we chose variants that differ in the aforementioned regions and cloned them into mammalian expression vectors using molecular biology techniques (Fig. 22 A, marked by a green rectangle).

As modifications in the sequence can affect protein expression, I tested whether the selected SGIP1 variants are expressed in the heterologous expression system by immunoblot using the antibody against SGIP1 N-terminal region conserved in all splice variants. In addition, I investigated whether the length of this novel SGIP1 variants can be compared to native SGIP1 of protein samples derived from the prefrontal cortex (PFC) of the mouse brain.

Immunoblot analysis demonstrated that all tested SGIP1 variants are expressed in the HEK293 cell line. A sample derived from the mouse brain produced two bands. The upper band of brain lysate migrated slower than the bands of tested splice variants (Fig. 22 B).

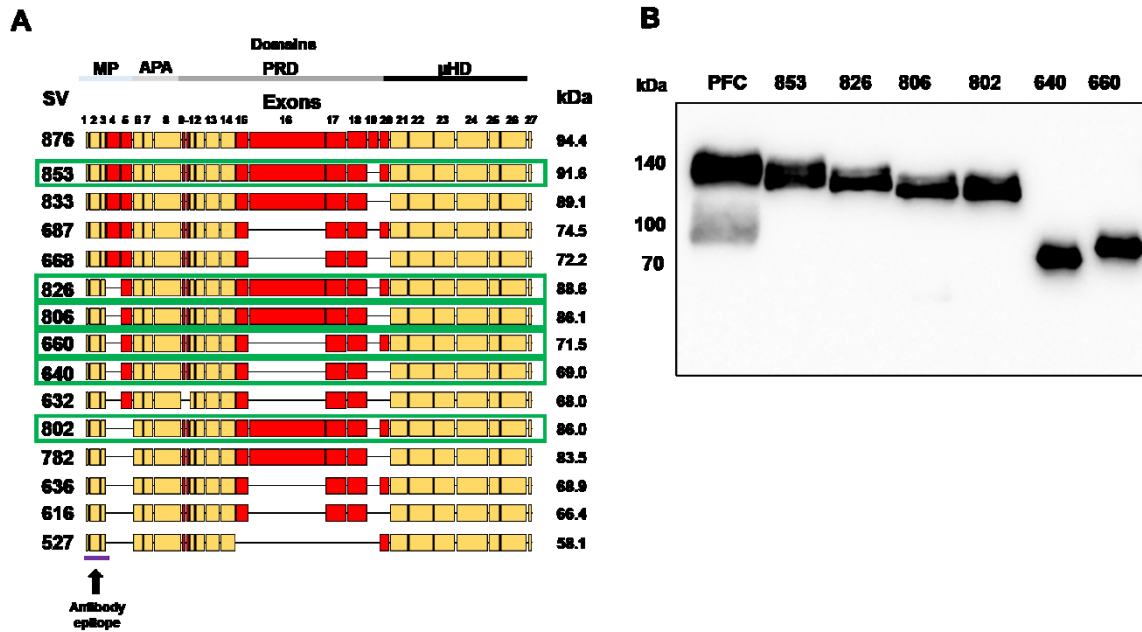


**Fig. 22 List of identified SGIP1 splice variants. Tested SGIP1 variants are expressed in HEK293 cells. A)** Schematic representation of SGIP1 variants, named according to the number of amino acids they are composed of. The SGIP1 variants selected for cloning into a mammalian expression vector and subsequently tested are marked by a green rectangle. Yellow color represents conserved exons, and red color depicts exons involved in the alternative splicing. MP – membrane binding domain, APA – AP2 activating domain, PRD – proline-rich domain,  $\mu$ HD –  $\mu$  homology domain SV – splice variant. **B)** Western blot analysis of selected SGIP1 variants and brain sample. HEK293 cells were transiently transfected with the indicated SGIP1 variant. Cell lysates and protein sample derived from the mouse's prefrontal cortex were separated by SDS-PAGE and subjected to Western blotting. Membranes were stained with anti-SGIP1 antibody that recognizes the conserved N-terminal region (marked by a purple line in A) section of this figure). PFC – prefrontal cortex.

#### 4.14. SGIP1 splice variants attenuate CB1R internalization

It was reported that SGIP1 significantly decreases WIN-induced CB1R internalization in HEK293 cells (Hajkova et al., 2016). Thus, I investigated whether SGIP1 variants with differences in the MP and PRD domain structures exhibit the same internalization-impeding properties as previously studied SGIP1 (which corresponds to the 806 amino acid variant). To assess the internalization of CB1R in the presence of SGIP1 variants in HEK293 cells, the HTRF-based method was used. The principle of this method lies in the resonance energy transfer between the energy donor fluorophore-tagged CB1R (terbium cryptate - SNAP-Lumi4-Tb) and energy acceptor fluorophore (fluorescein in the media). When the tagged receptor is present on the cellular membrane, its fluorescent signal

is quenched by the fluorescein in the media. Thus, receptor internalization can be observed as an increase in donor signal, as the signal is not quenched by fluorescein anymore.

WIN stimulation of CB1R in the absence of SGIP1 (mock) resulted in rapid receptor internalization with the maximum at 60 minutes. Interestingly, the presence of all SGIP1 variants inhibited CB1R internalization to comparable extent as previously described SGIP1 (806 aa) (Fig. 23 A). Therefore, alterations in N-terminal (exons 4, 5) and central (exons 16, 20) regions of SGIP1 did not affect the ability to suppress CB1R internalization. Next, to show that SGIP1 is a specific inhibitor of CB1R internalization, we tested DAMGO-induced internalization of  $\mu$ -opioid receptor (MOR) in the presence of SGIP1 isoforms. Neither of SGIP1 splice isoforms affected MOR endocytosis (Fig. 23 B).

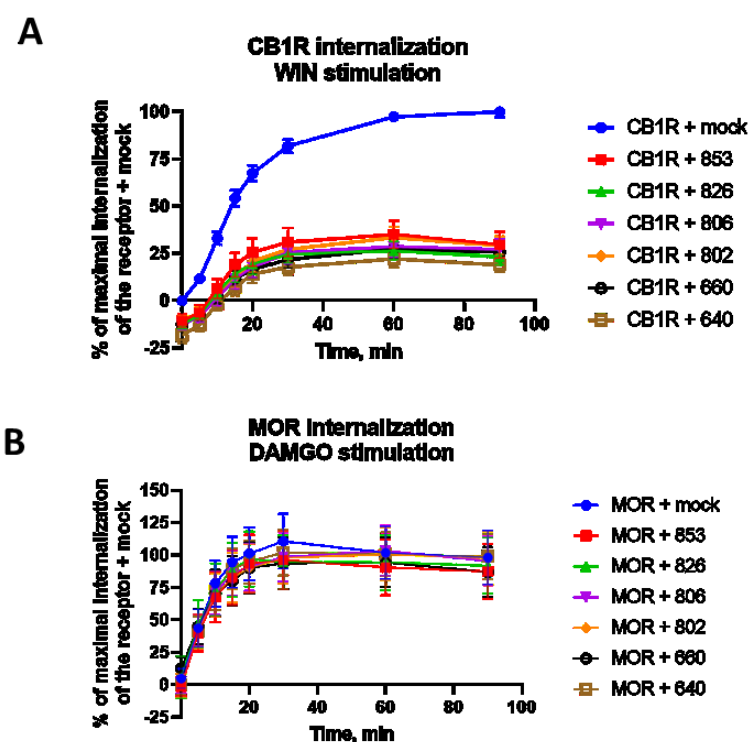


**Fig. 23 SGIP1 splice variants decrease the internalization of activated CB1R.** HEK293 cells were transiently co-transfected with the plasmids coding CB1R-SNAP/MOR-SNAP and SGIP1-Flag variant or empty plasmid pRK6 (1:2 ratio). Data were calculated from three experiments of independent cell preparations performed in three technical replicates. **A)** The kinetics of CB1R internalization in the presence of SGIP1 variants. Cells were stimulated by 1  $\mu$ M WIN. Data represent the relative level of CB1R internalization calculated as the percentage of the maximal CB1R + pRK6 internalization after 1  $\mu$ M WIN stimulation. **B)** The kinetics of MOR internalization in the presence of SGIP1 variants. Cells were stimulated by 1  $\mu$ M WIN. Data represent the relative level of MOR internalization calculated as the percentage of the maximal MOR + pRK6 internalization after 5  $\mu$ M DAMGO stimulation.

## 5. Discussion

The presented thesis aims to describe the roles of molecules involved in the regulation and desensitization of cannabinoid receptor 1. The role of GRK3 in facilitating the interactions of CB1R with proteins relevant to receptor regulation was evaluated using an array of techniques. Furthermore, events surrounding CB1R C-terminal tail phosphorylation during desensitization and interactions of regulatory proteins with the CB1R were studied and described. Lastly, I analyzed the impact of SGIP1 on the aforementioned events, and we depicted novel splice variants of SGIP1.

### 5.1. Activation of GRK3 is crucial for CB1R desensitization

GRK3, together with  $\beta$ -arrestins, execute a crucial role in the regulation and desensitization of numerous GPCRs, including CB1R (Appleyard et al., 1999; Bawa, Altememi, Eikenburg, & Standifer, 2003; Celver, Lowe, Kovoor, Gurevich, & Chavkin, 2001; Dautzenberg & Hauger, 2001; Dautzenberg, Wille, Braun, & Hauger, 2002; Jin et al., 1999; Luo & Benovic, 2003). Given the vital role of this kinase and arrestins, I studied the relationship between GRK3 activity and its ability to associate with CB1R and other signaling molecules like  $\beta$ -arrestin2 using a pharmacological inhibitor of GRK2/3 activity – cmpd101, in tandem with BRET-based sensors. As a heterologous expression system, transiently transfected human embryonic kidney 293 cells (HEK293) cells were used because they do not naturally express CB1R and SGIP1 and are widely used for studying the protein-protein interaction.

The GRK2/3 family contains a regulator of G protein signaling homology (RH) domain, which is essential for regulating its activity (Carman et al., 1999; Tesmer, 2009). The RH domain stabilizes the kinase domain in an open conformational state that renders GRK3 inactive (Homan & Tesmer, 2014; Lodowski, Tesmer, Benovic, & Tesmer, 2006). In order to become catalytically active, GRK3 undergoes conformation-induced rearrangement resulting in interaction with the activated GPCR and G $\beta\gamma$  subunits (Nogues et al., 2017). Cmpd101 binds deep in the active site (site responsible for kinase activity) of the GRK2/3 family but also partially binds to the ATP-binding site, stabilizing kinase in the inactive conformation and inhibiting the kinase activity (Ikeda S, 2007; Thal et al., 2011). This pharmacological tool thus allows studying the impact of inhibited GRK2/3 in the cells.

In the basal state, GRK3 is predominantly located in the cytoplasm. However, following the GPCR stimulation and subsequent G protein activation, cytosolic GRK3 translocates to the plasma membrane via interaction with G protein  $\beta\gamma$  dimer (Daaka et al., 1997; Touhara, Inglese, Pitcher, Shaw, & Lefkowitz, 1994). This interaction brings GRK3 to the close proximity of the receptor, which is consequently phosphorylated within its third intracellular loop and C-terminal tail (Boughton et al., 2011). Our results support these findings by showing that the activation of CB1R resulted in the rapid association of GRK3 with G $\beta\gamma$ . Interestingly, the application of cmpd101 significantly decreased the formation of GRK3-G $\beta\gamma$  complexes, albeit the interaction was not completely inhibited (Fig. 11 A). To exclude the option that the inhibition was due to altered WIN potency and not the activity of cmpd101 itself, a control experiment assessed WIN dose-response in cells treated or not with cmpd101 was performed. The results confirm that the potency of WIN in the presence of cmpd101 remains unchanged (Fig. 11 C). BRET is a sensitive technique for studying protein-protein interactions, and changes in the distance between the energy donor and acceptor, or their relative orientation, can result in modified BRET sensitivity (Bacart, Corbel, Jockers, Bach, & Couturier, 2008). However, structural data of cmpd101 binding to GRK3 do not support the notion that the lower BRET signal could result from the altered distance between cmpd101-bound GRK3-Rluc8 and G $\beta\gamma$ -YFP (Thal et al., 2011). Taken together, the decrease of BRET signal in the presence of cmpd101 is likely due to inhibited GRK3-G $\beta\gamma$  interaction, meaning GRK3 has to be in the active conformation in order to interact with G $\beta\gamma$  dimers optimally.

Next, the interaction between CB1R and GRK3 in the presence, or absence of cmpd101 was evaluated. Stimulation of CB1R resulted in the recruitment of GRK3 that peaked around 5 minutes and then progressively decreased to basal levels, indicating the transient nature of the GRK3-CB1R coupling. When the cells were pretreated with cmpd101, an inhibitor of GRK3 activation, this interaction was abolished (Fig. 12). Therefore, a catalytically active state of GRK3 is required for its interaction with activated CB1R. In light of the previous observation, hindered formation of CB1R-GRK3 complexes is likely due to inhibited interaction of GRK3 with G $\beta\gamma$  that would otherwise bring the cytosolic kinase to the membrane and close proximity of the receptor.

Accumulating evidence shows that CB1R desensitization and internalization depend on the activity of both GRK3 and  $\beta$ -arrestin2 (Daigle, Kwok, et al., 2008; Gyombolai, Boros, Hunyady, & Turu, 2013). The importance of  $\beta$ -arrestin2 was also demonstrated by *in vivo*

studies of  $\beta$ -arrestin2 knockout mice, which exhibited increased sensitivity to THC, enhanced nociception and decreased tolerance, typical symptoms of impaired CB1R desensitization (Breivogel, Lambert, Gerfin, Huffman, & Razdan, 2008; P. T. Nguyen et al., 2012). Given the importance of GRK3 and  $\beta$ -arrestin2 in CB1R desensitization, the role of GRK3 in mediating CB1R- $\beta$ -arrestin2 interaction was studied using cmpd101.

WIN activation of CB1R led to the recruitment of  $\beta$ -arrestin2, with the peak between 5 and 10 minutes, then gradually decreased. Conversely, cells pretreated with cmpd101 did not exhibit  $\beta$ -arrestin2 association after CB1R activation (Fig. 13). Unlike previous experiments, where the nature of transiently expressed GRK3 was studied, this experiment used the native pool of this kinase. However, as HEK293 cells naturally express both GRK3 and GRK2 (Moller et al., 2020), and cmpd101 is indeed the inhibitor of both these kinases, the possibility that the inhibition of native GRK2 played a certain role in the attenuation of CB1R- $\beta$ -arrestin2 interaction cannot be excluded. Future experiments could address this question by either using GRK2 knock-out cell line or GRK2 expression interference, for example, by introducing specific siRNA to the cells. Nevertheless, the work of Jin and colleagues showed that desensitization of CB1R expressed in *Xenopus* oocytes was dependent on the presence of both GRK3 and  $\beta$ -arrestin2. The expression of  $\beta$ -arrestin2 itself was not sufficient to promote CB1R desensitization (Jin et al., 1999). Our data support this observation, as the kinase activity of GRK2/3 is required for efficient and rapid  $\beta$ -arrestin2 recruitment to the activated CB1R.

Taken together, this study demonstrated the catalytically active state of GRK3 is required for its proper interaction with CB1R and G $\beta$  $\gamma$  heterodimers. Apart from this, the activity of the GRK3 is required for the recruitment of  $\beta$ -arrestin2 by activated CB1R in HEK293 cells.

## **5.2. Two regions of CB1R C-terminus play an essential role in mediating CB1R interactions with GRK3 and $\beta$ -arrestin2**

Like in all GPCRs, CB1R C-tail mediates signaling via direct interaction with signaling and regulatory molecules like G proteins, GRKs, or  $\beta$ -arrestins, and facilitates desensitization and receptor internalization (Stadel, Ahn, & Kendall, 2011). This region features two clusters of serine/threonine residues that are implied to participate in CB1R desensitization and internalization, namely <sup>425</sup>SMGDS<sup>429</sup> and <sup>460</sup>TMSVSTDTS<sup>468</sup> (human

CB1R numbering, corresponding to rat/mouse CB1R <sup>426</sup>SMGDS<sup>430</sup> and <sup>461</sup>TMSVSTDTS<sup>469</sup>) (Bakshi, Mercier, & Pavlopoulos, 2007; Daigle, Kwok, et al., 2008; Hsieh et al., 1999; Jin et al., 1999; Morgan et al., 2014; Singh et al., 2008; Straiker et al., 2012). Despite the reports, the relationship between these phosphorable regions and the binding of GRK3 or  $\beta$ -arrestins2 was not clear.

To address this, a set of CB1R C-tail phosphorylation mutants was created by mutating serine and threonine residues in <sup>425</sup>SMGDS<sup>429</sup> and <sup>460</sup>TMSVSTDTS<sup>468</sup> either to alanine or aspartic acid. Alanine was chosen for it is chemically inert, and most importantly, it cannot be phosphorylated, thus mimics an unphosphorylated state of a protein. On the other hand, aspartic acid mimics phosphoserine with its negative charge, thus allowing studying of protein in its phosphorylated-like form.

CB1R phosphorylation mutants were characterized prior their use in the protein-protein interaction experiments. Immunoblotting analysis demonstrated that CB1R mutants exhibited comparable expression levels to WT CB1R (Fig. 15 A). The cellular localization of mutant receptors was analyzed by fluorescent confocal imaging. All CB1R variants were, similarly to WT CB1R, predominantly localized on the cellular membrane. The detected intracellular portion of CB1R likely corresponds to trafficked receptors - newly synthesized or internalized from the membrane. Lastly, the functionality of mutated receptors was determined via activation of G protein in BRET-based assay. WIN stimulation of all CB1R receptors resulted in dissociation/conformational change of  $G\alpha_{i1}$ - $G\gamma_2$  complex, proving that C-tail phosphorylation mutants retain the ability to activate  $G\alpha_{i1}$  protein signaling pathway (Fig. 16).

GPCR signaling is not a linear progression of events where one type of receptor always elicits the same signaling response. A GPCR can activate different signaling cascades (a phenomenon called biased signaling), depending on various factors, including cellular context. Growing evidence supports a „phosphorylation barcode“ hypothesis, which states that different ligands induce specific patterns of the C-tail phosphorylation that mediate distinct signaling through interaction with different effectors (Liggett, 2011; Reiter, Ahn, Shukla, & Lefkowitz, 2012). Thus, the CB1R C-tail phosphorylation patterns mutants were tested to determine whether they exhibited altered G protein signaling. First, the efficiency with which the mutant receptors drive  $G\alpha_{i1}$  protein activity was studied. There was no significant difference in acute  $G\alpha_{i1}$  protein activation between WT CB1R and CB1R phosphorylation mutants (Fig. 17 A). Secondly, the extent of inositol monophosphate release

mediated by  $G\alpha_{qi9}$  activation was studied.  $G\alpha_{qi9}$  is a chimeric G protein that permits  $G_{i/o}$ -coupled receptors to activate  $G\alpha_q$ -driven inositol monophosphate production. Neither in this case was observed a change in activation of  $G_{qi9}$ , as IP1 production was comparable between WT CB1R and CB1R mutants (Fig. 17 B). These results show that G protein activation is not modified by CB1R phosphorylation pattern mutants.

The study of the interaction of GRK3 with CB1R phosphorylation pattern mutants yielded two significant findings. First, stimulation of CB1R\_2A (with the S425A, S429A mutations) resulted in a significantly enhanced and prolonged GRK3 recruitment (Fig. 19 B). On the other hand, the GRK3 recruitment profile of CB1R\_2D mutant, which mimics the phosphorylated state of these residues, resembled that of CB1R WT (Fig. 19 E). The results thus indicate that serines of  $^{425}\text{SMGDS}^{429}$  regulate the dynamics of GRK3-CB1R dissociation, presumably via GRK3 phosphorylation activity.

Secondly, the alanine replacement of serine and threonine residues within the  $^{460}\text{TMSVSTDTS}^{468}$  motif in CB1R\_6A significantly attenuated, but did not fully inhibited GRK3 recruitment to the receptor implying that serine/threonine residues in the  $^{425}\text{SMGDS}^{429}$  motif are sufficient for GRK3 binding, albeit with reduced efficiency. This observation is also supported by CB1R\_8A, with simultaneous mutation of both regions, which showed entirely inhibited GRK3 recruitment (Fig. 19 D). Mutation of serine/threonines of  $^{460}\text{TMSVSTDTS}^{468}$  into aspartic acid in mutant CB1R\_6D rescued GRK3 coupling only partially (Fig. 19 E). This was even more apparent in the CB1R\_8D mutant, with aspartic acid mutations in both motives, where the kinetics of GRK3 recruitment differed even more from that of WT CB1R (Fig. 19 E). Two possibilities can explain this partial recovery. Firstly, aspartic acid features only a single negative charge, while phosphoserine contains a double negative charge. Therefore, the aspartic acid charge could be insufficient for proper GRK3 binding. The second explanation is that phosphorylation is a dynamic process involving consecutive phosphorylation of the residues or partial phosphorylation of the motifs, which is not reflected by constitutively charged aspartic acid in the corresponding CB1R mutants.

Based on these observations, I propose a hypothesis that phosphorylation of  $^{425}\text{SMGDS}^{429}$  residues by GRK3 governs the dynamics of GRK3-CB1R coupling while the serines/threonines within  $^{460}\text{TMSVSTDTS}^{468}$  regions favor the kinase recruitment. Moreover, the subsequent phosphorylation of  $^{425}\text{SMGDS}^{429}$  induces the dissociation of GRK3 from the receptor.

Interestingly, for the most part, GRK3 was able to associate with G $\beta\gamma$  regardless of CB1R C-tail phosphorylation patterns, albeit the interaction was marginally altered. CB1R mutants that exhibited impaired GRK3 recruitment (CB1R\_6A and CB1R\_8A) also showed decreased GRK3-G $\beta\gamma$  coupling (Fig. 18 C & D), whereas CB1R\_2A, mutant with augmented CB1R-GRK3 association, facilitated increased GRK3-G $\beta\gamma$  complex formation (Fig. 18 B). As the phosphorylation patterns of CB1R did not modify the G protein activation, slightly altered GRK3-G $\beta\gamma$  coupling is not caused by a different quantity of released G $\beta\gamma$  available for GRK3 recruitment, but rather by the phosphorylation pattern of the CB1R C-tail that stabilizes the GRK3-G $\beta\gamma$  complex. The other possibility is that in the absence of GRK3 binding to CB1R mutants, GRK3 acquires different conformational states with G $\beta\gamma$  which is reflected as altered BRET signal in the experiment.

Several studies postulated that GRKs might modify G protein activity independently of the receptor phosphorylation (Breton, Lagace, & Bouvier, 2010; Dhimi, Anborgh, Dale, Sterne-Marr, & Ferguson, 2002). The GRK interactomes consist of a plethora of proteins involved in cellular signaling, including PI3K, GIT, MEK, AKT, RKIP, calmodulin, clathrin, and caveolin (Ribas et al., 2007). Since GRK3 is still able to sequester G $\beta\gamma$ , even in the absence of binding and phosphorylation of CB1R mutants, it is possible that the pool of signaling molecules that GRK3 interacts with may be modified. However, this hypothesis requires further investigation that is out of the scope of this thesis.

The crucial role of the <sup>425</sup>SMGDS<sup>429</sup> and <sup>460</sup>TMSVSTDTS<sup>468</sup> regions in the regulation of CB1R is also illustrated by the results obtained with the CB1R- $\beta$ -arrestin2 interaction assays. Mutation of serine residues to alanines within <sup>425</sup>SMGDS<sup>429</sup> motif in CB1R\_2A significantly reduced the recruitment of  $\beta$ -arrestin2 to the activated receptor (Fig. 20 B). This finding is interesting in light of previous observations made by Daigle and colleagues (Daigle, Kearns, et al., 2008). Using quantitative analysis of fluorescent confocal images, the authors observed that mutant CB1R\_2A recruited  $\beta$ -arrestin-2 to a similar extent as wild type receptor to the plasma membrane, while in our experiment, the interaction was decreased. This discrepancy can be explained by the distinct techniques used in each study. While Daigle and colleagues used quantitative analysis of fluorescent confocal images to reveal  $\beta$ -arrestin-2 translocation from the cytoplasm toward the membrane, our study facilitated BRET, a highly sensitive method allowing a more specific depiction of protein-protein interactions in comparison with the former technique. The other explanation of discrepancies

in studies is that  $\beta$ -arrestin2 might acquire a different conformational state with CB1R\_2A than with the wild type receptor (Cahill et al., 2017; Nuber et al., 2016). While the distinct conformational change could be reflected as decreased BRET signal, it cannot be observed by conventional confocal imaging. However based on data of CB1R-GRK3 recruitment, I hypothesize that decreased  $\beta$ -arrestin2 interaction with CB1R\_2A is a consequence of prolonged GRK3-CB1R\_2A interaction. Due to higher affinity between GRK3 and CB1R\_2A, this kinase could sterically block the interaction of  $\beta$ -arrestin2 with the CB1R\_2A.

CB1R\_8A, with all serines and threonines mutated to alanines in both <sup>425</sup>SMGDS<sup>429</sup> and <sup>460</sup>TMSVSTDTS<sup>468</sup> regions, completely lost the ability to recruit  $\beta$ -arrestin2 (Fig. 20 D). Interestingly, CB1R\_6A with mutated residues only within <sup>460</sup>TMSVSTDTS<sup>468</sup> exhibited a comparably impaired kinetic profile as CB1R\_8A. Thus, serine/threonine residues of <sup>460</sup>TMSVSTDTS<sup>468</sup> are critical for  $\beta$ -arrestin2 recruitment, and <sup>425</sup>SMGDS<sup>429</sup> region by itself is insufficient to mediate recruitment. Here, the data support and augment the findings of previous studies that <sup>460</sup>TMSVSTDTS<sup>468</sup> motif within extreme CB1R C-tail region serves as the primary initiation docking site for  $\beta$ -arrestin2 followed by the  $\beta$ -arrestin2 interaction with <sup>425</sup>SMGDS<sup>429</sup> region (Blume et al., 2017; Jin et al., 1999; Morgan et al., 2014).

All phosphomimetic aspartic acid CB1R mutants exhibited decreased  $\beta$ -arrestin2 binding (Fig. 20 E). This suggests that selective phosphorylation of serine and threonine residues or alternatively, a particular phosphorylation pattern – bar code is required for proper CB1R- $\beta$ -arrestin2 coupling. This possibility was tested in more detail by creating additional CB1R mutants with several combinations of alanine replacements within <sup>425</sup>SMGDS<sup>429</sup> and <sup>460</sup>TMSVSTDTS<sup>468</sup> and subsequently subjecting them to experiments. These CB1R variants with different triple alanine mutations in the extreme C-terminus tail exhibited similarly decreased, but not completely diminished recruitment of  $\beta$ -arrestin2 regardless of the presence/absence of alanine mutations in <sup>425</sup>SMGDS<sup>429</sup> region, meaning that both serine and threonine residues within <sup>460</sup>TMSVSTDTS<sup>468</sup> motif contribute to  $\beta$ -arrestin2 recruitment in a graded fashion (Fig. 21 D). This observation underlies the hypothesis that sequential and cumulative phosphorylation of serine/threonine residues in <sup>460</sup>TMSVSTDTS<sup>468</sup> region of CB1R regulates the rate of  $\beta$ -arrestin2 recruitment (Daigle, Kwok, et al., 2008). However, the possibility that the observed lower BRET signal induced by phosphorylation pattern CB1R mutants reflects unique  $\beta$ -arrestin2 conformation states cannot be discarded. Future research could resolve this question by using  $\beta$ -arrestin2-

NanoLuc or FAsH-based biosensors that can reveal distinct conformational signatures of  $\beta$ -arrestin2 (Haider et al., 2022).

The GRK3 recruitment experiments with the same CB1R phosphorylation pattern mutants revealed that serines rather than threonines in <sup>460</sup>TMSVSTDTS<sup>468</sup> are crucial for CB1R-GRK3 coupling. However, as the substitution of the threonines with alanine residues did not prevent CB1R-GRK3 recruitment entirely, it is possible that these residues play a role in the CB1R-GRK3 interaction. One of the possible scenarios is that the interplay between serine and threonine residues dictates the dynamics of GRK3 with the CB1R. Altogether, the data show that serines and threonines of CB1R <sup>425</sup>SMGDS<sup>429</sup> and <sup>460</sup>TMSVSTDTS<sup>468</sup> motifs distinctly govern the GRK3 and  $\beta$ -arrestin2.

The study of the presented thesis underlines the importance of GRK3 and multisite phosphorylation in the process of CB1R desensitization. It remains to be determined whether other GPCRs are subjected to similar phosphorylation mechanisms as those that regulate the dynamics of GRK3 and  $\beta$ -arrestin2 in CB1R interaction. Interestingly, Meiss and colleagues report that phosphorylation of extreme C-tail serine/threonine cluster is involved in GRK2 and  $\beta$ -arrestin2 recruitment, while the proximal serine/threonine cluster is involved in the stability of these interactions (Miess et al., 2018). This points to the parallel mechanism that is reported in this thesis. Detailed investigation of regions critical for GRKs and  $\beta$ -arrestins docking and activation may help us understand the mechanism governing receptor desensitization, potentially leading to new therapeutic strategies. One possible approach is targeting GRKs and their activity (Murga et al., 2019). This thesis demonstrates that inhibition of GRK activity, for example, by a small pharmacological inhibitor like cmpd101, can profoundly impact GPCR signaling and desensitization.

### **5.3. SGIP1 enhances GRK3-G $\beta$ $\gamma$ , CB1R-GRK3, and CB1R- $\beta$ -arrestin2 interactions**

SGIP1, an interaction partner of CB1R, is a protein with profound physiological impact (Cummings et al., 2012; Dergai et al., 2010; Dvorakova et al., 2021; Hajkova et al., 2016; Trevaskis et al., 2005; Yako et al., 2015). Co-expression of SGIP1 affects CB1R properties like enhanced and prolonged CB1R- $\beta$ -arrestin2 association upon the receptor activation and decreased ERK1/2 phosphorylation, presumably due to stalled CB1R internalization (Hajkova et al., 2016). Therefore, it is likely that SGIP1 affects other interactions upstream of CB1R- $\beta$ -arrestin2 coupling as well. This hypothesis was tested by studying additional protein-protein interactions mediated by CB1R in the presence and

absence of SGIP1. The GRK3 binding of G $\beta\gamma$  subunits following activation of the CB1R was enhanced by SGIP1. In addition, the presence of SGIP1 also augmented GRK3 association with CB1R. As GRK3-G $\beta\gamma$  and CB1R-GRK3 interactions occur virtually immediately after CB1R stimulation, these data support the previously postulated hypothesis that SGIP1 prevents CB1R internalization at early stages following the receptor activation.

Interestingly, SGIP1 augmented GRK3-G $\beta\gamma$ , CB1R-GRK3, and CB1R- $\beta$ -arrestin2 interactions in CB1R phosphorylation mutants that maintained the ability to associate with the interaction partners but could not rescue these interactions in mutants that exhibited no recruitment of GRK3 and  $\beta$ -arrestin2. This observation has two implications. Firstly, C-tail phosphorylation patterns of CB1R do not affect SGIP1 association with CB1R. This is in agreement with previously published data which showed using a yeast two-hybrid screen that SGIP1 binds to CB1R regardless of the presence of different phosphomimetic mutations in the C-terminus of CB1R (Hajkova et al., 2016). Secondly, SGIP1 modifies CB1R properties via stalling the internalization of CB1R bound to interaction partners as a whole interactome complex and not via direct interaction of SGIP1 with GRK3 and  $\beta$ -arrestin2.

#### **5.4. Characterization of novel SGIP1 splice variants**

Although Gene database reports as many as 20 possible SGIP1 splicing variants (NCBI, 2022), previous SGIP1 studies characterized only 4 isoforms. In our laboratory, the analysis of mRNA derived from a mouse brain resulted in identifying 12 unique previously undescribed SGIP1 splice variants. The subsequent sequence comparison showed that most splicing occurs in the PRD domain (between exons 16 and 20) and in the N-terminal MP domain (exons 4 and 5). As sequence alterations can change the expression and function of a protein, six SGIP1 splice variants were chosen for testing to cover the sequence variability of regions affected by alternative splicing. The expression of these splice variants in HEK293 cells was tested by immunoblot, and their length was compared with SGIP1 of protein samples derived from mouse brain. Interestingly, the bands of tested SGIP1 splice variants differed from those derived from the mouse prefrontal cortex. This disparity can be explained by distinct or missing posttranslational modifications of SGIP1 in HEK293 cells. The PRD domain of SGIP1 contains numerous potential phosphorylation sites, and indeed it was reported that SGIP1 is a heavily phosphorylated protein (Huttlin et al., 2010). On top of that, lysines of the FCHO2  $\mu$ HD domain (homolog of SGIP1) undergo ubiquitination (Uezu et al., 2011). As  $\mu$ HD domains between SGIP1 and FCHO2 exhibit a high level of

sequence conservation, SGIP1 in the brain may undergo ubiquitination that is different or absent in HEK293 cells.

Functional testing showed that all selected SGIP1 splice variants, including SGIP1 previously reported by Hájková and colleagues (corresponding to 806 aa) (Hajkova et al., 2016), hindered CB1R endocytosis. This observation implies that the variations in the MP and PRD domain sequences do not alter the inhibitory effect on CB1R internalization. The fact that SGIP1 variants lacking exon 4, 5, or both maintained the internalization-inhibiting feature demonstrates that these exons are not vital for the SGIP1 effect on CB1R. MP domain was shown to bind and deform cellular membranes (Trevaskis et al., 2005). The first three exons of SGIP1, conserved among variants, code the N-terminal part of the MP domain containing four arginine and eight lysine residues. These positively-charged residues are likely sufficient for SGIP1 to bind to the membrane. It has been demonstrated that SGIP1 interacts with CB1R via SGIP1  $\mu$ HD (Hajkova et al., 2016). As  $\mu$ HD and APA2 remain unaltered across SGIP1 splice variants, these regions may be essential for SGIP1 function. Further investigation is required to explain the function of exons 4 and 5. Neither of SGIP1 splice variants altered the specificity of the SGIP1-CB1R interaction, and none of the isoforms affected MOR internalization.

While this thesis establishes a basis for the characterization of SGIP1 splice variants, further studies are required to reason the existence of various SGIP1 forms. Different SGIP1 splice variants may be expressed in distinct brain regions or neuron subtypes with diverse functionalities. The immunohistochemistry of brain slices could answer this. However, the SGIP1 splice variant-specific antibodies would have to be developed as current SGIP1 antibodies target the regions that are conserved among splice variants.

## 6. Conclusions

The objective of this thesis was to describe and characterize molecular aspects that govern the regulation of cannabinoid receptor 1 (CB1R) signaling and desensitization.

Using bioluminescence.. method in tandem with pharmacological tools, I show that G protein-coupled receptor kinase 3 (GRK3) is an important regulator of CB1R. GRK3 must be in the active state to couple to the activated CB1R or G $\beta\gamma$  subunits of G proteins. In addition, the recruitment of  $\beta$ -arrestin2 to CB1R is dependent on the activity of GRK2/3.

CB1R C-terminal tail features two serine/threonine clusters, <sup>425</sup>SMGDS<sup>429</sup> and <sup>460</sup>TMSVSTDTS<sup>468</sup>, that are crucial in facilitating CB1R interactions with GRK3 and  $\beta$ -arrestin2. <sup>460</sup>TMSVSTDTS<sup>468</sup> motif favors GRK3 recruitment while <sup>425</sup>SMGDS<sup>429</sup> region regulates the stability of GRK3-CB1R interaction. In the case of  $\beta$ -arrestin2, the <sup>460</sup>TMSVSTDTS<sup>468</sup> motif serves as the primary initiation docking site, followed by the  $\beta$ -arrestin2 interaction with the <sup>425</sup>SMGDS<sup>429</sup> region. In addition, distinct phosphorylation patterns or “bar codes” within the CB1R C-terminal region are required for GRK3 and  $\beta$ -arrestin2 binding to CB1R. GRK3 couples to G $\beta\gamma$  regardless of CB1R C-tail phosphorylation patterns, albeit the interaction is likely stabilized by CB1R-GRK3 coupling.

Src homology 3-domain growth factor receptor-bound 2-like (endophilin) interacting protein 1 (SGIP1) enhances CB1R interactions with GRK3,  $\beta$ -arrestin2 as well as GRK3-G $\beta\gamma$  coupling. SGIP1 cannot rescue interactions that are inhibited by CB1R phosphorylation patterns. Thereby, SGIP1 regulates the dynamics of interactions between molecules that are part of the temporal CB1R signalosome established during desensitization. The alterations in SGIP1 proline-rich domain (PRD) and membrane phospholipid binding domain (MP) due to alternative splicing do not affect SGIP1 expression in HEK293 cells, nor the inhibitory effect on CB1R endocytosis.

In conclusion, this thesis's data and observations contribute to understanding the molecular mechanisms controlling CB1R signaling and desensitization. More profound knowledge of molecular events involved in these processes represents a crucial step in creating therapeutic approaches based on the modulation of the endocannabinoid system.

## 7. Summary

The endocannabinoid system is an important regulator of synaptic plasticity and plays a crucial role in many central nervous system (CNS) functions and its development. Cannabinoid receptor 1 (CB1R) is expressed most densely in CNS and is a target for endocannabinoids and phytocannabinoids, such as  $\Delta^9$ -THC. Activity and signaling of CB1R are tightly regulated, mainly via receptor desensitization and internalization, as abnormal activity and dysregulation of CB1R results in a broad spectrum of pathological conditions.

This study describes molecules and events surrounding CB1R desensitization in more details. The presented data and observations show that two serine/threonine-rich regions of CB1R, <sup>425</sup>SMGDS<sup>429</sup> and <sup>460</sup>TMSVSTDTS<sup>468</sup>, are involved in the recruitment of molecules involved in receptor desensitization: G protein-coupled receptor kinase 3 (GRK3) and  $\beta$ -arrestin2. I demonstrate that GRK3 has to be in active conformation to form complexes with CB1R or G protein subunits G $\beta\gamma$ . Furthermore, the recruitment of  $\beta$ -arrestin2 to CB1R depends on the activity of GRK2/3.

I show that the interaction partner of CB1R Src homology 3-domain growth factor receptor-bound 2-like (endophilin) interacting protein 1 (SGIP1) profoundly modifies the dynamics of signalosome interactions during CB1R desensitization. In addition, I characterize newly identified splice variants of SGIP1 and demonstrate that alternative splicing-based alteration in SGIP1 domains do not affect CB1R internalization-hindering properties of SGIP1.

Characterizing the events that drive the interactions involved in CB1R desensitization represents a pivotal step in understanding cannabinoid signaling and tolerance development. Such knowledge is central for further pharmacological management of disease states in which the endocannabinoid system is involved as well as for understanding the impact of regular cannabis use.

## 8. Shrnutí

Endokanabinoidní systém (ECS) hraje klíčovou roli v mnoha funkcích a vývoji centrálního nervového systému (CNS), je stěžejní v procesu synaptické plasticity, řídí homeostázu synaptických spojů. Centrální molekulou nervového ECS je kanabinoidní receptor 1 (CB1R). tento receptor je v CNS hojně exprimován, aktivován je endokanabinoidy a fyto-kanabinoidy, nejznámější je tetrahydrokanbinol  $\Delta^9$ -THC, jedna z aktivních složek marijuany. Signalizace CB1R podléhá sofistikované regulaci, především prostřednictvím desenzitizace a internalizace receptoru.

Tato práce podrobněji popisuje děje spjaté s desenzitizací CB1R, a popisuje interakce hlavních molekul zapojených v tomto procesu. Závěry našeho výzkumu naznačují, že dvě v koncové, nitro- buněčné části CB1R, bohaté na serin/treonin, <sup>425</sup>SMGDS<sup>429</sup> a <sup>460</sup>TMSVSTDTS<sup>468</sup>, se podílejí na vazbě molekul zapojených do desenzitizace receptoru: G proteinem spřažené receptorové kinázy 3 (GRK3) a  $\beta$ -arrestinu2. V této práci jsem prokázal, že GRK3 musí zaujmout aktivní konformaci proto, aby mohla vytvářet komplexy s CB1R nebo podjednotkami G proteinu G $\beta\gamma$ . Asociace  $\beta$ -arrestinu2 s CB1R je závislá na aktivitě GRK2/3.

Interakční partner CB1R Src homology 3-domain growth factor receptor-bound 2-like (endophilin) interacting protein 1 (SGIP1) zásadně modifikuje dynamiku interakcí CB1R signalosomu během desenzitizace. Námi nově identifikované sestřihové varianty SGIP1 se změnami ve sekvencích stěžejních domén SGIP1 způsobují asociaci s CB1R inhibici internalizace CB1R, avšak ani jedna varianta neovlivňuje mu- opioidní receptor.

Pochopení interakcí při desenzitizaci CB1R je stěžejní pro porozumění všech aspektů kanabinoidní signalizace, včetně rozvoje tolerance. Tyto znalosti jsou klíčové pro pochopení dopadu pravidelného užívání a rozvoje závislosti na marihuaně, avšak i na vývoj nových farmakologických přístupů, především vývoje látek pro léčbu chronické bolesti, posttraumatického syndromu, obezity a dalších patologických stavů, u nichž ovlivnění ECS má, nebo může mít prospěšné místo v moderní medicíně.

## 9. List of references

- Ahn, K. H., Mahmoud, M. M., & Kendall, D. A. (2012). Allosteric modulator ORG27569 induces CB1 cannabinoid receptor high affinity agonist binding state, receptor internalization, and Gi protein-independent ERK1/2 kinase activation. *J Biol Chem*, 287(15), 12070-12082. doi:10.1074/jbc.M111.316463
- Ahn K.H., Nishiyama, A., Mierke, D.F., Kendall, D.A. (2010). Hydrophobic residues in helix 8 of cannabinoid receptor 1 are critical for structural and functional properties. *Biochemistry*, 49:502–511. doi: 10.1021/bi901619r
- Antonny, B., Burd, C., De Camilli, P., Chen, E., Daumke, O., Faelber, K., . . . Schmid, S. (2016). Membrane fission by dynamin: what we know and what we need to know. *EMBO J*, 35(21), 2270-2284. doi:10.15252/embj.201694613
- Appleyard, S. M., Cerver, J., Pineda, V., Kovoov, A., Wayman, G. A., & Chavkin, C. (1999). Agonist-dependent desensitization of the kappa opioid receptor by G protein receptor kinase and beta-arrestin. *J Biol Chem*, 274(34), 23802-23807. doi:10.1074/jbc.274.34.23802
- Arshavsky, V. Y., & Burns, M. E. (2014). Current understanding of signal amplification in phototransduction. *Cell Logist*, 4, e29390. doi:10.4161/cl.29390
- Atwood, B. K., & Mackie, K. (2010). CB2: a cannabinoid receptor with an identity crisis. *British Journal of Pharmacology*, 160(3), 467-479. doi:10.1111/j.1476-5381.2010.00729.x
- Bacart, J., Corbel, C., Jockers, R., Bach, S., & Couturier, C. (2008). The BRET technology and its application to screening assays. *Biotechnol J*, 3(3), 311-324. doi:10.1002/biot.200700222
- Bakshi, K., Mercier, R. W., & Pavlopoulos, S. (2007). Interaction of a fragment of the cannabinoid CB1 receptor C-terminus with arrestin-2. *FEBS Lett*, 581(25), 5009-5016. doi:10.1016/j.febslet.2007.09.030
- Bawa, T., Altememi, G. F., Eikenburg, D. C., & Standifer, K. M. (2003). Desensitization of alpha 2A-adrenoceptor signalling by modest levels of adrenaline is facilitated by beta 2-adrenoceptor-dependent GRK3 up-regulation. *Br J Pharmacol*, 138(5), 921-931. doi:10.1038/sj.bjp.0705127
- Benard, G., Massa, F., Puente, N., Lourenco, J., Bellocchio, L., Soria-Gomez, E., . . . Marsicano, G. (2012). Mitochondrial CB1 receptors regulate neuronal energy metabolism. *Nature Neuroscience*, 15(4), 558-564. doi:10.1038/nn.3053
- Blume, L. C., Leone-Kabler, S., Luessen, D. J., Marrs, G. S., Lyons, E., Bass, C. E., . . . Howlett, A. C. (2016). Cannabinoid receptor interacting protein suppresses agonist-driven CB1 receptor internalization and regulates receptor replenishment in an agonist-biased manner. *Journal of Neurochemistry*, 139(3), 396-407. doi:10.1111/jnc.13767
- Blume, L. C., Patten, T., Eldeeb, K., Leone-Kabler, S., Ilyasov, A. A., Keegan, B. M., . . . Howlett, A. L. (2017). Cannabinoid Receptor Interacting Protein 1a Competition with beta-Arrestin for CB1 Receptor Binding Sites. *Molecular Pharmacology*, 91(2), 75-86. doi:10.1124/mol.116.104638
- Boguth, C. A., Singh, P., Huang, C. C., & Tesmer, J. J. (2010). Molecular basis for activation of G protein-coupled receptor kinases. *EMBO J*, 29(19), 3249-3259. doi:10.1038/emboj.2010.206
- Bond, R. A., & Ijzerman, A. P. (2006). Recent developments in constitutive receptor activity and inverse agonism, and their potential for GPCR drug discovery. *Trends Pharmacol Sci*, 27(2), 92-96. doi:10.1016/j.tips.2005.12.007
- Boughton, A. P., Yang, P., Tesmer, V. M., Ding, B., Tesmer, J. J., & Chen, Z. (2011). Heterotrimeric G protein beta1gamma2 subunits change orientation upon complex formation with G protein-coupled receptor kinase 2 (GRK2) on a model membrane. *Proc Natl Acad Sci U S A*, 108(37), E667-673. doi:10.1073/pnas.1108236108
- Brailoiu, G. C., Oprea, T. I., Zhao, P., Abood, M. E., & Brailoiu, E. (2011). Intracellular cannabinoid type 1 (CB1) receptors are activated by anandamide. *J Biol Chem*, 286(33), 29166-29174. doi:10.1074/jbc.M110.217463

- Breivogel, C. S., Lambert, J. M., Gerfin, S., Huffman, J. W., & Razdan, R. K. (2008). Sensitivity to delta9-tetrahydrocannabinol is selectively enhanced in beta-arrestin2 *-/-* mice. *Behav Pharmacol*, *19*(4), 298-307. doi:10.1097/FBP.0b013e328308f1e6
- Breton, B., Lagace, M., & Bouvier, M. (2010). Combining resonance energy transfer methods reveals a complex between the alpha2A-adrenergic receptor, Galphai1beta1gamma2, and GRK2. *FASEB J*, *24*(12), 4733-4743. doi:10.1096/fj.10-164061
- Brule, C., Perzo, N., Joubert, J. E., Sainsily, X., Leduc, R., Castel, H., & Prezeau, L. (2014). Biased signaling regulates the pleiotropic effects of the urotensin II receptor to modulate its cellular behaviors. *FASEB J*, *28*(12), 5148-5162. doi:10.1096/fj.14-249771
- Busquets-Garcia, A., Bains, J., & Marsicano, G. (2018). CB1 Receptor Signaling in the Brain: Extracting Specificity from Ubiquity. *Neuropsychopharmacology*, *43*(1), 4-20. doi:10.1038/npp.2017.206
- Butcher, A. J., Prihandoko, R., Kong, K. C., McWilliams, P., Edwards, J. M., Bottrill, A., . . . Tobin, A. B. (2011). Differential G-protein-coupled receptor phosphorylation provides evidence for a signaling bar code. *J Biol Chem*, *286*(13), 11506-11518. doi:10.1074/jbc.M110.154526
- Cahill, T. J., 3rd, Thomsen, A. R., Tarrasch, J. T., Plouffe, B., Nguyen, A. H., Yang, F., . . . Lefkowitz, R. J. (2017). Distinct conformations of GPCR-beta-arrestin complexes mediate desensitization, signaling, and endocytosis. *Proc Natl Acad Sci U S A*, *114*(10), 2562-2567. doi:10.1073/pnas.1701529114
- Calebiro, D., & Godbole, A. (2018). Internalization of G-protein-coupled receptors: Implication in receptor function, physiology and diseases. *Best Pract Res Clin Endocrinol Metab*, *32*(2), 83-91. doi:10.1016/j.beem.2018.01.004
- Cant, S. H., & Pitcher, J. A. (2005). G protein-coupled receptor kinase 2-mediated phosphorylation of ezrin is required for G protein-coupled receptor-dependent reorganization of the actin cytoskeleton. *Molecular Biology of the Cell*, *16*(7), 3088-3099. doi:10.1091/mbc.e04-10-0877
- Carman, C. V., Barak, L. S., Chen, C., Liu-Chen, L. Y., Onorato, J. J., Kennedy, S. P., . . . Benovic, J. L. (2000). Mutational analysis of Gbetagamma and phospholipid interaction with G protein-coupled receptor kinase 2. *J Biol Chem*, *275*(14), 10443-10452. doi:10.1074/jbc.275.14.10443
- Carman, C. V., Lisanti, M. P., & Benovic, J. L. (1999). Regulation of G protein-coupled receptor kinases by caveolin. *J Biol Chem*, *274*(13), 8858-8864. doi:10.1074/jbc.274.13.8858
- Castillo, P. E., Younts, T. J., Chavez, A. E., & Hashimoto, Y. (2012). Endocannabinoid signaling and synaptic function. *Neuron*, *76*(1), 70-81. doi:10.1016/j.neuron.2012.09.020
- Caterina, M. J., Schumacher, M. A., Tominaga, M., Rosen, T. A., Levine, J. D., & Julius, D. (1997). The capsaicin receptor: a heat-activated ion channel in the pain pathway. *Nature*, *389*(6653), 816-824. doi:10.1038/39807
- Celver, J. P., Lowe, J., Koo, A., Gurevich, V. V., & Chavkin, C. (2001). Threonine 180 is required for G-protein-coupled receptor kinase 3- and beta-arrestin 2-mediated desensitization of the mu-opioid receptor in *Xenopus* oocytes. *J Biol Chem*, *276*(7), 4894-4900. doi:10.1074/jbc.M007437200
- Craft, G.E., Graham, M.E., Bache, N., Larsen, M.R., Robinson, P.J., 2008. The in vivo phosphorylation sites in multiple isoforms of amphiphysin I from rat brain nerve terminals. *Mol. Cell. Proteomics* *7*, 1146–1161. <https://doi.org/10.1074/mcp.M700351-MCP200>.
- Cravatt, B. F., Giang, D. K., Mayfield, S. P., Boger, D. L., Lerner, R. A., & Gilula, N. B. (1996). Molecular characterization of an enzyme that degrades neuromodulatory fatty-acid amides. *Nature*, *384*(6604), 83-87. doi:DOI 10.1038/384083a0
- Cristino, L., De Petrocellis, L., Pryce, G., Baker, D., Guglielmotti, V., & Di Marzo, V. (2006). Immunohistochemical localization of cannabinoid type 1 and vanilloid transient receptor potential vanilloid type 1 receptors in the mouse brain. *Neuroscience*, *139*(4), 1405-1415. doi:10.1016/j.neuroscience.2006.02.074

- Cristino, L., Starowicz, K., De Petrocellis, L., Morishita, J., Ueda, N., Guglielmotti, V., & Di Marzo, V. (2008). Immunohistochemical localization of anabolic and catabolic enzymes for anandamide and other putative endovanilloids in the hippocampus and cerebellar cortex of the mouse brain. *Neuroscience*, *151*(4), 955-968. doi:10.1016/j.neuroscience.2007.11.047
- Cummings, N., Shields, K. A., Curran, J. E., Bozaoglu, K., Trevaskis, J., Gluschenko, K., . . . Jowett, J. B. (2012). Genetic variation in SH3-domain GRB2-like (endophilin)-interacting protein 1 has a major impact on fat mass. *Int J Obes (Lond)*, *36*(2), 201-206. doi:10.1038/ijo.2011.67
- Daaka, Y., Pitcher, J. A., Richardson, M., Stoffel, R. H., Robishaw, J. D., & Lefkowitz, R. J. (1997). Receptor and G betagamma isoform-specific interactions with G protein-coupled receptor kinases. *Proc Natl Acad Sci U S A*, *94*(6), 2180-2185. doi:10.1073/pnas.94.6.2180
- Daigle, T. L., Kearn, C. S., & Mackie, K. (2008). Rapid CB1 cannabinoid receptor desensitization defines the time course of ERK1/2 MAP kinase signaling. *Neuropharmacology*, *54*(1), 36-44. doi:10.1016/j.neuropharm.2007.06.005
- Daigle, T. L., Kwok, M. L., & Mackie, K. (2008). Regulation of CB(1) cannabinoid receptor internalization by a promiscuous phosphorylation-dependent mechanism. *Journal of Neurochemistry*, *106*(1), 70-82. doi:10.1111/j.1471-4159.2008.05336.x
- Dautzenberg, F. M., & Hauger, R. L. (2001). G-protein-coupled receptor kinase 3- and protein kinase C-mediated desensitization of the PACAP receptor type 1 in human Y-79 retinoblastoma cells. *Neuropharmacology*, *40*(3), 394-407. doi:10.1016/s0028-3908(00)00167-2
- Dautzenberg, F. M., Wille, S., Braun, S., & Hauger, R. L. (2002). GRK3 regulation during CRF- and urocortin-induced CRF1 receptor desensitization. *Biochem Biophys Res Commun*, *298*(3), 303-308. doi:10.1016/s0006-291x(02)02463-4
- De Luca, M. A., & Fattore, L. (2018). Therapeutic Use of Synthetic Cannabinoids: Still an Open Issue? *Clinical Therapeutics*, *40*(9), 1457-1466. doi:10.1016/j.clinthera.2018.08.002
- Dergai, O., Novokhatska, O., Dergai, M., Skrypkina, I., Tsyba, L., Moreau, J., & Rynditch, A. (2010). Intersectin 1 forms complexes with SGIP1 and Reps1 in clathrin-coated pits. *Biochem Biophys Res Commun*, *402*(2), 408-413. doi:10.1016/j.bbrc.2010.10.045
- Dhami, G. K., Anborgh, P. H., Dale, L. B., Sterne-Marr, R., & Ferguson, S. S. (2002). Phosphorylation-independent regulation of metabotropic glutamate receptor signaling by G protein-coupled receptor kinase 2. *J Biol Chem*, *277*(28), 25266-25272. doi:10.1074/jbc.M203593200
- Di Marzo, V., & Matias, I. (2005). Endocannabinoid control of food intake and energy balance. *Nat Neurosci*, *8*(5), 585-589. doi:10.1038/nn1457
- Dinh, T. P., Carpenter, D., Leslie, F. M., Freund, T. F., Katona, I., Sensi, S. L., . . . Piomelli, D. (2002). Brain monoglyceride lipase participating in endocannabinoid inactivation (vol 99, pg 10819, 2002). *Proceedings of the National Academy of Sciences of the United States of America*, *99*(21), 13961-13961. doi:10.1073/pnas.222439799
- Downes, G. B., & Gautam, N. (1999). The G protein subunit gene families. *Genomics*, *62*(3), 544-552. doi:10.1006/geno.1999.5992
- Dvorakova, M., Kubik-Zahorodna, A., Straiker, A., Sedlacek, R., Hajkova, A., Mackie, K., & Blahos, J. (2021). SGIP1 is involved in regulation of emotionality, mood, and nociception and modulates in vivo signalling of cannabinoid CB1 receptors. *Br J Pharmacol*, *178*(7), 1588-1604. doi:10.1111/bph.15383
- Edbauer, D., Cheng, D.M., Batterton, M.N., Wang, C.F., Duong, D.M., Yaffe, M.B., Peng, J. M., Sheng, M., 2009. Identification and Characterization of Neuronal Mitogenactivated Protein Kinase Substrates Using a Specific Phosphomotif Antibody. *Mol. Cell. Proteomics* *8*, 681-695. <https://doi.org/10.1074/mcp.M800233-MCP200>.
- Edwards, J. G. (2014). TRPV1 in the Central Nervous System: Synaptic Plasticity, Function, and Pharmacological Implications. *Capsaicin as a Therapeutic Molecule*, *68*, 77-104. doi:10.1007/978-3-0348-0828-6\_3

- ElSohly, M. A., & Slade, D. (2005). Chemical constituents of marijuana: The complex mixture of natural cannabinoids. *Life Sciences*, *78*(5), 539-548. doi:10.1016/j.lfs.2005.09.011
- Fauzan, M., Oubraim, S., Yu, M., Glaser, S. T., Kaczocha, M., & Haj-Dahmane, S. (2022). Fatty Acid-Binding Protein 5 Modulates Brain Endocannabinoid Tone and Retrograde Signaling in the Striatum. *Front Cell Neurosci*, *16*, 936939. doi:10.3389/fncel.2022.936939
- Fletcher-Jones, A., Spackman, E., Craig, T.J., Nakamura, Y., Wilkinson, K.A., Henley, J. M. (2023). SGIP1 binding to the  $\alpha$ -helical H9 domain of cannabinoid receptor 1 promotes axonal surface expression. bioRxiv, 2023-07. <https://doi.org/10.1101/2023.07.18.549510>.
- Fletcher-Jones, A., Hildick, K. L., Evans, A. J., Nakamura, Y., Wilkinson, K. A., & Henley, J. M. (2019). The C-terminal helix 9 motif in rat cannabinoid receptor type 1 regulates axonal trafficking and surface expression. *eLife*, *8*, e44252. <https://doi.org/10.7554/eLife.44252>
- Ford, B. M., Franks, L. N., Tai, S., Fantegrossi, W. E., Stahl, E. L., Berquist, M. D., . . . Prather, P. L. (2017). Characterization of structurally novel G protein biased CB1 agonists: Implications for drug development. *Pharmacological Research*, *125*(Pt B), 161-177. doi:10.1016/j.phrs.2017.08.008
- Freeman, J. L., De La Cruz, E. M., Pollard, T. D., Lefkowitz, R. J., & Pitcher, J. A. (1998). Regulation of G protein-coupled receptor kinase 5 (GRK5) by actin. *J Biol Chem*, *273*(32), 20653-20657. doi:10.1074/jbc.273.32.20653
- Gainetdinov, R. R., Premont, R. T., Bohn, L. M., Lefkowitz, R. J., & Caron, M. G. (2004). Desensitization of G protein-coupled receptors and neuronal functions. *Annu Rev Neurosci*, *27*, 107-144. doi:10.1146/annurev.neuro.27.070203.144206
- Giacobbe, J., Marrocu, A., Di Benedetto, M. G., Pariante, C. M., & Borsini, A. (2021). A systematic, integrative review of the effects of the endocannabinoid system on inflammation and neurogenesis in animal models of affective disorders. *Brain Behav Immun*, *93*, 353-367. doi:10.1016/j.bbi.2020.12.024
- Goodman, O. B., Jr., Krupnick, J. G., Santini, F., Gurevich, V. V., Penn, R. B., Gagnon, A. W., . . . Benovic, J. L. (1996). Beta-arrestin acts as a clathrin adaptor in endocytosis of the beta2-adrenergic receptor. *Nature*, *383*(6599), 447-450. doi:10.1038/383447a0
- Grabiec, U., & Dehghani, F. (2017). N-Arachidonoyl Dopamine: A Novel Endocannabinoid and Endovanilloid with Widespread Physiological and Pharmacological Activities. *Cannabis and Cannabinoid Research*, *2*(1), 183-196. doi:10.1089/can.2017.0015
- Gray, R. A., & Whalley, B. J. (2020). The proposed mechanisms of action of CBD in epilepsy. *Epileptic Disord*, *22*(S1), 10-15. doi:10.1684/epd.2020.1135
- Grimsey, N. L., Graham, E. S., Dragunow, M., & Glass, M. (2010). Cannabinoid Receptor 1 trafficking and the role of the intracellular pool: implications for therapeutics. *Biochemical Pharmacology*, *80*(7), 1050-1062. doi:10.1016/j.bcp.2010.06.007
- Gupte, J., Swaminath, G., Danao, J., Tian, H., Li, Y., & Wu, X. (2012). Signaling property study of adhesion G-protein-coupled receptors. *FEBS Lett*, *586*(8), 1214-1219. doi:10.1016/j.febslet.2012.03.014
- Gurevich, E. V., Tesmer, J. J., Mushegian, A., & Gurevich, V. V. (2012). G protein-coupled receptor kinases: more than just kinases and not only for GPCRs. *Pharmacol Ther*, *133*(1), 40-69. doi:10.1016/j.pharmthera.2011.08.001
- Gyombolai, P., Boros, E., Hunyady, L., & Turu, G. (2013). Differential beta-arrestin2 requirements for constitutive and agonist-induced internalization of the CB1 cannabinoid receptor. *Mol Cell Endocrinol*, *372*(1-2), 116-127. doi:10.1016/j.mce.2013.03.013
- Haider, R. S., Matthees, E. S. F., Drube, J., Reichel, M., Zabel, U., Inoue, A., . . . Hoffmann, C. (2022). beta-arrestin1 and 2 exhibit distinct phosphorylation-dependent conformations when coupling to the same GPCR in living cells. *Nat Commun*, *13*(1), 5638. doi:10.1038/s41467-022-33307-8
- Hajkova, A., Techlovská, S., Dvorakova, M., Chambers, J. N., Kumpost, J., Hubalkova, P., . . . Blahos, J. (2016). SGIP1 alters internalization and modulates signaling of activated cannabinoid

- receptor 1 in a biased manner. *Neuropharmacology*, 107, 201-214. doi:10.1016/j.neuropharm.2016.03.008
- Hao, S., Avraham, Y., Mechoulam, R., & Berry, E. M. (2000). Low dose anandamide affects food intake, cognitive function, neurotransmitter and corticosterone levels in diet-restricted mice. *European Journal of Pharmacology*, 392(3), 147-156. doi:10.1016/s0014-2999(00)00059-5
- Haring, M., Marsicano, G., Lutz, B., & Monory, K. (2007). Identification of the cannabinoid receptor type 1 in serotonergic cells of raphe nuclei in mice. *Neuroscience*, 146(3), 1212-1219. doi:10.1016/j.neuroscience.2007.02.021
- Hausdorff, W. P., Caron, M. G., & Lefkowitz, R. J. (1990). Turning off the signal: desensitization of beta-adrenergic receptor function. *FASEB J*, 4(11), 2881-2889.
- Hebert-Chatelain, E., & Marsicano, G. (2017). A new link between cannabinoids and memory - The mitochondria. *M S-Medecine Sciences*, 33(6-7), 579-581. doi:10.1051/medsci/20173306007
- Henley, J. R., Krueger, E. W., Oswald, B. J., & McNiven, M. A. (1998). Dynamin-mediated internalization of caveolae. *J Cell Biol*, 141(1), 85-99. doi:10.1083/jcb.141.1.85
- Henne, W. M., Boucrot, E., Meinecke, M., Evergren, E., Vallis, Y., Mittal, R., & McMahon, H. T. (2010). FCHO proteins are nucleators of clathrin-mediated endocytosis. *Science*, 328(5983), 1281-1284. doi:10.1126/science.1188462
- Henne, W.M., Kent, H.M., Ford, M.G.J., Hegde, B.G., Daumke, O., Butler, P.J.G., Mittal, R., Langen, R., Evans, P.R., McMahon, H.T., 2007. Structure and analysis of FCHO2F-BAR domain: A dimerizing and membrane recruitment module that effects membrane curvature. *Structure* 15, 839–852. <https://doi.org/10.1016/j.str.2007.05.002>.
- Herkenham, M., Lynn, A. B., Johnson, M. R., Melvin, L. S., de Costa, B. R., & Rice, K. C. (1991). Characterization and localization of cannabinoid receptors in rat brain: a quantitative in vitro autoradiographic study. *J Neurosci*, 11(2), 563-583.
- Herkenham, M., Lynn, A. B., Little, M. D., Johnson, M. R., Melvin, L. S., de Costa, B. R., & Rice, K. C. (1990). Cannabinoid receptor localization in brain. *Proc Natl Acad Sci U S A*, 87(5), 1932-1936. doi:10.1073/pnas.87.5.1932
- Higashijima, T., Ferguson, K. M., Sternweis, P. C., Smigel, M. D., & Gilman, A. G. (1987). Effects of Mg<sup>2+</sup> and the beta gamma-subunit complex on the interactions of guanine nucleotides with G proteins. *J Biol Chem*, 262(2), 762-766.
- Hollopeter, G., Lange, J. J., Zhang, Y., Vu, T. N., Gu, M., Ailion, M., . . . Jorgensen, E. M. (2014). The membrane-associated proteins FCHO and SGIP are allosteric activators of the AP2 clathrin adaptor complex. *Elife*, 3. doi:10.7554/eLife.03648
- Homan, K. T., & Tesmer, J. J. (2014). Structural insights into G protein-coupled receptor kinase function. *Curr Opin Cell Biol*, 27, 25-31. doi:10.1016/j.ceb.2013.10.009
- Howlett, A. C., Barth, F., Bonner, T. I., Cabral, G., Casellas, P., Devane, W. A., . . . Pertwee, R. G. (2002). International Union of Pharmacology. XXVII. Classification of cannabinoid receptors. *Pharmacological Reviews*, 54(2), 161-202. doi:DOI 10.1124/pr.54.2.161
- Hsieh, C., Brown, S., Derleth, C., & Mackie, K. (1999). Internalization and recycling of the CB1 cannabinoid receptor. *Journal of Neurochemistry*, 73(2), 493-501. doi:10.1046/j.1471-4159.1999.0730493.x
- Hua, T., Vemuri, K., Nikas, S. P., Laprairie, R. B., Wu, Y., Qu, L., . . . Liu, Z. J. (2017). Crystal structures of agonist-bound human cannabinoid receptor CB1. *Nature*, 547(7664), 468-471. doi:10.1038/nature23272
- Huang, H. C., & Klein, P. S. (2004). The Frizzled family: receptors for multiple signal transduction pathways. *Genome Biol*, 5(7), 234. doi:10.1186/gb-2004-5-7-234
- Huttlin, E. L., Jedrychowski, M. P., Elias, J. E., Goswami, T., Rad, R., Beausoleil, S. A., . . . Gygi, S. P. (2010). A tissue-specific atlas of mouse protein phosphorylation and expression. *Cell*, 143(7), 1174-1189. doi:10.1016/j.cell.2010.12.001

- Ibsen, M. S., Connor, M., & Glass, M. (2017). Cannabinoid CB1 and CB2 Receptor Signaling and Bias. *Cannabis Cannabinoid Res*, 2(1), 48-60. doi:10.1089/can.2016.0037
- Ikeda S, K. M., Fujiwara S. (2007). Japan Patent No.: T. P. C. Ltd.
- Ilyasov, A. A., Milligan, C. E., Pharr, E. P., & Howlett, A. C. (2018). The Endocannabinoid System and Oligodendrocytes in Health and Disease. *Front Neurosci*, 12, 733. doi:10.3389/fnins.2018.00733
- Jarrahan, A., Watts, V. J., & Barker, E. L. (2004). D2 dopamine receptors modulate Galpha-subunit coupling of the CB1 cannabinoid receptor. *J Pharmacol Exp Ther*, 308(3), 880-886. doi:10.1124/jpet.103.057620
- Jimenez-Blasco, D., Busquets-Garcia, A., Hebert-Chatelain, E., Serrat, R., Vicente-Gutierrez, C., Ioannidou, C., . . . Marsicano, G. (2020). Glucose metabolism links astroglial mitochondria to cannabinoid effects. *Nature*, 583(7817), 603-608. doi:10.1038/s41586-020-2470-y
- Jin, W., Brown, S., Roche, J. P., Hsieh, C., Celver, J. P., Koo, A., . . . Mackie, K. (1999). Distinct domains of the CB1 cannabinoid receptor mediate desensitization and internalization. *J Neurosci*, 19(10), 3773-3780.
- Johannes, L., Parton, R. G., Bassereau, P., & Mayor, S. (2015). Building endocytic pits without clathrin. *Nat Rev Mol Cell Biol*, 16(5), 311-321. doi:10.1038/nrm3968
- Josefsson, L. G. (1999). Evidence for kinship between diverse G-protein coupled receptors. *Gene*, 239(2), 333-340. doi:10.1016/s0378-1119(99)00392-3
- Joshi, N., & Onaivi, E. S. (2019). Endocannabinoid System Components: Overview and Tissue Distribution. *Adv Exp Med Biol*, 1162, 1-12. doi:10.1007/978-3-030-21737-2\_1
- Kaplan, J. S., Stella, N., Catterall, W. A., & Westenbroek, R. E. (2017). Cannabidiol attenuates seizures and social deficits in a mouse model of Dravet syndrome. *Proc Natl Acad Sci U S A*, 114(42), 11229-11234. doi:10.1073/pnas.1711351114
- Katona, I., & Freund, T. F. (2012). Multiple functions of endocannabinoid signaling in the brain. *Annu Rev Neurosci*, 35, 529-558. doi:10.1146/annurev-neuro-062111-150420
- Khan, S. M., Sleno, R., Gora, S., Zylbergold, P., Laverdure, J. P., Labbe, J. C., . . . Hebert, T. E. (2013). The expanding roles of Gbetagamma subunits in G protein-coupled receptor signaling and drug action. *Pharmacol Rev*, 65(2), 545-577. doi:10.1124/pr.111.005603
- Kirilly, E., Hunyady, L., & Bagdy, G. (2013). Opposing local effects of endocannabinoids on the activity of noradrenergic neurons and release of noradrenaline: relevance for their role in depression and in the actions of CB1 receptor antagonists. *Journal of Neural Transmission*, 120(1), 177-186. doi:10.1007/s00702-012-0900-1
- Kouznetsova, M., Kelley, B., Shen, M., & Thayer, S. A. (2002). Desensitization of cannabinoid-mediated presynaptic inhibition of neurotransmission between rat hippocampal neurons in culture. *Molecular Pharmacology*, 61(3), 477-485. doi:10.1124/mol.61.3.477
- Laporte, S. A., Oakley, R. H., Holt, J. A., Barak, L. S., & Caron, M. G. (2000). The interaction of beta-arrestin with the AP-2 adaptor is required for the clustering of beta 2-adrenergic receptor into clathrin-coated pits. *J Biol Chem*, 275(30), 23120-23126. doi:10.1074/jbc.M002581200
- Laporte, S. A., Oakley, R. H., Zhang, J., Holt, J. A., Ferguson, S. S., Caron, M. G., & Barak, L. S. (1999). The beta2-adrenergic receptor/betaarrestin complex recruits the clathrin adaptor AP-2 during endocytosis. *Proc Natl Acad Sci U S A*, 96(7), 3712-3717. doi:10.1073/pnas.96.7.3712
- Laprairie, R. B., Bagher, A. M., Kelly, M. E., & Denovan-Wright, E. M. (2016). Biased Type 1 Cannabinoid Receptor Signaling Influences Neuronal Viability in a Cell Culture Model of Huntington Disease. *Molecular Pharmacology*, 89(3), 364-375. doi:10.1124/mol.115.101980
- Latorraca, N. R., Masureel, M., Hollingsworth, S. A., Heydenreich, F. M., Suomivuori, C. M., Brinton, C., . . . Dror, R. O. (2020). How GPCR Phosphorylation Patterns Orchestrate Arrestin-Mediated Signaling. *Cell*, 183(7), 1813-1825 e1818. doi:10.1016/j.cell.2020.11.014

- Lauckner, J. E., Hille, B., & Mackie, K. (2005). The cannabinoid agonist WIN55,212-2 increases intracellular calcium via CB1 receptor coupling to Gq/11 G proteins. *Proc Natl Acad Sci U S A*, *102*(52), 19144-19149. doi:10.1073/pnas.0509588102
- Lee, S. E., Jeong, S., Lee, U., & Chang, S. (2019). SGIP1alpha functions as a selective endocytic adaptor for the internalization of synaptotagmin 1 at synapses. *Mol Brain*, *12*(1), 41. doi:10.1186/s13041-019-0464-1
- Lefkowitz, R. J. (1998). G protein-coupled receptors. III. New roles for receptor kinases and beta-arrestins in receptor signaling and desensitization. *J Biol Chem*, *273*(30), 18677-18680. doi:10.1074/jbc.273.30.18677
- Lemmon, M.A., 2008. Membrane recognition by phospholipid-binding domains. *Nat. Rev. Mol. Cell Biol.* *9*, 99–111. <https://doi.org/10.1038/nrm2328>.
- Levoye, A., Zwier, J. M., Jaracz-Ros, A., Klipfel, L., Cottet, M., Maurel, D., . . . Bachelierie, F. (2015). A Broad G Protein-Coupled Receptor Internalization Assay that Combines SNAP-Tag Labeling, Diffusion-Enhanced Resonance Energy Transfer, and a Highly Emissive Terbium Cryptate. *Front Endocrinol (Lausanne)*, *6*, 167. doi:10.3389/fendo.2015.00167
- Li, H. D., Liu, W. X., & Michalak, M. (2011). Enhanced clathrin-dependent endocytosis in the absence of calnexin. *PLoS One*, *6*(7), e21678. doi:10.1371/journal.pone.0021678
- Liggett, S. B. (2011). Phosphorylation Barcoding as a Mechanism of Directing GPCR Signaling. *Science Signaling*, *4*(185). doi:ARTN pe36  
10.1126/scisignal.2002331
- Ligresti, A., Petrosino, S., & Di Marzo, V. (2009). From endocannabinoid profiling to 'endocannabinoid therapeutics'. *Curr Opin Chem Biol*, *13*(3), 321-331. doi:10.1016/j.cbpa.2009.04.615
- Lindsley, C. W., Emmitte, K. A., Hopkins, C. R., Bridges, T. M., Gregory, K. J., Niswender, C. M., & Conn, P. J. (2016). Practical Strategies and Concepts in GPCR Allosteric Modulator Discovery: Recent Advances with Metabotropic Glutamate Receptors. *Chem Rev*, *116*(11), 6707-6741. doi:10.1021/acs.chemrev.5b00656
- Lodowski, D. T., Barnhill, J. F., Pyskadlo, R. M., Ghirlando, R., Sterne-Marr, R., & Tesmer, J. J. (2005). The role of G beta gamma and domain interfaces in the activation of G protein-coupled receptor kinase 2. *Biochemistry*, *44*(18), 6958-6970. doi:10.1021/bi050119q
- Lodowski, D. T., Pitcher, J. A., Capel, W. D., Lefkowitz, R. J., & Tesmer, J. J. G. (2003). Keeping G proteins at bay: A complex between G protein-coupled receptor kinase 2 and G beta gamma. *Science*, *300*(5623), 1256-1262. doi:DOI 10.1126/science.1082348
- Lodowski, D. T., Tesmer, V. M., Benovic, J. L., & Tesmer, J. J. (2006). The structure of G protein-coupled receptor kinase (GRK)-6 defines a second lineage of GRKs. *J Biol Chem*, *281*(24), 16785-16793. doi:10.1074/jbc.M601327200
- Luo, J., & Benovic, J. L. (2003). G protein-coupled receptor kinase interaction with Hsp90 mediates kinase maturation. *J Biol Chem*, *278*(51), 50908-50914. doi:10.1074/jbc.M307637200
- Luttrell, L. M., & Lefkowitz, R. J. (2002). The role of beta-arrestins in the termination and transduction of G-protein-coupled receptor signals. *J Cell Sci*, *115*(Pt 3), 455-465.
- Maccarrone, M., Bab, R., Biro, T., Cabral, G. A., Dey, S. K., Di Marzo, V., . . . Zimmer, A. (2015). Endocannabinoid signaling at the periphery: 50 years after THC. *Trends in Pharmacological Sciences*, *36*(5), 277-296. doi:10.1016/j.tips.2015.02.008
- Maccarrone, M., Dainese, E., & Oddi, S. (2010). Intracellular trafficking of anandamide: new concepts for signaling. *Trends Biochem Sci*, *35*(11), 601-608. doi:10.1016/j.tibs.2010.05.008
- Manev, H., Favaron, M., Guidotti, A., & Costa, E. (1989). Delayed increase of Ca<sup>2+</sup> influx elicited by glutamate: role in neuronal death. *Molecular Pharmacology*, *36*(1), 106-112.
- Marsicano, G., & Lutz, B. (1999). Expression of the cannabinoid receptor CB1 in distinct neuronal subpopulations in the adult mouse forebrain. *European Journal of Neuroscience*, *11*(12), 4213-4225. doi:DOI 10.1046/j.1460-9568.1999.00847.x

- Martini, L., Waldhoer, M., Pusch, M., Kharazia, V., Fong, J., Lee, J. H., . . . Whistler, J. L. (2007). Ligand-induced down-regulation of the cannabinoid 1 receptor is mediated by the G-protein-coupled receptor-associated sorting protein GASP1. *FASEB J*, *21*(3), 802-811. doi:10.1096/fj.06-7132com
- McMahon, H. T., & Boucrot, E. (2011). Molecular mechanism and physiological functions of clathrin-mediated endocytosis. *Nat Rev Mol Cell Biol*, *12*(8), 517-533. doi:10.1038/nrm3151
- Mees, I., Li, S.S., Tran, H., Ang, C.S., Williamson, N.A., Hannan, A.J., Renoir, T., 2022. Phosphoproteomic dysregulation in Huntington's disease mice is rescued by environmental enrichment. *Brain Communications* 4. <https://doi.org/10.1093/braincomms/fcac305>.
- Miess, E., Gondin, A. B., Yousuf, A., Steinborn, R., Mosslein, N., Yang, Y., . . . Canals, M. (2018). Multisite phosphorylation is required for sustained interaction with GRKs and arrestins during rapid mu-opioid receptor desensitization. *Sci Signal*, *11*(539). doi:10.1126/scisignal.aas9609
- Miller, L. J., Dong, M., & Harikumar, K. G. (2012). Ligand binding and activation of the secretin receptor, a prototypic family B G protein-coupled receptor. *Br J Pharmacol*, *166*(1), 18-26. doi:10.1111/j.1476-5381.2011.01463.x
- Milligan, G., & Kostenis, E. (2006). Heterotrimeric G-proteins: a short history. *Br J Pharmacol*, *147 Suppl 1*, S46-55. doi:10.1038/sj.bjp.0706405
- Moller, T. C., Pedersen, M. F., van Senten, J. R., Seiersen, S. D., Mathiesen, J. M., Bouvier, M., & Brauner-Osborne, H. (2020). Dissecting the roles of GRK2 and GRK3 in mu-opioid receptor internalization and beta-arrestin2 recruitment using CRISPR/Cas9-edited HEK293 cells. *Sci Rep*, *10*(1), 17395. doi:10.1038/s41598-020-73674-0
- Moore, C. A. C., Milano, S. K., & Benovic, J. L. (2007). Regulation of receptor trafficking by GRKs and arrestins. *Annual Review of Physiology*, *69*, 451-482. doi:10.1146/annurev.physiol.69.022405.154712
- Morgan, D. J., Davis, B. J., Kearns, C. S., Marcus, D., Cook, A. J., Wager-Miller, J., . . . Mackie, K. (2014). Mutation of putative GRK phosphorylation sites in the cannabinoid receptor 1 (CB1R) confers resistance to cannabinoid tolerance and hypersensitivity to cannabinoids in mice. *J Neurosci*, *34*(15), 5152-5163. doi:10.1523/JNEUROSCI.3445-12.2014
- Munro, S., Thomas, K. L., & Abushaar, M. (1993). Molecular Characterization of a Peripheral Receptor for Cannabinoids. *Nature*, *365*(6441), 61-65. doi:DOI 10.1038/365061a0
- Murakami, A., Yajima, T., Sakuma, H., McLaren, M. J., & Inana, G. (1993). X-arrestin: a new retinal arrestin mapping to the X chromosome. *FEBS Lett*, *334*(2), 203-209. doi:10.1016/0014-5793(93)81712-9
- Murga, C., Arcones, A. C., Cruces-Sande, M., Briones, A. M., Salaices, M., & Mayor, F., Jr. (2019). G Protein-Coupled Receptor Kinase 2 (GRK2) as a Potential Therapeutic Target in Cardiovascular and Metabolic Diseases. *Frontiers in Pharmacology*, *10*, 112. doi:10.3389/fphar.2019.00112
- Munton, R.P., Tweedie-Cullen, R., Livingstone-Zatchej, M., Weinandy, F., Waidelich, M., Longo, D., Gehrig, P., Potthast, F., Rutishauser, D., Gerrits, B., Panse, C., Schlapbach, R., Mansuy, I.M., 2007. Qualitative and quantitative analyses of protein phosphorylation in naive and stimulated mouse synaptosomal preparations. *Mol. Cell. Proteomics* 6, 283–293. <https://doi.org/10.1074/mcp.M600046-MCP200>
- Nakano, Y., Jahan, I., Bonde, G., Sun, X.S., Hildebrand, M.S., Engelhardt, J.F., Smith, R.J. H., Cornell, R.A., Fritsch, B., Banfi, B., 2012. A Mutation in the Srrm4 Gene Causes Alternative Splicing Defects and Deafness in the Bronx Waltzer Mouse. *PLoS Genet.* 8 <https://doi.org/10.1371/journal.pgen.1002966>.
- Nakano, Y., Wiechert, S., Banfi, B., 2019. Overlapping Activities of Two Neuronal Splicing Factors Switch the GABA Effect from Excitatory to Inhibitory by Regulating REST. *Cell Rep.* 27, 860-+. <https://doi.org/10.1016/j.celrep.2019.03.072>.

- NCBI. (2022, 30-Aug-2022). Sgip1 SH3-domain GRB2-like (endophilin) interacting protein 1 [ *Mus musculus* (house mouse) ]. Retrieved from <https://www.ncbi.nlm.nih.gov/gene?Db=gene&Cmd=DetailsSearch&Term=73094>
- Nguyen, A. H., Thomsen, A. R. B., Cahill, T. J., 3rd, Huang, R., Huang, L. Y., Marcink, T., . . . Lefkowitz, R. J. (2019). Structure of an endosomal signaling GPCR-G protein-beta-arrestin megacomplex. *Nat Struct Mol Biol*, *26*(12), 1123-1131. doi:10.1038/s41594-019-0330-y
- Nguyen, P. T., Schmid, C. L., Raehal, K. M., Selley, D. E., Bohn, L. M., & Sim-Selley, L. J. (2012). beta-arrestin2 regulates cannabinoid CB1 receptor signaling and adaptation in a central nervous system region-dependent manner. *Biol Psychiatry*, *71*(8), 714-724. doi:10.1016/j.biopsych.2011.11.027
- Nguyen, T., Li, J. X., Thomas, B. F., Wiley, J. L., Kenakin, T. P., & Zhang, Y. (2017). Allosteric Modulation: An Alternate Approach Targeting the Cannabinoid CB1 Receptor. *Med Res Rev*, *37*(3), 441-474. doi:10.1002/med.21418
- Nobles, K. N., Xiao, K., Ahn, S., Shukla, A. K., Lam, C. M., Rajagopal, S., . . . Lefkowitz, R. J. (2011). Distinct phosphorylation sites on the beta(2)-adrenergic receptor establish a barcode that encodes differential functions of beta-arrestin. *Sci Signal*, *4*(185), ra51. doi:10.1126/scisignal.2001707
- Nogueras-Ortiz, C., & Yudowski, G. A. (2016). The Multiple Waves of Cannabinoid 1 Receptor Signaling. *Molecular Pharmacology*, *90*(5), 620-626. doi:10.1124/mol.116.104539
- Nogues, L., Reglero, C., Rivas, V., Neves, M., Penela, P., & Mayor, F., Jr. (2017). G-Protein-Coupled Receptor Kinase 2 as a Potential Modulator of the Hallmarks of Cancer. *Molecular Pharmacology*, *91*(3), 220-228. doi:10.1124/mol.116.107185
- Nuber, S., Zabel, U., Lorenz, K., Nuber, A., Milligan, G., Tobin, A. B., . . . Hoffmann, C. (2016). beta-Arrestin biosensors reveal a rapid, receptor-dependent activation/deactivation cycle. *Nature*, *531*(7596), 661-664. doi:10.1038/nature17198
- Palczewski, K., Kumasaka, T., Hori, T., Behnke, C. A., Motoshima, H., Fox, B. A., . . . Miyano, M. (2000). Crystal structure of rhodopsin: A G protein-coupled receptor. *Science*, *289*(5480), 739-745. doi:10.1126/science.289.5480.739
- Park, P. S., Lodowski, D. T., & Palczewski, K. (2008). Activation of G protein-coupled receptors: beyond two-state models and tertiary conformational changes. *Annu Rev Pharmacol Toxicol*, *48*, 107-141. doi:10.1146/annurev.pharmtox.48.113006.094630
- Pavlos, N. J., & Friedman, P. A. (2017). GPCR Signaling and Trafficking: The Long and Short of It. *Trends Endocrinol Metab*, *28*(3), 213-226. doi:10.1016/j.tem.2016.10.007
- Penela, P., Murga, C., Ribas, C., Tutor, A. S., Peregrin, S., & Mayor, F., Jr. (2006). Mechanisms of regulation of G protein-coupled receptor kinases (GRKs) and cardiovascular disease. *Cardiovasc Res*, *69*(1), 46-56. doi:10.1016/j.cardiores.2005.09.011
- Penumarti, A., & Abdel-Rahman, A. A. (2014). The Novel Endocannabinoid Receptor GPR18 Is Expressed in the Rostral Ventrolateral Medulla and Exerts Tonic Restraining Influence on Blood Pressure. *Journal of Pharmacology and Experimental Therapeutics*, *349*(1), 29-38. doi:10.1124/jpet.113.209213
- Peterson, Y. K., & Luttrell, L. M. (2017). The Diverse Roles of Arrestin Scaffolds in G Protein-Coupled Receptor Signaling. *Pharmacol Rev*, *69*(3), 256-297. doi:10.1124/pr.116.013367
- Pin, J. P., Galvez, T., & Prezeau, L. (2003). Evolution, structure, and activation mechanism of family 3/C G-protein-coupled receptors. *Pharmacol Ther*, *98*(3), 325-354. doi:10.1016/s0163-7258(03)00038-x
- Piomelli, D. (2003). The molecular logic of endocannabinoid signalling. *Nature Reviews Neuroscience*, *4*(11), 873-884. doi:10.1038/nrn1247
- Pitcher, J. A., Inglese, J., Higgins, J. B., Arriza, J. L., Casey, P. J., Kim, C., . . . Lefkowitz, R. J. (1992). Role of beta gamma subunits of G proteins in targeting the beta-adrenergic receptor kinase to membrane-bound receptors. *Science*, *257*(5074), 1264-1267. doi:10.1126/science.1325672

- Porter, A. C., Sauer, J. M., Knierman, M. D., Becker, G. W., Berna, M. J., Bao, J., . . . Felder, C. C. (2002). Characterization of a novel endocannabinoid, virodhamine, with antagonist activity at the CB1 receptor. *J Pharmacol Exp Ther*, *301*(3), 1020-1024. doi:10.1124/jpet.301.3.1020
- Premont, R. T., & Gainetdinov, R. R. (2007). Physiological roles of G protein-coupled receptor kinases and arrestins. *Annual Review of Physiology*, *69*, 511-534. doi:10.1146/annurev.physiol.69.022405.154731
- Pronin, A. N., Satpaev, D. K., Slepak, V. Z., & Benovic, J. L. (1997). Regulation of G protein-coupled receptor kinases by calmodulin and localization of the calmodulin binding domain. *J Biol Chem*, *272*(29), 18273-18280. doi:10.1074/jbc.272.29.18273
- Reekie, T. A., Scott, M. P., & Kassiou, M. (2018). The evolving science of phytocannabinoids. *Nature Reviews Chemistry*, *2*(1). doi:ARTN 0101
- 10.1038/s41570-017-0101
- Reiter, E., Ahn, S., Shukla, A. K., & Lefkowitz, R. J. (2012). Molecular mechanism of beta-arrestin-biased agonism at seven-transmembrane receptors. *Annu Rev Pharmacol Toxicol*, *52*, 179-197. doi:10.1146/annurev.pharmtox.010909.105800
- Ribas, C., Penela, P., Murga, C., Salcedo, A., Garcia-Hoz, C., Jurado-Pueyo, M., . . . Mayor, F., Jr. (2007). The G protein-coupled receptor kinase (GRK) interactome: role of GRKs in GPCR regulation and signaling. *Biochim Biophys Acta*, *1768*(4), 913-922. doi:10.1016/j.bbamem.2006.09.019
- Rosenbaum, D. M., Rasmussen, S. G., & Kobilka, B. K. (2009). The structure and function of G-protein-coupled receptors. *Nature*, *459*(7245), 356-363. doi:10.1038/nature08144
- Ross, E. M. (2014). G Protein-coupled receptors: Multi-turnover GDP/GTP exchange catalysis on heterotrimeric G proteins. *Cell Logist*, *4*, e29391. doi:10.4161/cl.29391
- Rowland, N. E., Mukherjee, M., & Robertson, K. (2001). Effects of the cannabinoid receptor antagonist SR 141716, alone and in combination with dexfenfluramine or naloxone, on food intake in rats. *Psychopharmacology (Berl)*, *159*(1), 111-116. doi:10.1007/s002130100910
- Rozenfeld, R., & Devi, L. A. (2008). Regulation of CB1 cannabinoid receptor trafficking by the adaptor protein AP-3. *FASEB J*, *22*(7), 2311-2322. doi:10.1096/fj.07-102731
- Ryberg, E., Vu, H. K., Larsson, N., Groblewski, T., Hjorth, S., Elebring, T., . . . Greasley, P. J. (2005). Identification and characterisation of a novel splice variant of the human CB1 receptor. *Febs Letters*, *579*(1), 259-264. doi:10.1016/j.febslet.2004.11.085
- Sabatucci, A., Tortolani, D., Dainese, E., & Maccarrone, M. (2018). In silico mapping of allosteric ligand binding sites in type-1 cannabinoid receptor. *Biotechnol Appl Biochem*, *65*(1), 21-28. doi:10.1002/bab.1589
- Safran M, R. N., Twik M, BarShir R, Iny Stein T, Dahary D, Fishilevich S, and Lancet D. (2022). GeneCards – the human gene database. Retrieved from <https://www.genecards.org/cgi-bin/carddisp.pl?gene=SGIP1>
- Schioth, H. B., & Fredriksson, R. (2005). The GRAFS classification system of G-protein coupled receptors in comparative perspective. *Gen Comp Endocrinol*, *142*(1-2), 94-101. doi:10.1016/j.ygcen.2004.12.018
- Schulz, P., Hryhorowicz, S., Rychter, A. M., Zawada, A., Slomski, R., Dobrowolska, A., & Krela-Kazmierczak, I. (2021). What Role Does the Endocannabinoid System Play in the Pathogenesis of Obesity? *Nutrients*, *13*(2). doi:ARTN 373
- 10.3390/nu13020373
- Sente, A., Peer, R., Srivastava, A., Baidya, M., Lesk, A. M., Balaji, S., . . . Flock, T. (2018). Molecular mechanism of modulating arrestin conformation by GPCR phosphorylation. *Nat Struct Mol Biol*, *25*(6), 538-545. doi:10.1038/s41594-018-0071-3
- Seyedabadi, M., Ghahremani, M. H., & Albert, P. R. (2019). Biased signaling of G protein coupled receptors (GPCRs): Molecular determinants of GPCR/transducer selectivity and

- therapeutic potential. *Pharmacol Ther*, 200, 148-178.  
doi:10.1016/j.pharmthera.2019.05.006
- Shao, Z., Yin, J., Chapman, K., Grzemska, M., Clark, L., Wang, J., & Rosenbaum, D. M. (2016). High-resolution crystal structure of the human CB1 cannabinoid receptor. *Nature*, 540(7634), 602-606. doi:10.1038/nature20613
- Shiina, T., Arai, K., Tanabe, S., Yoshida, N., Haga, T., Nagao, T., & Kurose, H. (2001). Clathrin box in G protein-coupled receptor kinase 2. *J Biol Chem*, 276(35), 33019-33026.  
doi:10.1074/jbc.M100140200
- Shire, D., Carillon, C., Kaghad, M., Calandra, B., Rinaldi-Carmona, M., Le Fur, G., . . . Ferrara, P. (1995). An amino-terminal variant of the central cannabinoid receptor resulting from alternative splicing. *J Biol Chem*, 270(8), 3726-3731. doi:10.1074/jbc.270.8.3726
- Siderovski, D. P., Hessel, A., Chung, S., Mak, T. W., & Tyers, M. (1996). A new family of regulators of G-protein-coupled receptors? *Curr Biol*, 6(2), 211-212. doi:10.1016/s0960-9822(02)00454-2
- Singh, P., Wang, B., Maeda, T., Palczewski, K., & Tesmer, J. J. (2008). Structures of rhodopsin kinase in different ligand states reveal key elements involved in G protein-coupled receptor kinase activation. *J Biol Chem*, 283(20), 14053-14062.  
doi:10.1074/jbc.M708974200
- Sriram, K., & Insel, P. A. (2018). G Protein-Coupled Receptors as Targets for Approved Drugs: How Many Targets and How Many Drugs? *Molecular Pharmacology*, 93(4), 251-258.  
doi:10.1124/mol.117.111062
- Stadel, R., Ahn, K. H., & Kendall, D. A. (2011). The cannabinoid type-1 receptor carboxyl-terminus, more than just a tail. *Journal of Neurochemistry*, 117(1), 1-18. doi:10.1111/j.1471-4159.2011.07186.x
- Stella, N., Schweitzer, P., & Piomelli, D. (1997). A second endogenous cannabinoid that modulates long-term potentiation. *Nature*, 388(6644), 773-778. doi:10.1038/42015
- Stimpson, H. E., Toret, C. P., Cheng, A. T., Pauly, B. S., & Drubin, D. G. (2009). Early-arriving Syp1p and Ede1p function in endocytic site placement and formation in budding yeast. *Molecular Biology of the Cell*, 20(22), 4640-4651. doi:10.1091/mbc.E09-05-0429
- Straiker, A., Wager-Miller, J., & Mackie, K. (2012). The CB1 cannabinoid receptor C-terminus regulates receptor desensitization in autaptic hippocampal neurones. *Br J Pharmacol*, 165(8), 2652-2659. doi:10.1111/j.1476-5381.2011.01743.x
- Sugiura, T., Kishimoto, S., Oka, S., & Gokoh, M. (2006). Biochemistry, pharmacology and physiology of 2-arachidonoylglycerol, an endogenous cannabinoid receptor ligand. *Prog Lipid Res*, 45(5), 405-446. doi:10.1016/j.plipres.2006.03.003
- Sugiura, T., Kondo, S., Sukagawa, A., Nakane, S., Shinoda, A., Itoh, K., . . . Waku, K. (1995). 2-Arachidonoylglycerol - a Possible Endogenous Cannabinoid Receptor-Ligand in Brain. *Biochemical and Biophysical Research Communications*, 215(1), 89-97. doi:DOI 10.1006/bbrc.1995.2437
- Sylantsev, S., Jensen, T. P., Ross, R. A., & Rusakov, D. A. (2013). Cannabinoid- and lysophosphatidylinositol-sensitive receptor GPR55 boosts neurotransmitter release at central synapses. *Proc Natl Acad Sci U S A*, 110(13), 5193-5198.  
doi:10.1073/pnas.1211204110
- Syrovatkina, V., Alegre, K. O., Dey, R., & Huang, X. Y. (2016). Regulation, Signaling, and Physiological Functions of G-Proteins. *J Mol Biol*, 428(19), 3850-3868.  
doi:10.1016/j.jmb.2016.08.002
- Taylor, M. J., Perais, D., & Merrifield, C. J. (2011). A high precision survey of the molecular dynamics of mammalian clathrin-mediated endocytosis. *PLoS Biol*, 9(3), e1000604.  
doi:10.1371/journal.pbio.1000604
- Tesmer, J. J. (2009). Structure and function of regulator of G protein signaling homology domains. *Prog Mol Biol Transl Sci*, 86, 75-113. doi:10.1016/S1877-1173(09)86004-3

- Thal, D. M., Yeow, R. Y., Schoenau, C., Huber, J., & Tesmer, J. J. (2011). Molecular mechanism of selectivity among G protein-coupled receptor kinase 2 inhibitors. *Molecular Pharmacology*, *80*(2), 294-303. doi:10.1124/mol.111.071522
- Thomsen, W., Frazer, J., & Unett, D. (2005). Functional assays for screening GPCR targets. *Curr Opin Biotechnol*, *16*(6), 655-665. doi:10.1016/j.copbio.2005.10.008
- Tiberi, M., & Caron, M. G. (1994). High agonist-independent activity is a distinguishing feature of the dopamine D1B receptor subtype. *J Biol Chem*, *269*(45), 27925-27931.
- Touhara, K., Inglese, J., Pitcher, J. A., Shaw, G., & Lefkowitz, R. J. (1994). Binding of G-Protein Beta-Gamma-Subunits to Pleckstrin Homology Domains. *Journal of Biological Chemistry*, *269*(14), 10217-10220.
- Trevaskis, J., Walder, K., Foletta, V., Kerr-Bayles, L., McMillan, J., Cooper, A., . . . Collier, G. R. (2005). Src homology 3-domain growth factor receptor-bound 2-like (endophilin) interacting protein 1, a novel neuronal protein that regulates energy balance. *Endocrinology*, *146*(9), 3757-3764. doi:10.1210/en.2005-0282
- Turu, G., & Hunyady, L. (2010). Signal transduction of the CB1 cannabinoid receptor. *Journal of Molecular Endocrinology*, *44*(2), 75-85. doi:10.1677/JME-08-0190
- Ueda, N., & Tsuboi, K. (2012). Discrimination between Two Endocannabinoids. *Chemistry & Biology*, *19*(5), 545-547. doi:10.1016/j.chembiol.2012.05.001
- Uezu, A., Horiuchi, A., Kanda, K., Kikuchi, N., Umeda, K., Tsujita, K., . . . Nakanishi, H. (2007). SGIP1alpha is an endocytic protein that directly interacts with phospholipids and Eps15. *J Biol Chem*, *282*(36), 26481-26489. doi:10.1074/jbc.M703815200
- Uezu, A., Umeda, K., Tsujita, K., Suetsugu, S., Takenawa, T., & Nakanishi, H. (2011). Characterization of the EFC/F-BAR domain protein, FCHO2. *Genes Cells*, *16*(8), 868-878. doi:10.1111/j.1365-2443.2011.01536.x
- van der Blik, A. M., Redelmeier, T. E., Damke, H., Tisdale, E. J., Meyerowitz, E. M., & Schmid, S. L. (1993). Mutations in human dynamin block an intermediate stage in coated vesicle formation. *J Cell Biol*, *122*(3), 553-563. doi:10.1083/jcb.122.3.553
- Villapol, S. (2018). Roles of Peroxisome Proliferator-Activated Receptor Gamma on Brain and Peripheral Inflammation. *Cellular and Molecular Neurobiology*, *38*(1), 121-132. doi:10.1007/s10571-017-0554-5
- Wilhelm, B. G., Mandad, S., Truckenbrodt, S., Krohnert, K., Schafer, C., Rammner, B., . . . Rizzoli, S. O. (2014). Composition of isolated synaptic boutons reveals the amounts of vesicle trafficking proteins. *Science*, *344*(6187), 1023-1028. doi:10.1126/science.1252884
- Williams, C. M., & Kirkham, T. C. (1999). Anandamide induces overeating: mediation by central cannabinoid (CB1) receptors. *Psychopharmacology (Berl)*, *143*(3), 315-317. doi:10.1007/s002130050953
- Yako, Y. Y., Echouffo-Tcheugui, J. B., Balti, E. V., Matsha, T. E., Sobngwi, E., Erasmus, R. T., & Kengne, A. P. (2015). Genetic association studies of obesity in Africa: a systematic review. *Obes Rev*, *16*(3), 259-272. doi:10.1111/obr.12260
- Yang, F., Yu, X., Liu, C., Qu, C. X., Gong, Z., Liu, H. D., . . . Sun, J. P. (2015). Phospho-selective mechanisms of arrestin conformations and functions revealed by unnatural amino acid incorporation and (19)F-NMR. *Nat Commun*, *6*, 8202. doi:10.1038/ncomms9202
- Yeo, G., Holste, D., Kreiman, G., Burge, C.B., 2004. Variation in alterYeo, G., Holste, D., Kreiman, G., Burge, C.B., 2004. Variation in alternative splicing across human tissues. *Genome Biol*, *5*, 15. <https://doi.org/10.1186/gb-2004-5-10-r74>.  
Genome Biol. 5, 15. <https://doi.org/10.1186/gb-2004-5-10-r74>.
- Yona, S., Lin, H. H., Siu, W. O., Gordon, S., & Stacey, M. (2008). Adhesion-GPCRs: emerging roles for novel receptors. *Trends Biochem Sci*, *33*(10), 491-500. doi:10.1016/j.tibs.2008.07.005
- Zhang, X., & Kim, K. M. (2017). Multifactorial Regulation of G Protein-Coupled Receptor Endocytosis. *Biomol Ther (Seoul)*, *25*(1), 26-43. doi:10.4062/biomolther.2016.186

Zou, S. L., & Kumar, U. (2018). Cannabinoid Receptors and the Endocannabinoid System: Signaling and Function in the Central Nervous System. *International Journal of Molecular Sciences*, 19(3). doi:ARTN 83310.3390/ijms19030833

## 10. List of publications

The results of this dissertation thesis are part of the following publication:

**Gazdarica, M.**, Noda, J., Durydivka, O., Novosadova, V., Mackie, K., Pin, J. P., Blahos, J. (2021). SGIP1 modulates kinetics and interactions of the cannabinoid receptor 1 and G protein-coupled receptor kinase 3 signalosome. *Journal of Neurochemistry*. doi:10.1111/jnc.15569

Durydivka O., **Gazdarica M.**, Vecerkova K., Radenkovic S., Blahos J. (2023). Multiple Sgip1 splice variants inhibit cannabinoid receptor 1 internalization. *Gene*. Doi: 10.1016/j.gene.2023.147851

Other publications of the author:

Sevcovicova, A., Plava, J., **Gazdarica, M.**, Szabova, E., Huraiova, B., Gaplovska-Kysela, K., Cipakova, I., Cipak, L., Gregan, J. (2021). Mapping and Analysis of Swi5 and Sfr1 Phosphorylation Sites. *Genes (Basel)*. doi: 10.3390/genes12071014.

Ferenc, J., Červenák, F., Birčák, E., Juríková, K., Goffová, I., Gorilák, P., Huraiová, B., Plavá, J., Demecsová, L., Ďuríková, N., Galisová, V., **Gazdarica, M.**, Puškár, M., Nagy, T., Nagyová, S., Mentelová, L., Slaninová, M., Ševčovicová, A. and Tomáška, Ľ. (2018), Intentionally flawed manuscripts as means for teaching students to critically evaluate scientific papers. *Biochem. Mol. Biol. Educ.*, doi.org/10.1002/bmb.21084

## 11. Appendices

1. Results of statistical analysis of protein-protein interaction are presented in Tables 2-9.
2. **Gazdarica, M.**, Noda, J., Durydivka, O., Novosadova, V., Mackie, K., Pin, J. P., Prezeau, L., Blahos, J. (2021). SGIP1 modulates kinetics and interactions of the cannabinoid receptor 1 and G protein-coupled receptor kinase 3 signalosome. *Journal of Neurochemistry*. doi:10.1111/jnc.15569; IF 5.372
3. Durydivka O., **Gazdarica M.**, Vecerkova K., Radenkovic S., Blahos J. (2023). Multiple Sgip1 splice variants inhibit cannabinoid receptor 1 internalization. *Gene*. doi.org/10.1016/j.gene.2023.147851; IF 3.913